The Pennsylvania State University

The Graduate School

IRON PROFILING IN GLIOBLASTOMA

A Dissertation in

Biomedical Sciences

by

Bhavyata Shesh

Submitted in Partial Fulfillment of the
Requirements
for the Degree of

Doctor of Philosophy

December 2023

The dissertation of Bhavyata Shesh was reviewed and approved by the following:

James R Connor
University Distinguished Professor
Vice-Chair of the Department of Neurosurgery Dissertation Advisor
Chair of Committee

Desai Dhimant
Professor of the Department of Pharmacology, Next-Generation Therapies.

Jeffrey Sundstrom
Assistant Professor of Ophthalmology, Neural and Behavioral Sciences, and Cellular & Molecular Physiology

Mohammed A. Ali
Associate Professor of Human Capital Management, Director of the MBA Program

Alicia McDonald
Principal Scientist, Merck

Rhoda Joseph
Professor of Information Systems, School of Business Administration, and Professor-in-Charge, Ph.D. in Biomedical Sciences / Master of Business Administration (Ex-Director)

Lisa Shantz
Program Head, Biomedical Sciences Graduate Program
Associate Professor of Biochemistry and Molecular Biology

ABSTRACT

Ferritin is a 450 kDa protein composed of 24 subunit polypeptides of two kinds: heavy (H) and light (L) chains. The ratio of these chains varies depending on the tissue in which ferritin is found. Ferritin protein is expressed ubiquitously and was historically believed to be solely involved in cytosolic intracellular iron sequestration, preventing the availability of excess redox-active iron for Fenton chemistry and the production of reactive oxygen species that can damage cells. However, recent studies have revealed additional functions beyond iron sequestration. In addition to its role in iron sequestration, ferritin has been found to act as an iron-delivery molecule. It has been shown that extracellular ferritin can deliver iron to organs throughout the body, including the brain. Due to its ability to carry more iron atoms than the traditional iron delivery protein transferrin, ferritin uptake is believed to be occurring in tissues or conditions that require higher levels of iron, such as during developmental stages and cancer. However, the uptake of ferritin by cancer tissues from the extracellular environment and its role in cancer growth and progression are still poorly understood.

In this thesis, I explore whether glioblastoma (GBM), a highly aggressive and malignant form of brain cancer, can uptake extracellular ferritin as an iron delivery agent and investigate the subsequent role of ferritin in tumor development. The first experimental section of this dissertation focuses on the uptake of extracellular H-ferritin by patient-derived glioblastoma cancer stem cell lines (GSCs). These cells, characterized by their ability to self-renew and differentiate within the tumor, contribute to tumor growth, recurrence, therapy resistance, and poor prognosis. Moreover, these cell types have been shown to acquire iron aggressively and preferentially from the tumor microenvironment. But the mechanism and mode of iron uptake are unclear. Thus, understanding the mechanism and functional implications of ferritin uptake in these cells is crucial. I demonstrate that GSCs can uptake extracellular H-ferritin as an iron delivery agent and that blocking transferrin receptor reduces ferritin uptake, suggesting the involvement of the receptor in this process. Moreover, I investigate the impact of extracellular ferritin uptake on the invasive potential of GSCs and find that H-ferritin reduces invasiveness without affecting proliferation capacity. This study sheds light on the H-ferritin mediated iron uptake mechanism in GSCs, providing valuable insights into GBM biology.

The next experimental section of my thesis focuses on understanding the factors that affect the uptake of extracellular H-ferritin. Using in vivo mouse models of GBM, I investigate whether the Homeostatic Iron Regulator (HFE) and the sex of the mice have any effect on H-ferritin uptake. Differences in GBM occurrence, characteristics, and outcomes between sexes

suggest that sex may regulate different mechanisms in tumors. Additionally, findings from the previous section indicated a potential sex difference in the binding of H-ferritin to human GBM tissues. However, my mouse model data reveals no significant difference in H-ferritin uptake between male and female GBM tissues. HFE protein is an iron sensor in cells, it monitors the levels of iron within the body and through its interaction with TfR helps regulate the uptake of iron at this receptor. Considering TfR's association with H-ferritin uptake in the previous section, and the sex-specific role of HFE in GBM survival, I investigate whether the Homeostatic Iron Regulator (HFE) affects the uptake of extracellular H-ferritin. Downregulation of HFE does not significantly affect the uptake of H-ferritin or transferrin proteins in GBM tissues either. Interestingly, mice with HFE downregulation exhibit a significant survival benefit compared to control levels of HFE in tumors. Although there are differences between the mouse models and human GBM tissues, the survival benefit observed in these mice models provides a useful tool to study mechanisms affecting survival in male GBMs and explore their translatability in human patients.

The final section of my thesis explores the role of H-ferritin beyond tumor expression levels. I investigate the impact of systemically downregulating H-ferritin in a novel mouse model of GBM. The results show that the extrinsic status of H-ferritin significantly impacts the survival of female GBM mice but not males. Sequencing of the tumors from these mice reveals differentially regulated pathways between male and female tumors. Female GBM tumors exhibit increased expression of genes related to immune system activation, cytokines, and chemokines, while male tumors show a reduction in immune system gene expression. Further analysis reveals decreased infiltration of T-cells and CD8+ T-cells but increased infiltration of mast cells in female mice, highlighting a novel role played by tumor extrinsic H-ferritin in regulating tumor-infiltrating T-cell populations and emphasizing the sex-biased nature of its functions. This section uncovers a sex-specific role of tumor extrinsic H-ferritin in modulating GBM tumors and elucidates sex-biased molecular mechanisms in tumor growth and development.

In conclusion, this dissertation provides evidence of the complex role of H-ferritin in GBM. It demonstrates the dynamic nature of H-ferritin, from its role in delivering iron to regulating tumor-infiltrating cells. The findings suggest a sex-specific role of H-ferritin in GBM tumor modulation. Overall, this research offers deeper insights into GBM biology and provides a new frame of reference in furthering our understanding of these tumors.

TABLE OF CONTENTS

LIST OF FIGURES

LIST OF TABLES

LIST OF ABBREVIATIONS

1FHA	PDB ID Human H Ferritin
2FFX	PDB ID Human L Ferritin
AKT	Ak Strain Transforming Serine/Threonine Kinase
ANOVA	Analysis Of Variance
AP1	Activator Protein 1
APC	Allophycocyanin
APOC2	Apolipoprotein C2
ARE	Antioxidant/Electrophile Response Element
ATF1	Activating Transcription Factor 1
ATG8	Autophagy Related 8
ATP	Adenosine Triphosphate
BBB	Blood Brain Barrier
BCNU	Bis-Chloroethylnitrosourea, Carmustine
BD	Inductively Coupled Plasma Emission Spectrometry
BHQ-3	Black Hole Quencher
BMP	Bone Morphogenetic Protein
cAMP	Cyclic Adenosine Monophosphate
CCE	Mouse Embryonic Stem Cell Line
CD133	Horse Radish Peroxidase

CD15	Honestly Significant Difference
CD44	Cluster Of Differentiation 44
CD44	Guanosine Triphosphatase
CD8	Cluster Of Differentiation 8
CDC42	Glioblastoma Initiating Cells
CDC42BPA	Glioblastoma
CDH2	Cadherin 2
CE	Corneal Epithelium
CNS	Central Nervous System
CO2	Extracellular Matrix
COPZ1	Coatomer Subunit Zeta-1
COVID-19	Coronavirus Disease 2019
CPZ	Epithelial-Mesenchymal
CRC	Colorectal Cancer
CREB	Camp-Response Element Binding Protein
CSCs	Cancer Stem Cells
CSF	Cerebro Spinal Fluid
CT	Computer Tomography
CXCL12	C-X-C Motif Chemokine Ligand 12
CXCR4	C-X-C Motif Chemokine Receptor 4
DAPI	Cluster Of Differentiation 44
DEGs	Differentially Expressed Genes

DMT1	Divalent Metal Transporter 1
DMT1	Divalent Metal Transporter
DNA	Deoxyribonucleic Acid
EBV	Epstein-Barr Virus
ECM	Cluster Of Differentiation 15
EDTA	Ethylenediaminetetraacetic Acid
EGF	Epidermal Growth Factor
EGFR	Epidermal Growth Factor Receptor
EMT	Epithelial Mesenchymal Transition
EMT	Cluster Of Differentiation 133
ER	Endoplasmic Reticulum
ES	Embryonic Stem
FBS	Fetal Bovine Serum
FC	Fold Change
FDA	Food And Drug Administration
FDR	False Discovery Rate
FeCl3	Ferric Chloride
FGS	Fluorescence Image-Guided Surgery
FOXM1	Forkhead Box M1
FTH1	Ferritin Heavy Chain
FTL	Ferritin Light Chain
GABARAP	Gaba Type A Receptor-Associated Protein

GADD45	Growth Arrest And DNA Damage Inducible Alpha
GADD45A	Growth Arrest And DNA Damage Inducible Alpha
GBM	Glioblastoma
GBM	Chlorpromazine
Gd-DO3A	Gadobutrol
GEPIA	Gene Expression Profiling Interactive Analysis
GICs	Cell Division Control Protein 42 Homolog
GL261	Mouse GBM Cell Line
GPCR	G-Protein-Coupled Receptors
GPX4	Glutathione Peroxidase
GSCs	GBM Cancer Stem Cells
GSEA	Gene Set Enrichment Analysis
GSK3	Glycogen Synthase Kinase 3 Beta
GTPases	Cdc42 Binding Protein Kinase Alpha
H2O2	Hydrogen Peroxide
H3R17	Epigenetic Methylation Of Histone 3 On Arginine 17
H4R3	Epigenetic Methylation Of Histone 3 On Arginine 3
HA	Hyaluronic Acid
HaCaT	Human Epidermal Keratinocytes
HCC	Hepatocellular Carcinoma
HCCLM3	Human Hepatocellular Carcinoma Cell Line
HCT116	Human Colorectal Carcinoma Cell

HEK293T	Human Embryonic Kidney Cells
HepG2	Hepatoblastoma Cell Line
HER2	Human Epidermal Growth Factor Receptor 2
HFE	Homeostatic Iron Regulator
HH	Hereditary Hemochromatosis
HIF	Hypoxia Inducible Factor
HIF1A	Hypoxia Inducible Factor 1 Subunit Alpha
HIV1	Human Immunodeficiency Virus
HKa132	Human High Molecular Weight Kininogen
HNSC	Head And Neck Squamous Cell Carcinoma
HRE-3	Hypoxia Response Element -3
HRP	Carbon Dioxide
HSD	Becton, Dickinson And Company
HT29	Human Colorectal Adenocarcinoma Cell Line
IACUC	The Institutional Animal Care And Use Committee
ICG	Indocyanine Loaded
ICP-AES	4',6-Diamidino-2-Phenylindole
IDH	Isocitrate Dehydrogenase
IgG	Immunoglobulin G
IL-1	Interleukin -1
InsR	Insulin Receptor
IRB	Institutional Review Board

IRE	Iron Responsive Element
IRP	Iron Regulatory Protein
JAK2	Janus Kinase 2
JNK	C-Jun N-Terminal Kinases
JunB	Transcription Factor Junb
JunD	Transcription Factor Jund
KD	Knockdown
KEAP1	Kelch Like Ech Associated Protein 1
LAML	Leukemia
LC3	Light Chain 3
LDs	Lipid Droplets
LGG	Lower Grade Glioma
LICAM	L1 Cell Adhesion Molecule (L1CAM)
LIME	Laboratory For Isotopes and Metals In The Environment
LIP	Labile Iron Pool
LIP	Labile Iron Pool Measurements Labile Iron Pool
MAPK	Mitogen-Activated Protein Kinase 1
MARE	Maf Recognition Element
MCF7	Breast Cancer Cell Line
MCs	Mast Cells
MDA-MB-231	Breast Cancer Cell Line
MDR	Multi Drug Resistant

MDR1a	Multidrug Resistance Mutation 1 A
MFI	Median Fluorescence Intensity
MG-63	Osteosarcoma Cell Line
MGMT	Methylguanine-DNA Methyltransferase
MHCC97H	Hepatocellular Carcinoma
mMCP	Murine Microenvironment Cell Population
MMP-9	Matrix Metalloprotease 9
MMPs	Matrix Metalloproteinases
MOLT4	T Lymphoblast Cell Line
MRI	Magnetic Resonance Imaging
mRNAs	Messenger RNA
MtFt	Mitochondrial Ferritin
NCOA4	Nuclear Receptor Coactivator 4
NDRG1	N-Myc Downstream-Regulated Gene-1
NHS	-Hydroxysuccinimide
NIH	National Institutes of Health
NIR	Near Infrared
NIRF	Near-Infrared Fluorescence
NLS	Nuclear Localization Signal
NRF2	Nfe2 Like Bzip Transcription Factor 2
NSCLC	Non-Small Cell Lung Cancer
NTA	Nitrilotriacetic Acid

OE	Overexpressed
PBS	Phosphate Buffered Saline
PCR	Polymerase Chain Reaction
PDAC	PDAC Models of Pancreatic Ductal Adenocarcinoma
PDB	Protein Data Bank
PDT	Photodynamic Cancer Therapy
PDX	Patient Derived Xenografts
PHD	Plant Homeodomain
PIAS3	Protein Inhibitor Of Activated Stat 3
PIGF	Placental Growth Factor
PKA	Protein Arginine Methyltransferase 4
PLAA	Poly-L-Aspartic Acid
PRMT1	Protein Arginine Methyltransferase 1
PRMT4	Protein Arginine Methyltransferase 4
PTT	Photothermal Therapy
PUFA	Polyunsaturated Fatty Acid
PyMOL	Open-Source Molecular Visualization System
qPCR	Quantitative PCR
Rap1A	Ras-Related Protein 1A
RAS	Rat Sarcoma Gene
RIN	RNA Integrity Number
RIPA	Radioimmunoprecipitation Assay Buffer

RNA	Ribonucleic Acid
ROS	Reactive Oxygen Species
RPMI	Roswell Park Memorial Institute Medium
RSL	RAS-Selective Lethal
SARS-CoV-2-	Severe Acute Respiratory Syndrome Coronavirus 2
SF	Serum Ferritin
SH-SY5Y	Human Neuroblastoma Cell Line
SIREs	Searching For Iron Responsive Elements
SKBR3	Human Adenocarcinoma Cell Line
SKOV3	Human Ovarian Cancer Cell Line
SMPs	Stress Mitigation Pathways
STAT3	Signal Transducer and Activator Of Transcription 3
STAT5	Signal Transducer and Activator of Transcription 5
SW480	Primary Adenocarcinoma Cell Line
T47D	Human Breast Cancer Cell Line
TAMs	Tumor Associated Macrophages
TCGA	The Cancer Genome Atlas
TF	Transferrin
TfR	Transferrin Receptor
TGF	Transforming Growth Factor
TME	Tumor Microenvironment
TMIGD3	Transmembrane And Immunoglobulin Domain Containing 3

TNF	Tumor Necrosis Factor
TopGO	Gene Set Enrichment Analysis for Gene Ontology (GO) Terms
TPM	Transcript Per Million
UTR	Untranslated Region
UTRs	Untranslated Regions
UV	Ultraviolet Rays
UVM	Uveal Melanoma
VEGF	Vascular Endothelial Growth Factor
WT	Wild Type

This thesis is dedicated to all the chocolate cakes that I ate through the process of making it.

Oh, and to Shesh (Who (thankfully) hates chocolate cakes)

ACKNOWLEDGEMENTS

I am deeply grateful to Dr. James Connor for providing the invaluable opportunity to work in his laboratory. Dr. Connor’s unwavering dedication, motivation, and passion have been truly inspiring, propelling my own drive to excel. Under his mentorship, I have experienced significant personal and professional growth. Dr. Connor possesses a remarkable ability to guide and support me, enabling me to reach my fullest potential and pushing me to develop in areas where I need to hone my skills further. His exceptional qualities as a motivated individual across various roles are truly admirable, and I aspire to emulate them throughout my career and life. Furthermore, I am grateful for his encouragement and motivation to help me pursue an MBA program, demonstrating his genuine interest in my progress. I extend my heartfelt appreciation to Dr. Connor for his immeasurable contributions to my growth and success. Working under his guidance has been a privilege, and I am confident that his mentorship will continue to impact my future endeavors.

In Dr. Connor's laboratory, the list of individuals I would like to express my gratitude to is extensive! To each person, past and present, whom I have had the opportunity to interact with as a member of the Connor lab, I extend my heartfelt thanks. I would like to start by acknowledging Brian, Vagisha, and Insung, who were my initial points of contact and played a pivotal role in guiding my decision to join the lab. Your support and guidance have been instrumental in shaping the path that led me to where I am today. I am truly grateful for the immense love, assistance, training, and support provided by Becky, Beth, and Lisa Harman (Lisa, you hold a special place in my heart!) over the past five years. You are the pillars of this lab, forming its solid foundation. I also want to express my appreciation to past members whom I have enjoyed working with and with whom I cherish the opportunity to maintain connections. Madhan, Stephanie, Mandy, Yunsung, Jennifer, Sang, Ganesh, Vladimir, Dasha, and Mark, I consider myself fortunate to have had the opportunity to work alongside you and learn from each of you. I look forward to staying connected with all of you in the future. To the current members of the lab, Quinn, Savannah, Tim, Stephanie, Palsa, Rebecka, Emily, Pappus, and Makenzie, I couldn't have asked for better colleagues to collaborate with. Your dedication, teamwork, and camaraderie have made my experience in the lab truly enjoyable. I extend my sincerest gratitude to every Connor lab individual who I had the opportunity to interact with. Your contributions, support, and camaraderie have played an invaluable role in my personal and professional growth. I am grateful for the opportunity to work with such a remarkable group of individuals.

I would also like to express my gratitude to my committee members for their unwavering support and

encouragement throughout this journey. Their presence and guidance have been invaluable to me. I am incredibly thankful to Dr. Alicia McDonald for providing me with the opportunity to begin my career in this country. Her continued guidance as my committee member has helped me see the bigger picture in this research. I extend my appreciation to Dr. Dhimant Desai for consistently showing kindness by attending our early morning meetings and dedicating valuable time to developing new drug compounds for this research. Additionally, Dr. Desai has gone above and beyond by providing support beyond the confines of Penn State Hershey. I would like to acknowledge Dr. Jeffrey Sundstrom for ensuring the rigor of our research and constantly pushing for excellence. Dr. Rhoda Joseph has played a crucial role by approaching the research from a business perspective, prompting me to consider the dimensions of life sciences research in the context of business. I also thank her for her willingness to be on my committee despite her moving states. Lastly, I am grateful to Dr. Mohammed Ali for his support and willingness to join my committee at short notice. Dear committee members, I truly and greatly appreciate all the effort and support you have shown in my development and progress throughout this PhD.

I would like to express my immense gratitude to several individuals at Penn State whose help has made a lot of this research possible. Firstly, I would like to thank Dr. Thomas Abraham and Wade Edris for their invaluable assistance in helping me learn confocal microscopy techniques. Additionally, I am grateful to Dr. Vonn Walter, Dr. Sirisha Pochareddy, Dr. Yuka Imamura, and Oana Bolt for their unwavering support and guidance in mRNA sequencing-related analysis. Special thanks go to Lisa Clark and Stephanie Pomraning for their kindness and helpfulness throughout the PhD process.

Above all, I want to extend my deepest appreciation to my husband and the love of my life, Shesh. His dedication to this PhD journey has been as remarkable as my own. Without his unwavering love, patience, humor, friendship, encouragement, and gentle reminders to push myself towards my goals and dreams, this thesis would not have been possible. I would also like to express my heartfelt thanks to my parents, Shaivangi mom, sister, and nephews for their unconditional love and unwavering support throughout this journey.

Lastly let me be practical and not forget the one thing that keeps everyone rolling: the $$$$! Thank you, National Institute of Health (NIH), for funding this research. I appreciate you being generous. (This work was funded by grant P01CA245705 by the National Institutes of Health. The contents of this paper are solely the responsibility of the authors and do not necessarily represent the official views of the NIH).

Chapter 1: A Novel View of Ferritin in Cancer

This work has been previously submitted as:
Bhavyata (Pandya) Shesh, James R. Connor, A novel view of ferritin in cancer, Biochimica et Biophysica Acta (BBA) - Reviews on Cancer, 2023

1.1 Abstract

Since its discovery more than 85 years ago, ferritin has principally been known as an iron storage protein. However, new roles, beyond iron storage, are being uncovered. Novel processes involving ferritin such as ferritinophagy and ferroptosis and as a cellular iron delivery protein not only expand our thinking on the range of contributions of this protein but present an opportunity to target these pathways in cancers. The key question we focus on within this review is whether ferritin modulation represents a useful approach for treating cancers. We discussed novel functions and processes of this protein in cancers. We are not limiting this review to cell-intrinsic modulation of ferritin in cancers, but also focus on its utility in the trojan horse approach in cancer therapeutics. The novel functions of ferritin as discussed herein realize the multiple roles of ferritin in cell biology that can be probed for therapeutic opportunities and further research.

1.2 Introduction

Ferritin has long been established as an iron storage protein with a central role in iron regulation. In mammals ferritin is composed of 24-subunits and consists of two distinct subunits, H (Heavy, 21 kDa) and L (Light, 19 kDa) chains[1,2]. The H subunit (FTH1) has ferroxidase activity, which converts Fe2+ to Fe3+ for storage inside the shell, and L subunit (FTL) has a nucleation site for iron. Ferritin H and L subunits are encoded by two different genes, and the proteins co-assemble in various ratios (isoferritins) with a tissue-specific distribution. For example, H chain is expressed highly in the heart, whereas L-chain expressed predominantly in the liver[3]. In the brain, the oligodendrocytes, microglia, and neurons express ferritin[4]. Oligodendrocytes express equal amounts of both H and L subunits, whereas microglia are enriched in L-ferritin, and neurons predominantly have the H-subunit of ferritin. In physiological states, ferritin can store nearly 2000 $Fe^{3+.}$ When the cavity is completely saturated, ferritin can store up to 4500 Fe^{3+} This form of iron storage prevents peroxide and reactive oxygen species production which occurs typically via a Fenton reaction between Fe^{2+} and H_2O_2, making ferritin not only a crucial part of the cellular iron trafficking machinery but also an important cellular defense against stress and

inflammation[5–9]. Sequestering iron and converting it to a non-toxic Fe^{3+} thereby protecting nucleic acids, proteins, and lipids from ROS, is crucial for cell survival as increased ROS could lead to cell death. This is further highlighted by the observation that homozygous murine knock outs of H-ferritin are embryonically lethal[10].

Our laboratory has been focusing on ferritin, especially H-ferritin as a potential iron-delivery protein[11]. Furthermore, our and other studies also demonstrated that ferritin is a multi-functional protein with possible roles in proliferation, angiogenesis, antioxidation, and immunosuppression[12]. In this review, we discuss structure, ferritin uptake and release followed by regulation of ferritin synthesis and an overview of types of ferritins. Additionally, we will be focusing H-ferritin's role in cancers and its potential as a therapeutic target and as a targeting molecule in cancer therapeutics.

1.2.1 Ferritin Structure

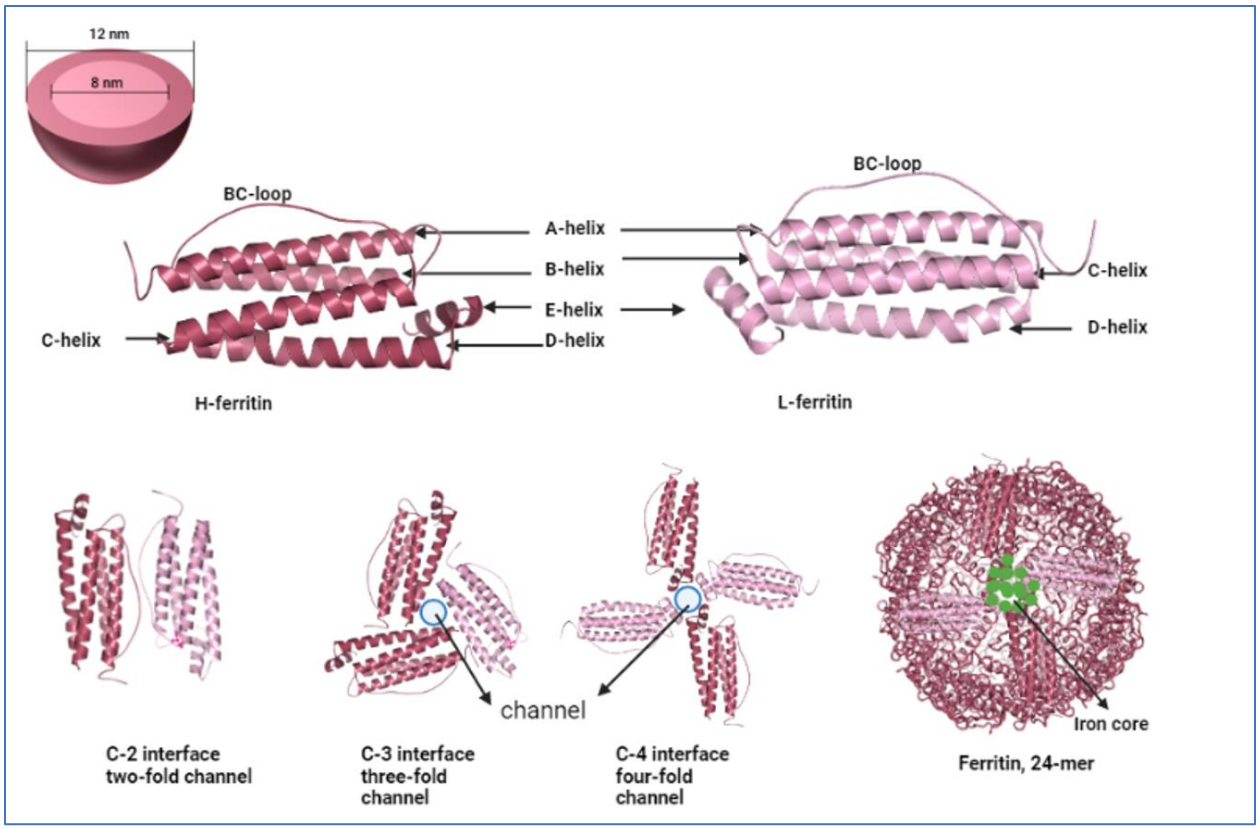

Fig. 1-1 Structure of ferritin (A) A representation of ferritin as a sphere showing the inner core and outer core diameter. (B) Graphical representation of the identical ferritin H- and L- peptides. Images were built in PyMOL 2.5.4 using ferritin heavy chain PDB ID 1FHA and ferritin light chain PDB ID 2FFX. (C) The various interfaces of the heavy and light chain ferritin. The three- and four-fold channels represent the open channels through which iron atoms can flow in and out of the structure. Finally, a 24-mer representation of the ferritin structure containing iron atoms is also presented. The image is inspired from the review by Chenxi Zhang et al[13].

The H and L subunits are essentially made up of 4 α- helices, A, B, C and D, which form the main bundle and a 5th C-terminal small α-helix, E (Fig. 1-1). The helices are assembled in a 4-3-2 symmetry to form a hollow spherical cage with an inner and outer diameter of 7~8 nm and 12~14 nm respectively and a thickness of 2~2.5 nm[13,14]. The symmetrical assembly of helices leaves openings aka channels at 3- and 4-fold subunit junctions which are lined with hydrophilic and hydrophobic residues allowing iron entry-exit and exchange of electron transport respectively[15,16]. Fe^{2+} ions enter the protein via the hydrophilic channels and are guided towards the Glu and His rich ferroxidase centers of the H-subunit which oxidize 2 Fe^{2+} to 2 Fe^{3+} at a time. Fe^{3+} ions being unstable at the ferroxidase center migrate to a, Glu rich, nucleation center of the L-subunit[6,17–19].

Iron mineralization grows at the nucleation centers inside the shell of the protein accommodating up to 4500 oxygen- and hydroxyl-bridged iron atoms[6,16]. Mineralized iron in ferritin is in the form of a crystalline ferric oxyhydroxide, $(Fe^{3+})2O_3 \bullet 0.5H_2O$, typically accompanied by phosphate in ratio of ≥10:1. Iron mineralization grows at the nucleation centers inside the shell of the protein accommodating up to 4500 oxygen- and hydroxyl-bridged iron atoms[6,16].

1.2.2 H-Ferritin Uptake and Release

Several studies have indicated H-ferritin is taken up into the brain parenchyma[11] and its trafficking across the blood brain barrier (BBB) via endothelial cells[20–23]. One of the important functions of ferritin being taken from extracellular environment is to deliver iron. Our laboratory has previously established that H-ferritin can replace transferrin as an iron source for oligodendrocytes[24]. In addition to oligodendrocytes, H-ferritin uptake has been observed in hepatocytes, reticulocytes, lymphoid cells, and erythroid precursor cells[25,26]. The mechanism of H-ferritin uptake is reported via a receptor mediated binding and endocytic uptake of this protein (Fig. 1-2)[27]. Some of the receptors implicated in its uptake, by cells, include TfR1[28], Tim1[20,29], Tim2 (rodent models)[30,31], CXCR4[32], and Scara 5 (for FTL specifically)[33–35]. Some studies focusing on the downstream fate of ferritin, post uptake, have shown ferritin entering the endosomal and lysosomal compartments in MOLT4 T-lymphoblast cell line[28].

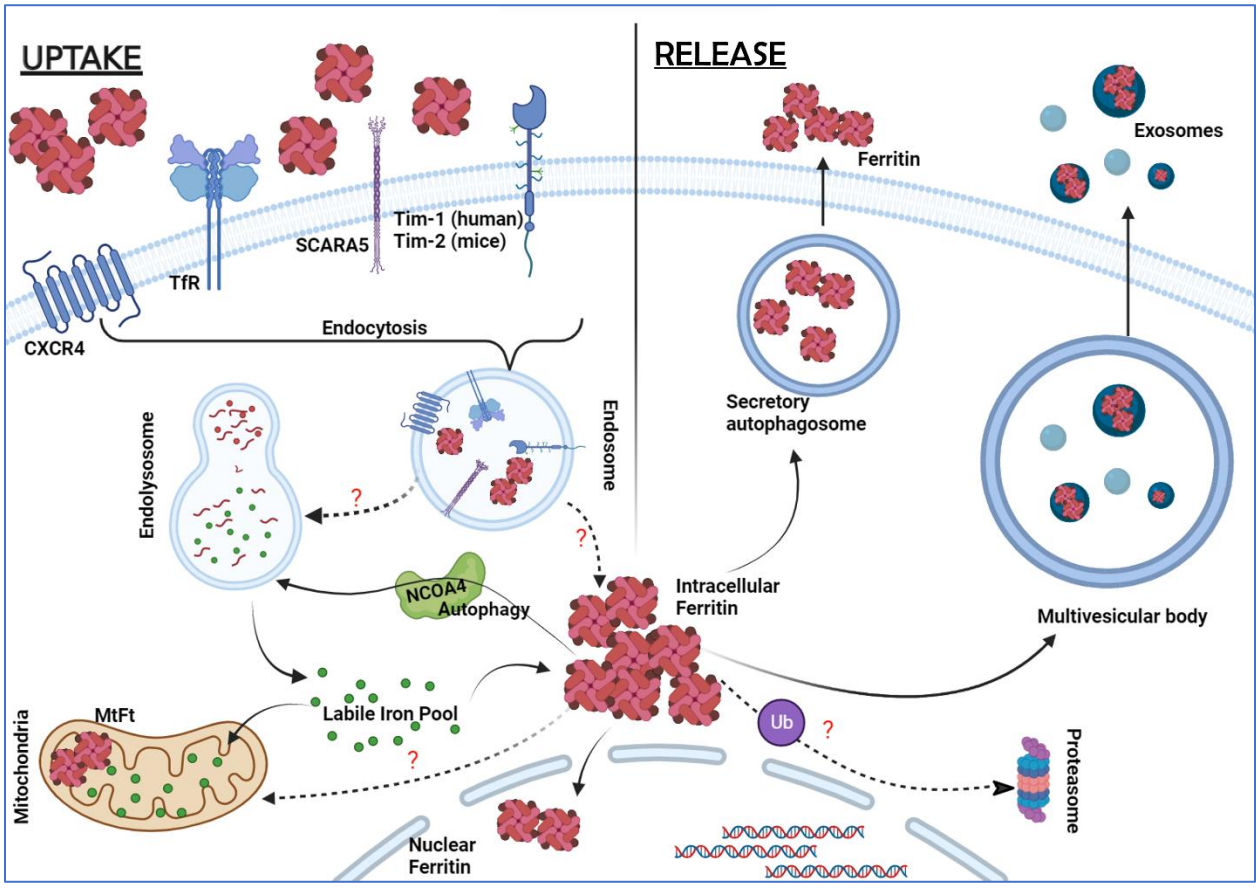

Fig. 1-2 Ferritin uptake and release Schematic of ferritin uptake and its downstream journey. Left: Ferritin H-chain binding and uptake has been shown to be mediated by receptors TfR1, Tim-1 (human), and Tim-2 (mice). Ferritin L-chain has been shown to bind Scara5 and CXCR4 receptors. Post binding at the cell surface, ferritin is endocytosed into the endosomes. While not all receptors are required simultaneously for endocytosis of ferritin, the schematic represents information from the various reports that have identified the presence of the receptors in question in the endosomes. The hypothesized fate of ferritin post endocytosis is shown. The dotted lines from the endosomal compartments to the endolysosome compartment represent one of the hypotheses for ferritin fate: which states that ferritin enters the lysosome and is degraded due to the acidic milieu of the compartment. Degradation of ferritin causes the release of the stored iron atoms which subsequently leave the compartment and become part of the labile iron pool. Another hypothesis is that ferritin leaves the endosomal compartment as is and becomes part of the intracellular ferritin levels. Intracellular ferritin can be shuttled to the lysosome, via NCOA4, during iron deplete conditions or transported to the nucleus or ubiquitinated and degraded in proteasome. Mitochondrial ferritin (MtFt) is shown in this figure for completeness. See text for discussion. Right: Ferritin has been shown to be secreted via two regulated pathways: (1) secretory autophagy/lysosomal secretory pathway or (2) encapsulation in exosomes, released extracellularly via multivesicular bodies. This image was created by using BioRender.

However, there is a gap in our current understanding of the uptake pathway and the downstream fate of ferritin in cancer cells[36]. For example, does ferritin enter the endo-lysosomal compartment and release iron in the acidic milieu of that compartment? How do the cells handle the surge in iron (as exogenous ferritin carries anywhere from 100 to 1000 times as much iron as transferrin)? If ferritin is broken down in the lysosomes, do the individual polypeptides of ferritin assemble back into the nanocage and are recycled? All in all, it seems clear that endocytosis of ferritin results in increased intracellular iron suggesting a more efficient iron delivery system at play in times of high iron demand, such as during neural development, rapid growth, and cancers[11]. Riding on this potential of efficient delivery (of iron) to cells ferritin has been extensively studied for its use as a nanoparticle that can deliver chemotherapeutics to various cancer cells in vivo. It is even more attractive as a nanoparticle delivery agent especially in brain tumors because it can easily cross the BBB. We will discuss this delivery potential of ferritin detail later in this article.

While uptake of ferritin is believed to deliver iron to the cells it is also released from cells potentially as a signal regarding local cellular iron status that can be communicated to other cells or as a mechanism to decrease the cellular iron content. As stated later in this article, newer research has suggested that some of the extracellular ferritin is part of extracellular vesicles which are now beginning to emerge as signaling vesicles between the cells. Because cancer cell signaling in crucial for cell survival, proliferation, drug-and radio resistance ferritin release might emerge as a critical signaling mechanism.

1.3 Regulation

Cellular iron status is the primary regulator of ferritin synthesis inside the cells[37]. Regulation by iron mainly occurs at the post-transcriptional level when mRNA binding proteins, iron regulatory protein (IRP) 1 and 2, bind to the 5’ stem loop structure on ferritin mRNA to inhibit its translation. The 5’ stem loop structure aka iron responsive element (IRE) is highly conservative in nature and is found on other proteins that are regulated by iron levels (for example, transferrin receptor) as well. During iron scarcity cells rely on iron content stored in their ferritin and allow ferritin degradation by proteasomal or lysosomal machinery to balance the intracellular iron levels. In such iron scarce situations additional ferritin translation is unnecessary and cells accomplish this translation blocking using IRP1/IRP2 binding to 5’ IREs. IRP1 usually exists as a cytosolic aconitase in presence of abundant iron but assumes an open conformation that allows it to bind to IRE. Both FTH1 and FTL, encoded by different highly conserved genes having 3 introns and 4 exons, encode the highly conserved 5’ IRE[38,39]. Both IRP1 and IRP2 have tissue specific expressions and regulate FTH and FTL in a highly context dependent manner in cancers.

For example, FTH1 but not FTL is specifically downregulated by IRP2 in breast and prostate cancer cell lines[40,41]. Post transcriptional regulation by miRNAs, binding to mRNA 3' untranslated regions (UTRs) to inhibit translation or induce degradation of the transcript, is also known. miR335 for example, has been shown to directly bind to FTH1 transcript and direct it for degradation[42]. Unlike post transcriptional regulation, transcriptional regulation of the ferritin genes particularly FTH1 are less well elucidated. Tissue specific transcription activation of FTH1 gene was shown to be mediated by cyclic AMP and hemin via a 0.1kb B- site located upstream of transcription initiation sequence. However, much work needs to be done to understand the transcription factors binding to the B-site and the various regulators regulating FTH1 transcription[43]. Apart from iron, pro-inflammatory cytokines (TNFα and IL-1α), growth factors, hormones, oxidative stress, hypoxia, non-coding RNAs (ncRNAs), and some proteins such as p53 have been shown to play a role in regulating ferritin levels in an iron-independent manner[44,45]. Regulation by these factors is briefly discussed below.

1.3.1 Regulation by oxidative stress

Ferritin is an antioxidant and has a cytoprotective roles against iron catalyzed ROS and oxidative stress. Hence, its regulation by oxidative stress is predictable. Oxidative stress proteins such as Nrf2 activate ferritin gene transcription via the conserved antioxidant/electrophile response element (ARE). FTH1 ARE consists of two activator protein 1 (AP1) binding sites, upstream of the transcription start site. While FTL ARE consists of an additional Maf recognition element (MARE) which makes it highly responsive to oxidative stress; even more than by iron levels[46]. Nrf2 directly binds to the AP1 binding sites to activate FTH1 and FTL transcription. Binding of Nrf2 to FTH1 ARE however is highly dependent on epigenetic methylation. In human HaCaT keratinocytes for example methylation of histone H4R3 and H3R17 in the FTH1 ARE region and subsequent binding of protein arginine (R) methyltransferases 1 and 4 (PRMT1 and PRMT4) to the methylated histones drives the activation of transcription[47,48]. Like Nrf2, other b-zip transcription factors, JunD and JunB, are also involved in binding FTH1 ARE and activating its transcription in HepG2 hepatocarcinoma cells[43,49]. In erythroleukemia, transcription factor regulatory protein PIAS3 (protein inhibitor of activated STAT3) indirectly activates FTH1 transcription by inhibiting the DNA binding capacity of a repressor, ATF1 (Activating Transcription Factor 1), on ARE sequence[49]. These studies demonstrate that various oxidative stress responsive proteins potently activate FTH1 in various cancer cells.

1.3.2 Regulation by hypoxia

Hypoxia is a common pathological feature of cancers. Hypoxia promotes tumor malignancy, EMT,

angiogenesis and drug resistance. In U87 and U251 glioma cells, FTL was shown to be upregulated under hypoxia and hypoxia inducible FTL was a positive regulator of epithelial mesenchymal transition (EMT). In these cells, Hypoxia-inducible factor 1-alpha (HIF 1α) directly bound to the HRE-3 region on the FTL promoter to activate its transcription[50]. HIF1α is upregulated in hypoxia and is implicated in promoting tumor growth and metastasis in multiple tumors including glioma, breast, hepatocellular, and hypernephroma[51]. FTH1 regulation by HIF1A is complex. FTH1 is known to stabilize HIF1A by reducing PHD (HIF prolyl hydroxylase that targets HIF1A for proteasomal degradation) activity through deprivation of Fe^{2+}. Additionally, FTH1 interacts with FIH (factor inhibiting HIF inhibits the transcriptional activity of HIF-1α) and activates its hydroxylase activity that inhibits HIF1A. Thus, FTH1 has opposing effect on two negative regulators of HIF1A. In hypoxic human primary macrophages FTH1 and mitochondrial ferritin expression was elevated and protected these cells from iron induced cell death[52]. In cancer cells, K562, however, hypoxia only marginally activated FTH1 translation by reducing the IRE-IRP interactions. In the same study, cobalt chloride, a hypoxia mimetic, was shown to reduce FTH1 expression by increasing the IRE-IRP interactions, resulting in translational block of the FTH1 mRNA[53]. These studies depict a reciprocal regulation between hypoxia/HIF1A and ferritin and further highlight the differences in use of hypoxia mimetics such as cobalt chloride versus hypoxic conditions developed via maintaining 1% O_2 gas conditions. A point to remember here is that hypoxia in the tumor microenvironment is a complex state that employs distinct mechanisms for expression of various genes including ferritin genes by targeting both DNA and RNA regulatory elements. While FTH1 might play a role in protecting normal cells from hypoxic damage, cancer cells on the other hand might utilize this same machinery to their advantage in sustaining and promoting tumorigenesis processes.

1.3.3 Regulation by oncogenes and tumor suppressors

One of the first reports of an oncogene regulating FTH1 came in 1993, from a report by Y Tsuji et al., describing preferential repression of FTH1 but not FTL by E1A oncogene in fibroblast cells[54]. Consistent with this report, proto-oncogene c-myc was also shown to repress FTH1 and stimulate IRP2 expression in highly tumorigenic, c-myc–transformed, Epstein-Barr virus–immortalized B cells[55]. Another report in U937 cells, a pro-monocytic, human myeloid leukemia cell line, showed c-myc downregulation corresponding with upregulation of FTH1 levels[38]. C-myc, a proto-oncogene and a transcription factor, is often hyper-activated in cancers. One way to explain reduction in ferritin in presence of c-myc (and other oncogenes described above) is to look at ferritin's classical role in the cells which is to sequester iron. Repressing ferritin causes an increase in the labile iron pool (LIP) which is considered actively available iron for cellular processes[56]. In cancer cells, which are often known to be 'iron addicted', intracellular iron

funds multiple different processes such as cellular proliferation, invasion, migration, and drug metabolism[57]. Increase in LIP might thus ultimately feed into cancer cell progression mechanisms. This idea has support in a related study showing c-myc expression increasing TfR1 expression suggesting an increase in iron uptake, and thereby LIP, in cancer cells[58].

Tumor suppressor p53 regulates cell cycle and apoptosis. Cellular stress, including DNA damage, hypoxia, ribosomal stress, and loss of adhesion activates p53. Once activated p53 can lead to activation of genes that promote growth arrest, cell death, or senescence and repress certain genes that mediate cell proliferation, growth and metastasis[59,60]. The relationship between p53 and FTH1 is anything but simple. On one hand excess p53 downregulates FTH1 gene via a trimeric transcription factor, NF-Y, in HeLa cells[61]. On the other, in lung cancer cells, H1299, excess p53 upregulates FTH1 via reducing its binding to IRP1[59]. FTH1 in return also regulates p53. In HEK293T, H1299, and MCF7 cell lines, FTH1 was shown to bind directly with p53 and upregulate its levels during hydrogen peroxide mediated oxidative stress[62]. In a more recent report, FTH1 upregulated p53 levels, in non-small cell lung cancer (NSCLC) cells, via miR-125b[63]. These studies suggest that FTH1 perhaps has a tumor suppressive role in conjunction with p53 and can be targeted for specific cancer therapeutics to enhance this activity.

1.3.4 Regulation by non-coding RNA (ncRNA) and pseudogenes

The role of ncRNAs, especially miRNAs, in regulating gene expression, has been extensively studied and continues to attract attention of researchers in cancer and other diseases. miRNAs are 19–25 nucleotides long and can modulate gene expression by inhibiting translation or inducing degradation of mRNA transcripts. A single miRNA could regulate multiple genes and it has been suggested that around 60% of the protein coding genome is regulated by miRNAs. Specific patterns of miRNA expression (miRNome) during different stages, subtypes, tissue- cell type specific, have been explored for cancer diagnosis, prognosis, and therapeutics[64,65]. Reciprocal regulation exists between miRNAs and FTH1. FTH1 regulates let-7g, let-7f, let-7i and miR-125b expression, and their down-stream genes, in K562 erythroleukemia cell line. While oncogenic miRNA (oncomiRs) miR-200b targets FTH1 expression in highly aggressive breast cell line MDA-MB-231. Moreover, downregulation of FTH1 by miR200b increased the sensitivity of the breast cancer cells to doxorubicin chemotherapy[66]. miR-335 has been shown to target FTH1 and induce ferroptotic cell death in Parkinson's disease[42]. A recent study in prostate cancer identified FTH1 and its pseudogenes to be top targets of oncogenic miRNA, miR638, hinting at a larger miRNA:gene:pseudogene network. Pseudogenes are ncRNA transcripts that act as a sponge for the miRNAs that are targeted to their ancestral genes and thus possess competing endogenous RNAs (ceRNA) activity. Apart from miRNAs, long non-coding RNAs (lncRNA), circular RNAs (circ RNA), pseudogenes, and some mRNAs

could compete for and sequester shared miRNAs thus displaying ceRNA activity. Some other oncogenic miRNAs targeting the FTH1 gene:pseudgene network in prostate cancer are miR-19b-3p, 19b-1-5p, 181a-5p, 210-3p, 362-5p and 616-3p[67]. Interestingly, this network of miRNAs that target FTH1 and its pseudogenes is targetable. In prostate cancer cell lines, FTH1 and pseudogenes have a tumor suppressive role and hence targeting miRNAs that degrade FTH1 gene and pseudogenes could prove to be a beneficial therapeutic strategy[67].

Apart from the above discussed modes of regulation, growth hormones, cytokines, inflammation also regulate ferritin expression. The readers are guided to the excellent review on these additional regulatory mechanisms by F. M. Torti et al[38]. These different regulatory pathways of ferritin highlight the diversity and complexity of its post-transcriptional regulation. Considering the intra and inter- tumoral heterogeneity and specialized roles of ferritin in the different cells in the tumor microenvironment (TME) these different modes of regulation seem very plausible.

1.4 Types of Ferritin

Ferritin mainly exists in the cytosolic compartment of the cells. However, it has also been observed in the nuclear and mitochondrial compartments[68–71]. Extracellularly, ferritin has been reported in the serum, urine, synovial and cerebrospinal fluids[10,72,73]. The presence of ferritin in different sub-cellular and extracellular regions provides evidence of its multi-functional capacity which is discussed in this review further below.

1.4.1 Cytosolic ferritin

Cytosolic ferritin is the most abundant form of ferritin. The structure and function of ferritin discussed above are of a typical cytosolic ferritin.

1.4.2 Mitochondrial ferritin

Mitochondrial ferritin, as the name suggests, is located, specifically in the mitochondrion. Mitochondrial ferritin (MtFt) resembles H-ferritin subunit in structure and function but lacks the IRE sequence and is synthesized as a precursor that is targeted to mitochondria with the help of a 60 amino acid leader sequence[74,75]. The leader sequence is processed inside the mitochondria yielding a 22 kDa H-ferritin like protein which assembles into a 24 subunit homopolymer shell possessing ferroxidase activity[76]. Since, MtFt lacks IRE sequence, it is found to be regulated by epigenetic mechanisms activated in response to oxidative stress[77]. MtFt functions to regulate mitochondrial iron levels thereby reducing the reactive

oxygen species (ROS) formation and instigating a cytoprotective effect on the cells. MtFt is maintained at low levels in normal cells as higher levels siphon off iron from cytosol to mitochondria, leading to a reduced availability of iron in cytosol, causing an iron deficient phenotype. However, higher expression of MtFt is observed in tissues that have high oxygen consumption and increased metabolic activity such as testes, brain, and erythrocytes[74,78]. Higher expressions of MtFt have also been observed in disease states such as sideroblastic anemia, refractory anemia with ringed sideroblasts, and in in vivo cancer cells[79]. In normal cells, MtFt functions to regulate mitochondrial iron levels thereby reducing the reactive oxygen species (ROS) formation and instigating a cytoprotective effect on the cells. For example, cytoprotective effects of MtFt were observed when its overexpression inhibited erastin induced ferroptosis (iron induced cell death) in SH-SY5Y, neuroblastoma, cells. Overexpression of MtFt even rescued transgenic drosophila, fed an erastin-containing diet, from dying as compared to the drosophila with normal MtFt levels[80].

In cancer cells, however, MtFt plays an important role in being a tumor suppressor. For example, MtFt was found to be overexpressed in the HeLa and leukemic (K562) cells causing apoptosis of cells via cytosolic iron deprivation induced activation of Janus kinase 2 (JAK2) - signal transducer and activator of transcription 5 (STAT5) pathway[71,79,81]. Tumor inhibitory effects of high MtFt levels, likely due to cytosolic iron deprivation, were also observed in non-small cell lung carcinoma (H1299) cells[82]. High expressions of MtFt in neuroblastoma cell lines (SH-SY5Y) were shown to have an inhibitory effect on cellular proliferation. In SH-SY5Y, MtFt caused upregulation of tumor suppressors p53 and N-myc downstream-regulated gene-1 (NDRG1) and downregulation tumor promotors such as C-myc, N-myc and p-Rb[75]. Another example of tumor suppressor function of MtFt was observed when ovarian cancer cells overcame cisplatin resistance in presence roflumilast induced up-regulation of MtFt via the activation of cAMP/PKA/CREB signals[83,84]. Thus, MtFt plays key roles in iron metabolism impacting important cellular functions such as proliferation, apoptosis, ferroptosis, iron metabolism and oxidative stress management.

1.4.3 Nuclear ferritin

Nuclear ferritin has been observed in some cell types such as macrophages, hepatocytes, reticular, muscle, and nerve cells. It has also been observed in some brain tumors and glial cell lines in vitro. Unlike mitochondrial ferritin, nuclear ferritin is translated from the same mRNA that generates cytosolic ferritin. However, O-linked glycosylation of the six putative glycosylation sites on the nuclear ferritin sets it apart from the cytosolic ferritin and at the same time it enables it to translocate into the nucleus via an ATP dependent mechanism[57,69]. Since nuclear ferritin is produced from the same mRNA as FTH1, its

expression is also primarily regulated by the IRE-IRP system. Functionally, nuclear ferritin protects cells from the UV and iron-induced oxidative stresses. In 2002, our group showed for the first time, that nuclear ferritin binds to DNA and protects it from iron-induced oxidative damage by sequestering excess iron[70,85,86]. Structurally, nuclear ferritin, like mitochondrial ferritin, is mainly composed of the H-subunits. However, unlike mitochondrial ferritin which has a leader sequence, nuclear ferritin lacks a nuclear localization signal (NLS)[87]. Even though no specific NLS has been found on the nuclear ferritin, a separate transporter called ferritoid which contains an NLS has been shown transporting nuclear ferritin in the corneal epithelium (CE) cells. Ferritoid mediated transport of nuclear ferritin is believed to be specific to CE cells. CE cells are in fact believed to be highly tolerant to UV mediated DNA damage due to the protective effect of nuclear ferritin[88]. Protective role of nuclear ferritin led our group to perform studies on the role of nuclear ferritin in cancer cells where we have shown that reducing ferritin levels in the cancer cells increases their sensitivity to radiation and chemotherapy[89,90]. Thus, nuclear ferritin seems to be facilitating tumorigenesis.

1.4.4 Serum and other extracellular ferritins

Extracellular ferritin is the secreted form of ferritin present in various body fluids such as serum, urine, synovial, and cerebrospinal fluid. Serum ferritin (SF) is an extracellular ferritin that is the most clinically assessed biomarker as its concentrations may reflect systemic iron levels with < 100 ng/ml corelating with iron deficiency and > 800 ng/ml corelating with iron overload. SF, a 24-mer protein that resembles L-ferritin immunologically and structurally, is thus, a marker of choice when iron deficiency or anemia is suspected[91–94]. SF levels are also upregulated in many other diseases with inflammatory biology including COVID-19 infections[95], autoimmune diseases[96], and cancers[97]. High SF levels are in fact reported in numerous cancers including glioblastoma, neuroblastoma, breast, renal, and cervical cancers and is often associated with poor survival in these patients[57]. Nevertheless, because increased levels of SF are reported during inflammatory conditions, which often confounds several diseases, much caution must be administered in using SF as a disease detection marker[95]. Iron saturation levels of SF are a matter of controversy in the existing literature as differing reports have been published. One group demonstrated that hemochromatosis patients have SF which is iron poor while another demonstrated that hemochromatosis patients have iron rich SF[98,99]. In general, however, it can be summarized that SF is found to be saturated with iron from anywhere between 5% to almost 50% depending on certain factors such as inflammation or developmental stage. Inflammation in general causes SF to have low iron saturation due to an obstruction in the mobilization of iron from the reticuloendothelial system. In terms

of relative iron content, SF is known to carry less iron atoms when compared to liver ferritin. Liver ferritin can carry 4500 iron atoms[100] while SF can carry ~ 700 iron atoms. Although SF carries less iron atoms relative to other cytoplasmic ferritins it still carries higher iron atoms than Transferrin (TF) protein which can carry only two iron atoms[26].

Many cell types including hepatocytes and macrophages have been shown to secrete ferritin in normal and disease states. Bone marrow derived macrophages secrete extracellular ferritin that is composed of 50% H- and 50% L- subunits. This composition is slightly different from the typical SF, which is primarily of the L subunit type, suggesting that macrophage secreted ferritin could be carrying a larger iron payload than the typical SF[101]. Tumor associated macrophages (TAMs) in certain cancers such as melanoma and breast cancer have been shown to secrete ferritin into the tumor microenvironment[102,103]. In breast cancer, secreted ferritin from TAMs, induced by tumor necrosis factor alpha (TNFα) and interleukin 1 beta (IL-1β), was found to stimulate proliferation of the cancer cells[102–104]. Taken together, this raises the possibility that released/secreted ferritin, with higher H- subunit composition, could be functioning as an iron delivery protein during times when cells need considerably more iron, such as during development, growth, and in iron addicted tumors (tumor cells), than what can be delivered by just TF.

Ferritin in cerebrospinal fluid (CSF) is a secreted, extracellular, form of ferritin that has been shown to be elevated in certain inflammatory neurologic disease and in patients with malignant involvement of the CNS. In 2008, a group from Brazil showed that CSF ferritin levels were highest in group of patients with malignant infiltration as compared to 4 other groups; (1) that had no malignancy, (2) with inflammatory neurological diseases, (3) with neurocysticercosis, (4) and with acute bacterial meningitis. This data led to the conclusion that CNS ferritin could be used as an adjuvant biomarker for diagnosing CNS malignant infiltrations[105–107].

A portion of the SF has been shown to be glycosylated and binds to concanavalin A[91,108]. Because of glycosylation of SF, classical endoplasmic reticulum (ER) - Golgi secretory pathway is believed to be involved in secretion of some portion of SF. However, some other reports have shown a lack of secretion signal on SF ruling out the classical endoplasmic reticulum - Golgi secretory pathway[101]. In such cases, two non-classical secretory pathways that have been identified, so far, for ferritin are: a lysosomal secretory pathway demonstrated by Cohen et al. in 2010 and a multivesicular body-exosome pathway described by Truman-Rosentsvit et al. in 2018[102,109–111]. Ferritin is found in exosomes of neuroblastoma cells[112,113] and more recently in exosomes released from brain endothelial cells[114]. Thus, secretion/release via lysosomal secretory, exosomal, or ER-Golgi pathway, all organelle-based, regulated pathways, suggests that ferritin's presence in the extracellular milieu is not a product of cell damage or death but a

regulated signaling mechanism. All in all, iron content of the ferritin, its mode of release, cell type from which it is released, and the target cell type where it is taken up might drive the function of the released ferritin. For example, ferritin released in extracellular vesicles might play a significant role in cell-cell signaling or might be ousted from the cancer cells as a way to export iron out of the cells to avoid iron mediated cell death (ferroptosis)[111]. Whereas ferritin released from macrophages, containing high iron content, might play a role in iron delivery to the neighboring tumor cells in the tumor microenvironment. Thus, there are multiple functions to ferritin that are released via multiple different pathways showing the ability of cells including cancer cells to fine tune mechanisms that help drive their survival and growth.

1.5 Ferritin in Cancer

Dysregulation of iron metabolism has been associated with multiple cancers. Frequently termed as "iron addicted", cancer cells have evolved to regulate the expression of multiple iron metabolism proteins to not only suffice their abnormal iron demands but to utilize them in various capacities exceeding their specified roles[115]. Ferritin protein and mRNA levels are reportedly dysregulated in many cancers including breast[103], glioblastoma[116], and prostate[117]. The significance of altered ferritin levels in cancer is highlighted in the following section and a schematic overview of the cancer processes affected by FTH1 is also presented (Fig. 1-3).

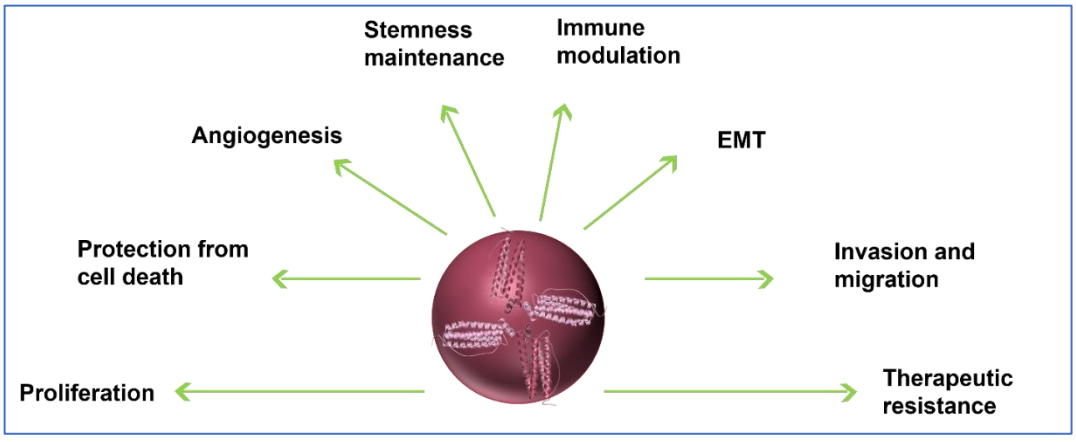

Fig. 1-3 Ferritin in cancer Schematic of a broad overview of ferritin's impact on multiple processes in cancer.

Functional role of ferritin in cancer

Functionally ferritin impacts various cellular processes in cancer cells ranging from proliferation, apoptosis, and EMT. Its individual role in cellular processes is summarized below.

1.5.1 Proliferation

Uncontrolled proliferation is a hallmark of cancer cells. Ferritin has been shown to support proliferation of cells irrespective of its iron content. Breast cancer cell lines such as MCF7 and T47D, for example, were shown to proliferate in presence of ferritin in an iron independent manner[103]. Upregulated FTH1 expression is associated with poor survival in multiple cancers, such as, Brain lower grade glioma (LGG), Acute myeloid leukemia (LAML), Head and neck squamous cell carcinoma (HNSC), and uveal melanoma (UVM). A recent study in hepatocellular carcinoma (HCC) cells, HCCLM3 and MHCC97H, showed that upregulated FTH1 expression enhanced cell proliferation by reducing peroxide and ROS levels[118]. FTL levels are also associated with cancer proliferation. For example, in Glioblastoma (GBM) FTL is upregulated, and it promotes cell growth via deactivation of pro-apoptotic GADD45A/JNK pathway. FTL was shown to bind GADD45A further suggesting that it could be inhibiting dimerization, essential for activation of GADD45A. In the same study, FTL was shown to be associated with upregulation of c-myc and cyclin D1 which further contributed to promoting proliferation of the cells[119]. In HeLa cells, upregulation of FTL levels was shown to increase proliferation in an iron - independent manner[120]. FTL was also shown to promote proliferation of osteosarcoma, MG-63, cells via GADD45/JNK pathway regulation[121]. It is not just the intracellular expression of ferritin that affects proliferation. As described in the previous section, extracellular ferritin secreted from TAMs also stimulates cancer cell proliferation via tumor microenvironment reprogramming. All in all, ferritin behaves as a positive regulator of proliferation in many different cancers.

1.5.2. Apoptosis

While many cancer cells have increased proliferation in presence of increased FTH1, association of FTH1 with tumor suppressor p53 has been shown to decrease the proliferation in H460 and A549 non-small-cell lung cancer (NSCLC) cells. In the H460 and A549 cell lines, FTH1 was shown to upregulate the expression of p53 by downregulating a p53 inhibitor miR125b via an indirect epigenetic mechanism. Increased p53 in presence of increased FTH1 led to induction of apoptotic pathway in these cells[63,122]. In human erythroleukemic K562 cell line high MtFt led to increased apoptosis in cells through cytosolic iron sequestration and JAK2/STAT5 pathway activation[79]. Contrasting the apoptotic activity, downregulation

of the FTH1 at transcriptional and translational levels, by using antisense oligonucleotides, led to specific increase in apoptosis in MCF7 breast cancer cell line, suggesting FTH1's role in protecting the cancer cells from apoptotic cell death[123]. In another report, increased expression of a ferroxidase mutant and wild type FTH1 in HeLa cells was shown to rescue from TNFα induced apoptosis in these cells[124]. Further suggesting that FTH1 participates in anti-apoptotic activity in some cancer cells irrespective of its iron content potentially by physically binding and inhibiting apoptotic activators. Indeed, in a separate report, in 293T cells, FTH1 was shown to bind and inhibit key apoptotic activating protein Bax[125]. In melanoma cells derived from a primary cutaneous melanoma, FTL downregulation was shown to inhibit cell proliferation in vitro and cell growth in vivo and increase sensitivity to apoptosis[126]. All this evidence suggests that although ferritin has a context dependent role in different cancers it primarily behaves as an oncogenic protein in protecting cancer cells from apoptotic cell death and supporting cell growth and proliferation.

1.5.3 Epithelial-mesenchymal transition (EMT)

EMT is a process whereby epithelial cells take on mesenchymal features i.e., they acquire fibroblast-like phenotype with reduced adhesive and augmented motility. Regulated EMT is mainly seen during development and adult tissue regeneration stages. Whereas in cancers, EMT is highly deregulated allowing cancer metastasis and invasion[127]. In lung cancer cell line A549, transforming growth factor beta 1 (TGFβ1) triggered EMT was enhanced in presence of autophagic degradation of FTH1. It was shown that autophagic degradation of FTH1 induced iron-driven oxidant injury that caused a feed forward loop which further increased autophagy during EMT[128,129]. FTH1 downregulation was shown to induce EMT in breast cancer cell lines MCF7 and H460 as well. In MCF7 and H460 cells, FTH1 silencing was associated with activation of two crucial EMT regulating pathways; c-x-c motif chemokine 4 (CXC4)/ c-x-c motif chemokine ligand 12 (CXCL12) CXCR4/CXCL12 and iron/ROS. In contrast to FTH1, FTL levels were observed to either increase or decrease the metastatic, proliferative, and invasive capacities of the cancers in a context specific manner. For example, in osteosarcoma cancer cell line, MG-63, high FTL levels decreased the metastatic potential via a reduction in metastatic protein players such as CDH2 and Vimentin[121]. Whereas, in GBM, FTL downregulation repressed EMT via AKT/GSK3β/ β-catenin signaling both in vitro and in vivo[130]. A process closely dependent on acquisition of EMT features in the cancer cells is invasion capacity[131]. Ferritin affects EMT in cancer cells suggesting that it might directly or indirectly (through iron delivery) affect the invasion capacity of the cells as well.

1.5.4 Angiogenesis

New growth in vascular network is required for cancer cell progression, dissemination, attainment of nutrients and oxygen, and removal of waste products. New growth of blood vessels from the existing ones, aka angiogenesis, depends on several activating and inhibiting factors. FTH1 has been shown to have either inhibitory or activating roles in angiogenesis depending on its interactions with these factors. For example, in human prostate cancer xenograft model, FTH1 was shown to support vessel growth by binding to and subsequently inhibiting the 22 amino acid antiangiogenic subdomain of HKa[132,133]. On the other hand, in colon cancer cell lines, HCT116 and SW480, FTH1 was shown to repress the HIF1α transcriptional activity in normoxic and hypoxic conditions[134]. HIF1α is an oxygen sensitive transcriptional mediator of hypoxia which regulates angiogenesis via activating factors such vascular endothelial growth factor (VEGF), placental growth factor (PIGF), and angiopoietins[135]. The current literature on the relationship of FTH1 is contradictory and the impact may relate to its iron status. For example, FTH1 activity on blood vessels was shown to be independent of iron.[132]

1.5.5. Therapeutic resistance

Normal cells activate various endogenous stress mitigation pathways (SMPs) to survive when they are exposed to stressors such as DNA damage, starvation, toxins, infections, etc. Cancer cells utilize these endogenous SMPs to survive when they are exposed to stressors such as those coming from a variety of cancer therapeutics. These SMPs are not limited to individual cells but also encompass heterotypic cell-cell signaling which is required for maintaining the right tumor microenvironment that can support in mitigating the stresses. Genetic modulations such as upregulation of multi drug resistant (MDR) genes, reinforcement of DNA repair systems, and rewiring of the cell signaling pathways such as incapacitation of cell death pathways, and fortification of antioxidant defenses are some of the SMPs evolved by cancer cells[136]. Intrinsic drug resistance mechanisms include pre-existing clones and some genetic mutations while acquired drug resistance mechanisms include non-genetic modifications such as cancer cell plasticity, and microenvironment modulations. Drug efflux, inactivation and/or alterations in the drug targets are also commonly acquired drug resistance mechanisms[136,137]. Since ferritin is an important player in antioxidant defense, many cancer cells utilize altered ferritin expression to survive the stresses from various cancer therapeutics such as chemo-, radio-, and immunotherapies. One of the first reports of FTH1 involvement in cancer resistance came from a study in leukemia cells that had enhanced resistance to oxidants in presence of elevated FTH1 levels[138]. FTL is also implicated in conferring resistance against oxidants in melanoma cells[126]. In erythroleukemia cells, increased FTH1 levels increased resistance to oxidative stress via increasing expression of multidrug resistance mutation 1 a (MDR1a) protein[139].

Nuclear ferritin's ability to protect the DNA is involved in resistance against DNA alkylating agents such as doxorubicin, BCNU, and cisplatin in glioma, breast, and leukemia cells[66,89,140,141]. Given nuclear ferritin's role in protecting the DNA from damage, our laboratory has established its role in conferring radioresistance in U251 glioma cells in vitro and in vivo[142]. Another report of FTH1's involvement in radioresistance comes from a recent study of lipid droplets (LDs) in breast, bladder, lung, neuroglioma, and prostate cancer cells. In this study, it was shown that increased number of LDs, carrying elevated FTH1, was associated with radioresistance in these cells[143]. While FTH1 seems to be conferring radio resistance in some cancers, its absence in certain others such as ovarian cancer cells, SKOV3, activates NF-κB induced chemoresistance[144]. Based on these reports modulating FTH1 levels in cancer cells might be a mechanism to alleviate therapeutic resistance in cancers.

1.5.6. Cancer initiating cells

Cancer initiating cells aka cancer stem cells (CSCs) have been shown to be iron addicted. CSCs demonstrate increased iron uptake, and storage along with a reduced export. There is considerable evidence that suggests that iron is essential for maintaining stem- cell phenotype. High FTH1 expression was recently associated with CSC features in breast[145], prostate[145], and cholangiocarcinomas[146]. FTH1 downregulation in GBM CSCs has been shown to inhibit it's in vivo tumorigenic potential. In these cells, FTH1-STAT3-FOXM1 axis was uncovered to be maintaining stemness and survival[116]. Reports from our laboratory have also confirmed FTH1's role in survival and stemness of GBM CSCs[90].

1.6 Ferritin in Cancer Therapy

Ferritin is an attractive target for cancer therapy. It has been shown that siRNA mediated downregulation of FTH1 in HeLa cells[147], and human glioma cells[89] increases chemosensitivity. FTH1 downregulation by siRNA also showed selective radiation sensitivity of GBM CSCs[90]. Thus, cellular processes that influence ferritin levels such as ferritinophagy and ferroptosis may be targetable for therapeutic purposes. Below, we discuss the potential of targeting these pathways for cancer therapy and further discuss the potential of ferritin itself aiding in transporting therapeutics to tumors.

1.6.1 Ferritinophagy

Ferritinophagy is the selective autophagy process whereby nuclear receptor coactivator 4 (NCOA4) binds to ferritin to traffic it to the lysosomes where it is degraded, and iron stored within it released[148]. NCOA4

is crucial for iron homeostasis at cellular and systemic levels as dysregulation of NCOA4 renders cells susceptible to ferroptosis. During selective autophagy, degradation cues guide the selective receptors, such as NCOA4, to recognize, bind and link their bound cargo to the autophagosomal membrane by interacting with lipidated ATG8 proteins (LC3/GABARAP). NCOA4 binds directly with a conserved c-terminal domain on FTH1 subunit. NCOA4 is regulated by the iron levels in the cells. During iron replete conditions, NCOA4 is recognized by a multifunctional ubiquitin E3 ligase, HERC2, and directed for degradation via the ubiquitin–proteasome system[149]. NCOA4 mRNA and protein levels have been shown to be relevant to carcinogenesis in many different cancers. In ovarian cancer for example, NCOA4 mRNA and protein levels were upregulated in multiple malignant subtypes; serous, serous papillary, and mucinous. A knockdown of NCOA4 in the malignant ovarian cancer cells increased FTH1 levels which was accompanied by reduced cell survival[150]. Recently, upregulation of NCOA4 has also been reported in patient derived and murine PDAC models of pancreatic ductal adenocarcinoma (PDAC). Ablation of NCOA4 in these PDAC models, improved survival and delayed tumor progression emphasizing the critical role of NCOA4 mediated ferritinophagy in survival and tumor progression[151]. Low NCOA4 levels, on the other hand, were recently discovered to be associated with high grade malignancy, poor survival, and defective immune cell infiltration in clear cell renal carcinoma (ccRCC). NCOA4 depletion in ccRcc increased FTH1 levels and lowered the occurrence of ferroptosis (iron mediated cell death)[152]. Thus, an imbalance in FTH1 levels due to dysregulated NCOA4 plays a crucial role in carcinogenesis and ferroptosis. NCOA4 from the ferritinophagy pathway can thus be targeted depending on the cancer type, to initiate mechanisms that trigger cancer cell death. Further evidence and importance of NCOA4/FTH1 mediated ferritinophagy in ferroptotic cell death is provided below.

1.6.2 Ferroptosis

Ferroptosis is a recently discovered form of regulated, iron-dependent, cell death pathway. Membrane damage due to oxidation of polyunsaturated fatty acid (PUFA)-containing phospholipids because of a reduction in glutathione peroxidase (GPX4) activity and accumulation of redox active iron are the trademarks of ferroptotic cell death[153]. Multiple different cellular pathways such as KEAP1/NRF2, iron metabolism, EMT, cell adhesion, ferritinophagy, and RAS/MAPK, and cell intrinsic molecules such as p53, GPX4, and system xc^- regulate ferroptotic cell death[153]. Small molecules that can inhibit GPX4 or system xc^- (an antiporter which imports cystine into the cells) such as (1S, 3R)-RSL3 and erastin, respectively, have been shown to induce ferroptosis[154]. One of the first reports of ferroptotic cell death induction by RSL3 and erastin came from a screen to identify small molecules that can selectively be lethal to RAS-mutant tumor cells (hence the name RAS-selective lethal (RSL) compounds)[155,156]. There

are various other small molecules that can induce ferroptosis via multiple different routes that have been covered in excellent reviews by Dixon and Stockwell[153], Mou et al.[157], and Lu et al.[154]. Clinically, immunotherapy and a combination of immuno- and radiotherapy have been shown to synergistically induce cancer cell death via ferroptosis[158,159]. Administering drugs that might trigger ferroptosis in drug resistant cancer cells is an area that is actively under research. There are three main pathways that can be targeted to induce ferroptosis to reverse drug resistance cancers: (1) canonical GPX4-regulated pathway, (2) iron metabolism pathway, (3) and lipid metabolism pathway[160]. One of the ways iron metabolism pathway can be targeted is via modulating labile iron pool of the cells. For example, dihydroartemisinin, an antimalarial drug, was found to increase labile iron pool in cisplatin resistant pancreatic ductal adenocarcinoma consequently triggering ferroptototic cell death[161]. Similarly, inhibitors of the divalent metal transporter 1 (DMT1), a membrane protein which allows translocation of ferrous iron (Fe^{2+}) to the cytosol following iron endocytosis, were shown to increase labile iron pool and subsequently trigger ferroptosis in drug resistant breast cancer stem cells[162]. Another way to target iron metabolism pathway to induce ferroptosis is via modulating FTH1 levels. One of the first reports of involvement of FTH1 in ferroptosis comes from a study by N. D. Yang et al. where an anti-malarial repurposed for cancer therapy, artesunate, was reported to induce ferroptosis in HeLa and hepatocellular carcinoma, HepG2, cells. In that study, overexpression of FTH1 directly and indirectly, via knockdown of NCOA4, was able to rescue artesunate mediated ferroptosis[163,164]. Artesunate was found to induce ferroptosis, in a similar manner, in the highly apoptotic resistant pancreatic cancer cells as well[165]. A role for FTH1 in ferroptosis was further confirmed in a study by Y. Q. Wang et al. that showed that overexpressing FTH1 in neuronal cells inhibited erastin induced ferroptosis[80,166]. In another report degradation of NCOA4 in pancreatic and fibrosarcoma cancer cells was shown to suppress ferroptosis[167]. In GBM mice models, downregulation of COPZ1 (Coatomer protein complex subunit zeta 1) was shown to induce ferroptosis by increasing NCOA4 mediated ferritinophagy downregulation of FTH1. Thus, COPZ1/NCOA4/FTH1 axis could be another target for destroying GBM cells[168]. Taken together, high FTH1 levels protect cancer cells from ferroptotic cell death and therapeutic strategies that can downregulate FTH1 levels, thereby triggering ferroptosis, might prove to be a promising target for cancer therapeutics.

1.6.3 Ferritin Nanoparticles

Ferritin's use as nanoparticles is an area that has expanded in the past few decades. Detailed descriptions on ways to engineer ferritin for its use as a therapeutic carrier can be found in literature[169–174]. Here we provide an overview on ferritin and its various uses in cancers. As described previously, 24-mer ferritin has a hollow spherical core where iron atoms are stored in a mineralized form. The self- assembling

property of the ferritin 24-mers, into a spherical shape, is highly pH dependent. Where extreme pH of 2-3 or 10-12 causes the spherical shell to decompose into subunits, physiological pH causes the re-assembly of the protein into a spherical shell. This renders ferritin a highly useful drug carrier as it is easy to package the drug in it with mere pH manipulations. Apart from easy packaging some of the other properties that make ferritin an ideal nanocarrier are: (1) robust tumor targeting ability: ferritin is highly permeable through the vasculature and is often enriched at the tumor site. Speculated reasoning behind this enrichment is the uptake of ferritin by tumors for their superior iron needs. Indeed, we have recently demonstrated that FTH1 binds to GBMs, and the amount of binding is sex-dependent providing novel

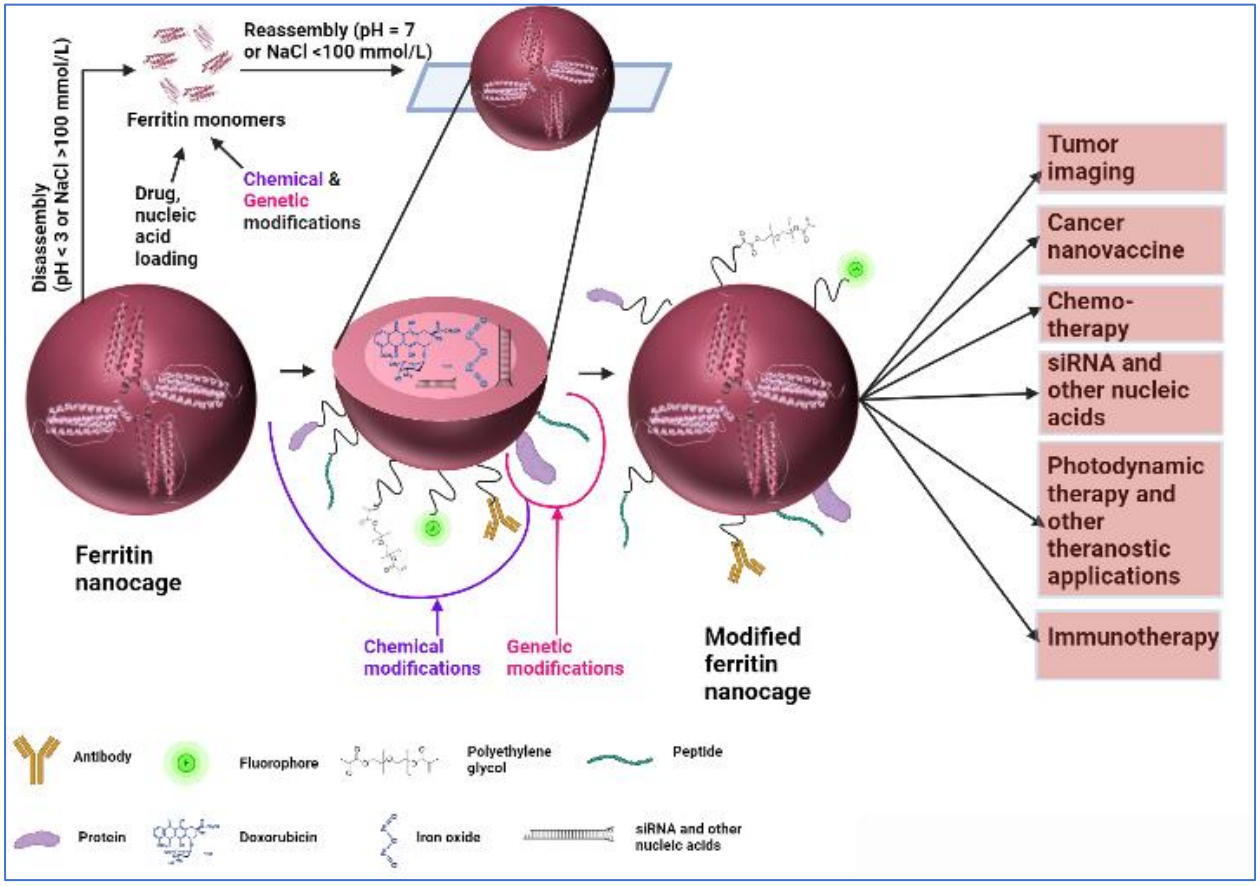

clinical considerations for using ferritin as a therapeutic target,

Fig. 1-4 Ferritin in nanotherapeutics Ferritin 24-mer hollow sphere can be utilized in a trojan horse approach to deliver chemotherapeutics to tumors. Specific targeting of the ferritin protein can be achieved by genetically or chemically attaching peptide or peptide ligand molecules that bind to tumor specific receptors. Apart from peptides a variety of other molecules such as polyethylene glycol, fluorophores, and antibodies can be attached to ferritin surface. Furthermore, ferritin nanocage can also be loaded with imaging agents, iron oxide, and nucleic acids such as siRNA. Loading and modifying ferritin with these different molecules makes it useful in a wide variety of applications such as tumor imaging, photodynamic and immunotherapy, and tumor nano-vaccines. This presentation was created with the help of BioRender.

(2) excellent biocompatibility and non-immunogenicity: ferritin is highly conserved among various organisms[38]. Moreover, recombinant human ferritin can also be easily expressed in E.coli and scaled up as required, (3) good stability: ferritin can withstand high temperatures up to 75 °C for 10 min. It is also highly stable in presence of various denaturants[175,176], (4) easily modifiable: lysine and cysteine residues on the outer surface of ferritin allow easy modifications to obtain better targeting capabilities. For example, EGF ligand has been conjugated on the surface of recombinant human ferritin to target it to the EGFR receptors in breast cancers, (5) hydrophobic drug packaging: the inner surface of the protein allows packaging of hydrophobic drugs as well and since most of the cancer therapeutics are hydrophobic in nature it can carry a vast variety of hydrophobic molecules[177–180], (6) versatility: ferritin is straightforwardly genetically and chemically modifiable increasing its versatile use in medical therapeutics, imaging, diagnostics, bioelectronics, and non-medical applications such as water purification, and as a bioactuator for potential development as artificial muscles[181,182]. This can open doors to combined photo- and chemotherapy treatments. All in all, ferritin has the potential to become an ideal drug carrier for various chemotherapeutics (Fig. 1-4)[183–185].

There are numerous reports of ferritin being used as a nanocage drug carrier for a variety of chemotherapeutics in different cancers[186]. Typically, metal containing drugs such as cisplatin, Gd-DO3A, and deferoxamine B are encapsulated in the ferritin nanocage via passive loading i.e., allowing the molecules to enter ferritin via its six hydrophobic channels and eight hydrophilic channels at room temperature. In a study in U87 GBM cells, doxorubicin conjugated with Cu^{2+} is packaged, via hydrophilic channels, in surface engineered human ferritin molecules. It was shown that doxorubicin-Cu^{2+} complex packaged this way in ferritin had significantly enhanced pharmacokinetics such as prolonged circulation and half-life, reduced non-specific cardiotoxicity, and much higher uptake in the tumor cells[187]. Similarly, Gefitinib, a tyrosine kinase inhibitor was passively encapsulated, via hydrophobic channels, within human heavy chain apoferritin. Gefitinib packaged in H-ferritin nanocage demonstrated increased cellular uptake and potency, against HER2 overexpressing SKBR3 cell line, as compared to Gefitinib alone[188]. Release of the chemotherapeutic drugs from ferritin is also mediated by these hydrophobic and hydrophilic channels/pores. In a study by Luo et al., daunomycin was packaged with poly-L-aspartic acid (PLAA) to enhance its sustained release from the hyaluronic acid (HA) surface modified ferritin. Daunomycin packaged HA-ferritin allowed specific binding of ferritin to CD44 markers on A549 lung cancer cells and improved sustained release of the drug from the nanocarrier[189]. Apart from passive loading, disassembly (and reassembly) of ferritin, to load drugs, in presence of 8M urea and extreme pH conditions has also

been reported. Fat soluble drugs such as curcumin, paclitaxel, etc. have been packaged using such dissociation methods[180].

Because of its ability to traffic across the blood brain barrier (BBB), via receptors such as Tim1 and TfR, ferritin could prove effective in carrying drugs across the BBB to treat various neurological diseases. Treatment of many of the diseases of the brain is challenged by permeability of drugs across the BBB. In fact, it is well known that only 2% of the pharmaceutical compounds can cross the BBB. In highly aggressive brain tumors such as neuroblastoma or glioblastoma, ferritin thus, represents newer opportunities to explore. As an example, Huang et al. had recently shown a 2- fold increase in mice glioma tumor targeting capability, after crossing BBB, of H ferritin nanocarriers packed with doxorubicin. The H-ferritin carriers in the study were genetically modified to carry a surface peptide that targets α2β1 integrins[190]. In another study, by Chen et al., ferritin packed with doxorubicin was shown to reliably cross the BBB and increase survival period of mice treated with the doxorubicin in H-ferritin nanocarrier (30 days) as compared to doxorubicin alone (19 days)[191]. These examples highlight the potential of using ferritin to package drugs for brain related ailments including lethal glioblastomas. As mentioned, our studies have demonstrated FTH11 binding to GBMs and uptake into orthotopic animal models[192]. In further support of the potential to use FTH1 delivery to the brain in non-tumor diseases, we have demonstrated that FTH1 is taken up into the brain in normal mice where the uptake patterns are influenced by both age and sex[193]. Thus, the data strongly support the exploration of ferritin as a mechanism for therapeutic interventions strategies for the brain.

Apart from chemotherapeutics ferritin is being studied for carrying nucleic acids as well. Because of the labile nature of siRNA its delivery in the in vivo systems has been hampered. Ferritin encapsulated delivery of siRNA not only protects it from extracellular nuclease degradation but also from scavenging activity of immune cells. Ongoing efforts for using naïve and modified ferritins for siRNA delivery are proving to be successful in many different cancers. For example, a study by Li et al., has shown that siRNA against insulin receptor (anti-InsR) can be easily packaged in ferritin via a pH modulated disassembly-reassembly method. Anti-InsR-ferritin complexes were then shown to transfect human colon adenocarcinoma cell line, Caco-2, with high efficiency[194]. Recently, Yuan et al. have developed genetically modified H-ferritin carriers containing cationic inner surface. Arginine mutations in the inner surface of the protein presented robust electrostatic forces that enhanced the siRNA encapsulation efficacy of the nanoparticle[195]. Chemical modifications of the inner surface by chemoselective conjugation of cationic piperazine-based compounds have also been proven to be highly efficient in encapsulation and delivery of siRNA to cancer cells[196]. Ferritin is thus emerging as a nanocarrier of choice for nucleic acids.

Use of ferritin nanocarriers is not limited to carrying chemotherapeutics, and anti-tumor siRNAs. Ferritin nanocarriers have been developed for various imaging methods such as computer tomography (CT), magnetic resonance imaging MRI, and near-infrared fluorescence (NIRF) imaging. For example, Zhao et al., developed magnetoferritin probes loaded with iron oxide in 125I radionuclide- surface modified ferritin for multimodal imaging in tumors of living mice[197]. In another example, gadolinium-loaded ferritin was developed to image endothelial cells in tumors by contrast MRI[198]. Ferritins loaded and/or conjugated with fluorophores are not only being studied for advanced diagnostic imaging but for image-guided surgery of cancers as well. For example, indocyanine loaded (ICG) loaded ferritin was shown to trace cancer cells in a preclinical model of breast cancer. Since ICG is already used in the clinics for lymph node mapping and NIR fluorescence image-guided surgery (FGS), its encapsulation in the ferritin increases its potential to be used in FGS in cancers[199]. As mentioned previously, ferritin is highly versatile, and that can be seen in the study by Lin et al. in which they developed a hybrid ferritin nanoparticle that is activated in presence of tumor matrix metalloproteinases (MMPs). These hybrid nanoparticles are developed by generating two different ferritin peptides, one that is conjugated with infrared activated Cy5.5 fluorophore and a second type that has a black hole quencher (BHQ-3) conjugation. Upon encountering the tumor MMPs the quencher molecule is released, and the fluorophore fluoresces in presence of NIRF[200].

Ferritin carrying ICG has been explored in cancer photothermal therapy (PTT) as well. ICG is a, FDA approved photothermal agent that can absorb near-infrared light and convert it into heat. This high then induces apoptosis a characteristic that can prove crucial in cancer therapy[201]. ICG derivative, IR820, packaged in ferritin was shown to achieve 100% tumor elimination, without any evident non-specific toxicity, in subcutaneous mice model of breast cancer[202]. Combination of PTT with chemotherapy is another tool that has drawn interest in cancer therapy. A very interesting example of this comes from a recent study by Lin et al. They developed grenade-like nanoparticles, covered in NIR dye, that upon laser irradiation burst open into smaller cluster warheads which are basically ferritin nanocages carrying doxorubicin. Release of doxorubicin from these nanoparticles is further controlled by low pH found in tumors and within the acidic compartments of tumor cells[203]. Use of ferritin as a carrier for hydrophobic photosensitizers is also gaining traction for photodynamic cancer therapy (PDT). Photosensitizers generate ROS, in the presence of oxygen, when activated by specific light. High amounts of ROS can kill tumor cells, destroy tumor vasculature and/or activate the immune system to kill tumor cells[180180].

A surprising use of ferritin nanocarrier came from a study, in 2006, when Li et al. first reported HIV1 Tat antigen functionalization on the outer surface of ferritin. Since then, several studies have shown ferritin nanoparticle use in antigen/vaccine delivery. A more comprehensive review on the vaccine

development using ferritin nanoparticle can be found in the review by Rodrigues et al[204]. More recently, there have been numerous studies that have shown ferritin nanoparticles carrying SARS-CoV-2/COVID-19 vaccine to induce robust innate immune activity in hosts[205–209]. One of these SARS-CoV-2- vaccines, by Joyce et al., is active in phase I clinical trial (ClinicalTrials.gov ID NCT04784767). Besides SARS-CoV-2, ferritin nanoparticle based vaccines against Influenza and Epstein Barr Virus have also moved to phase I clinical trials (ClinicalTrials.gov ID NCT04579250 and NCT04645147). Combining drug resistance and ferroptosis in ferritin delivery, iron saturated ferritin nanoparticles carrying doxorubicin were recently shown to activate ferroptotic cell death in leukemia, CRC, breast, liver, cervical, and lung cancer cells[210].

1.7 Conclusions

Ferritin is a protein that wears multiple hats when it comes to cancers and other potential medical uses. While it performs its classical role of storing iron and protecting DNA inside the nucleus quite efficiently, ferritin's role as a tumor suppressor or an oncogene, depending on the type of cancer, presents it as a potential target for cancer therapy. Cell-cell communication via exosomes in the tumor microenvironment is also a recent novel concept for ferritin. One of the most beneficial roles of ferritin is emerging in its use as a biological nanocarrier for delivering chemotherapeutics. The current state of the art of the scientific interrogation into the versatility of ferritin is likely just the tip of the iceberg when it comes to understanding the role of this unique protein in cancer and its dynamic roles in both a target and trojan horse for treating cancers.

Chapter 2: Uptake of H-ferritin by Glioblastoma stem cells and its impact on their invasion capacity

This work has been previously submitted as:
Bhavyata (Pandya) Shesh, Becky Slagle-Webb, Ganesh Shenoy, Vladimir Khristov, Brad E. Zacharia, James R. Connor, Uptake of H-ferritin by Glioblastoma stem cells and its impact on their invasion capacity, Journal of Cancer Research and Clinical Oncology, 2023

2.1 Abstract

Purpose: Iron acquisition is key to maintaining cell survival and function. Cancer cells in general are considered to have an insatiable iron need. Iron delivery via the transferrin/transferrin receptor pathway has been the canonical iron uptake mechanism. Recently, however, our laboratory and others have explored the ability of ferritin, particularly the H-subunit, to deliver iron to a variety of cell types. Here we investigate whether Glioblastoma (GBM) initiating cells (GICs), a small population of stem-like cells, known for their iron addiction and invasive nature acquire exogenous ferritin, as a source of iron. We further assess the functional impact of ferritin uptake on the invasion capacity of the GICs. **Methods:** To establish that H-ferritin can bind to human GBM tissue binding assays were performed on samples collected at the time of surgery. To interrogate the functional consequences of H-ferritin uptake, we utilized two patient-derived GIC lines. We further describe H-ferritin's impact on GIC invasion capacity using a 3D invasion assay. **Results:** H-ferritin bound to human GBM tissue at the amount of binding was influenced by sex. GIC lines showed uptake of H-ferritin protein via transferrin receptor. FTH1 uptake correlated with a significant decrease in the invasion capacity of the cells. H-ferritin uptake was associated with a significant decrease in the invasion related protein Rap1A. **Conclusion:** These findings indicate that extracellular H-ferritin participates in iron acquisition to GBMs and patient-derived GICs. The functional significance of the increased iron delivery by H-ferritin is a decreased invasion capacity of GICs potentially via reduction of Rap1A protein levels.

2.2 Introduction

Glioblastoma (GBM) is both the most common and almost always fatal primary brain malignancy with a median overall survival of only 15 months [211]. Multiple challenges, including the highly invasive nature [212], presence of tumor heterogeneity [213], and presence of glioblastoma initiating cells (GICs) [214], burden the treatment course and almost guarantee treatment failure and recurrence [215]. GICs are a subgroup of cancer cells that exhibit stem-like properties of self-renewal and express putative cell markers such as CD133, CD15, CD44, LICAM [214]. Some of the hallmarks of GICs are high tumorigenic potential in vivo [216], increased capacity for angiogenesis [217,218], elevated invasive potential [219,220], and immune system evasion [221,222]. Given the essential role GICs play in GBM treatment challenges it is crucial we further dissect and characterize these cells to ultimately lead to the development of better targeting strategies for treatments.

Iron is an essential element required for cellular growth and function and cancer cells are particularly noted to be "iron addicted" [223,224]. The iron addicted phenotype of cancer cells pertains to increased expression of iron uptake genes and abnormal expression of iron-regulating genes supporting cell growth. One of the ways cells can acquire iron is via the uptake of extracellular ferritin protein [28]. Ferritin, a canonical cytoplasmic iron storage protein, has also been shown to bind specifically and saturably, to deliver iron, to multiple cell types including erythroid precursors, lymphocytes, and brain oligodendrocytes [11,26,30]. Additionally, this binding and subsequent uptake of the extracellular ferritin in most cell types has been observed by the ferritin composed primarily of H-ferritin (FTH1) subunits rather than L-ferritin (Lft) subunits [28]. Well-studied cell surface receptors for FTH1 uptake include T Cell Immunoglobulin Mucin 2 (Tim-2) on rat oligodendrocytes [31], Tim-1 (Tim-2 is not found in humans) on human oligodendrocytes [29], and Transferrin receptor (TFR1) on mitogen-activated lymphocytes and circulating reticulocytes [28]. Some cancer cells have also been shown to uptake ferritin composed of FTH1 subunits. For example, FTH1 was shown to be taken up and subsequently promote proliferation in breast cancer and hepatocellular carcinoma cells [103,225]. However, whether GBM cells uptake FTH1, for their various cellular needs, is not known. Moreover, understanding the mechanisms of uptake and downstream functional impact could further our understanding of 'iron addicted' GBM's iron acquisition strategies and exploit them for drug targeting.

In the studies presented here we show that FTH1 binds to human GBM male and female tissues. We further characterize the uptake of FTH1 by GICs and demonstrate its impact on their cell invasion capacity in two patient derived GIC lines. We show that GICs uptake FTH1 potentially via TFR1

receptor. We find that FTH1 significantly reduces the cell invasion capacity of the GICs but has no significant impact on the proliferation capacity. Moreover, inhibition of cell invasion capacity is also accompanied by a decrease in Rap1A protein expression. Rap1A is a member of the RAS oncogene family and has been previously implicated in enhancing invasion capacity of GICs [226]. Our bioinformatic analysis on the Rap1A gene further predicted the presence of a non-canonical iron responsive element (IRE) in all 6 transcripts of this gene, suggesting that increased intracellular iron levels due to FTH1 uptake might play a role in regulating the invasion capacity of GICs via directly modulating the invasion related genes such as Rap1A.

Our findings describe the role of extracellular ferritin in GBM cell biology, its mechanism of uptake, and its functional effect on cell invasion. Considering that GBM cells from patient tumors have high expression of TFR along with a high infiltrating population of macrophages, that could secrete iron rich H-ferritin in the tumor microenvironment [101,227] (potentially making H-ferritin available for tumor cells), make our observations highly relevant from a clinical standpoint. Our findings warrant further studies to evaluate the role of extracellular ferritin on clinical patient survival outcomes in glioblastoma.

2.3 Materials and Methods

2.3.1 Cell culture

T387 and T3691 are xenograft derived (PDX) CD133+ GICs generated from primary tumor tissues of GBM patients (Catalog numbers of materials are provided in supplementary materials and methods). The cell lines were a gift from Dr. Jeremy Rich at University of California, San Diego and were generated as previously described [116]. PDX GICs were cultured as neurospheres in Neurobasal™ medium without phenol red (Gibco) supplemented with 2% B27 without vitamin A (Gibco), 1% sodium pyruvate (Gibco), 1% GlutaMax™ (Gibco) and 20 ng/mL of recombinant human epidermal growth factor and 4 ng/mL of fibroblast growth factor (R & D systems) at 37°C and 5% CO_2.

2.3.2 Preparation of protein and fluorophore conjugation

Recombinant FTH1 was isolated from Escherichia coli (E.coli) as previously described [24,31,228] and conjugated with Atto 647N NHS ester dye (Sigma) following manufacturer's protocol. The iron content of the protein was approximately 110ng/mL Fe per mg of protein as measured by

ThermoFisher iCAP 7400, Inductively Coupled Plasma Emission Spectrometry (ICP-AES). A brief description of the protocol can be found in the supplementary information.

2.3.3 FTH1 binding on human GBM membranes

Human GBM tissues (Males n = 6, Females n = 6) were obtained from the Penn State Hershey Neuroscience Institute Biorepository under institutional review board protocol (IRB #2914, approved). We adapted the binding assay protocol as described previously [229]. Briefly, male, and female tissues were minced and homogenized in 0.3M sucrose (VWR Chemicals). Debris removal from the homogenate was carried via a centrifugation spin at 800 x g for 20 minutes followed by second spin at 120,000 x g for 1 hour. Resulting pellets were re-suspended in 0.05 M potassium phosphate buffer (pH 7.4) supplemented with 10% glycerol (Fisher-Scientific) to isolate plasma membrane extracts. Radiolabeled Iodine, ^{125}I (Sigma-Aldrich), tagged H-ferritin was then added to 20 µg of plasma membrane extract, for 1 hour at room temperature, in a 96-well filter plate (Millipore-Sigma). The reaction was then terminated by the addition of ice-cold PBS. Finally, the mixture was vacuum filtered using 0.2 µm hydrophilic membranes and then washed three times with ice-cold PBS to remove unbound radiolabeled transferrin and H-ferritin. Radioactivity in the filters was then quantified using a Beckman Gamma 4000 Analyzer. Methodology of radiolabeling the protein is provided in the Supplementary Information.

2.3.4 Fluorescent protein uptake

Uptake of the fluorophore conjugated proteins was performed as previously described [28,29.] Briefly, 8-well chamber slides (ThermoFisher) were coated with Geltrex™ (1.6 µl/mL) (ThermoFisher Scientific) for 1h after which $5x10^4$ cells/mL were plated, in each well, for 24h. Next, 50 µg/mL FTH1-Atto 647, and 50 µg/mL Transferrin (TF)-Alexa 488 were added to the plated cells and incubated for 1h and 4 h at 37°C. Next, cells were washed thrice with 1x DPBS and fixed with 4% paraformaldehyde. Finally, fixed cells were washed thrice with 1x DPBS, mounted with mountant containing DAPI (ThermoFisher Scientific) and visualized on a confocal microscope (Leica).

2.3.5 Labile iron pool measurements

Labile iron pool (LIP) of the cells was assessed using FerroFarRed ™ (Sigma) following manufacturer's protocol. Briefly, $2x10^5$ cells were plated in 6 well plates and allowed to adhere overnight. Cells were then treated with 50-300 µg/mL FTH1 or TF proteins for 24 h. Next, cells were washed with serum-free media and incubated with 5 µM FerroFarRed in serum-free media for 1h at 37°C. Cells were then lifted using StemPro™ Accutase™ (ThermoFisher Scientific) and washed thrice with double the volume of 1x

DPBS to remove the unbound fluorophore.

Cells were finally resuspended in flow cytometry staining buffer and assessed on flow cytometer (BD Symphony, BD Biosciences). Allophycocyanin (APC) filter was used to collect ten thousand events.

2.3.6 Receptor blocking

Receptor mediated endocytosis was blocked using Chlorpromazine (CPZ) (Sigma) at 50 µM as described previously [230]. Briefly, $8x10^4$ cells were plated and allowed to adhere overnight. Cells were then gently washed with 1x DPBs and CPZ added for 1h at 37°C. FTH1-Atto 647N and TF-Alexa 488 were then added to the wells at 50 µg/mL concentration and allowed to incubate for 4h at 37°C. Next, cells were washed, fixed, mounted and visualized as described in the fluorescent protein uptake protocol described above. Individual TFR1 or Tim-1 receptors were blocked using anti-TFR1 (25µg/ml), Tim-1 (25µg/ml), or IgG (25µg/ml) blocking antibodies. Antibody blocking was performed for 2h at 37°C. Post blocking, the cells were incubated with FTH1-Atto 647N and TF-Alexa 488 at 50 µg/mL for 4h at 37°C. After incubation cells were washed, fixed, mounted and visualized as described in the fluorescent protein uptake protocol described above.

2.3.7 Proliferation assay

To determine cell viability of the cells, alamarBlue™ cell viability reagent (Thermo Fisher) was used according to manufacturer guidelines. Briefly, around $1x10^4$ cells were plated and allowed to adhere for 24h. Next, cells were treated with FTH1 for 24, 48, and 72h at 37°C. FTH1 treated cells were then incubated with Alamar Blue reagent for 4h at 37°C. Fluorescence was measured with excitation wavelength at 560 nm and emission wavelength at 590 nm via SpectraMax Gemini EM plate reader (Molecular Devices).

2.3.8 3D spheroid invasion assay

IncuCyte® S3 3D Spheroid Invasion Assay was followed as per the manufacturer's protocol. Briefly, 3000 cells were added to Nunc™ 96-well, U-bottom plates and allowed to form spheres for 72h. Spheroids were then treated with FTH1 (10 µL/well) at 20x final assay concentration. The spheroids were then layered with Geltrex™ (90 µL/well) at 50% final assay concentration. Polymerization of the gel matrix was allowed at 37ºC for 30 minutes. The spheroids were then monitored for 72h on Incucyte® Live-Cell imaging system to assess and invasion capacity of the cells.

2.3.9 Spheroid formation assay

Spheroid formation assay was performed as described previously [231]. Briefly, 1000 cells/well were added to Nunc™ 96-well, U-bottom plates along with the different concentrations of the recombinant FTH1. Spheroid formation was evaluated at 72h, and images captured on Echo revolve light microscope (Discover Echo Inc., CA). Spheroid sizes were analyzed using ImageJ software.

2.3.10 Immunoblotting

Immunoblotting was carried out as previously described [114]. Briefly, cells, pre-treated with FTH1, were lysed in RIPA buffer with protease inhibitors. 10–20 μg of total protein was run on 4–20% TGX gradient SDS gel (BioRad). Proteins transferred on nitrocellulose membrane were then probed with Rap1A antibody (Cell Signaling, 1:1000) and β-actin (Sigma-Aldrich, 1:5000). Corresponding secondary antibodies conjugated to HRP were added (1:5000, GE Amersham) to visualize bands on an Amersham Imager 600 (GE Amersham). Densitometry was performed using Image studio lite v5.2 (Licor). Expression levels were normalized to β-actin.

2.3.11 Statistical and image analysis

Statistical analyses were performed using GraphPad Prism 9.5 (GraphPad Software Inc., San Diego, CA). Microscopy image analysis was performed using CellProfiler 4.2 application. Bioinformatic analysis was performed using the SIRE (searching for Iron Responsive Elements bioinformatic) webtool. TCGA_GBM database was accessed from Gliovis on 25 January 2023 for Rap1A survival and expression analysis.

2.4 Results

2.4.1 Human GBM membranes bind to exogenous H-ferritin

To demonstrate that FTH1 is a component of the iron acquisition system in GBMs, we investigated if exogenous FTH1 binds to human GBM tissues by performing a radiolabeled protein binding assay on the male and female human GBM membranes. Information on patient sex, age, and genetic mutations can be found in Supplementary Table S1. We found that both male and female tumor tissues bind to FTH1. Interestingly there is a sex-effect with a significantly increased binding on male tumor tissues as compared to females (Fig. 2-1).

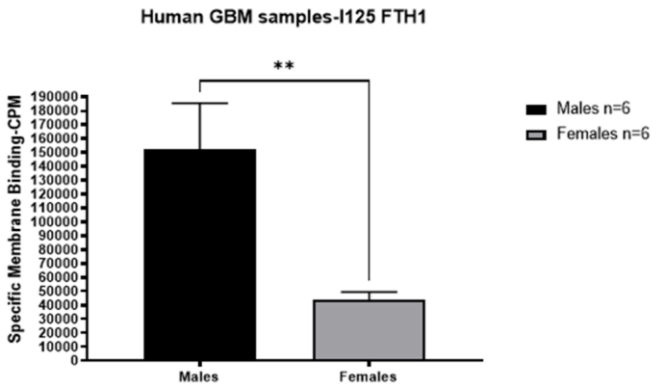

Fig. 2-1 H-ferritin binding on human GBM tissues Binding of ^{125}I-tagged FTH1 to extracted plasma membrane fractions from homogenized human glioblastoma tumors (n = 6 male, n = 6 female). Male tumors had significantly higher binding of radiolabeled FTH1 as compared to female tumors. The data were analyzed for statistical significance by unpaired T-test between the two groups and the differences were found to be significant. *: $p < 0.05$, **: $p < 0.01$, ***: $p < 0.001$, ****: $p < 0.0001$

2.4.2 FTH1 uptake in GICs in cell culture

To investigate if GICs take up FTH1 we incubated them with fluorophore conjugated FTH1 (red fluorophore, Atto 647N) and green fluorophore conjugated TF (Alexa 488) (Fig.2-2 a, b). Since uptake of TF by cells is very well documented [28] it was used as a positive control for studying FTH1 uptake. The uptake was observed on a scanning confocal microscope. We observed that TF uptake occurred within 1h of incubation while FTH1 uptake was not measurable until 4h in T387 and T3691 cells. To confirm the delivery of iron from FTH1 we used FerroFarRed iron probe to measure the LIP within the cells (Fig.2-2 c, d). We found that GBM cells treated with FTH1 had increased LIP, as compared to the cells not treated with FTH1, confirming iron delivery by FTH1 protein inside the cells.

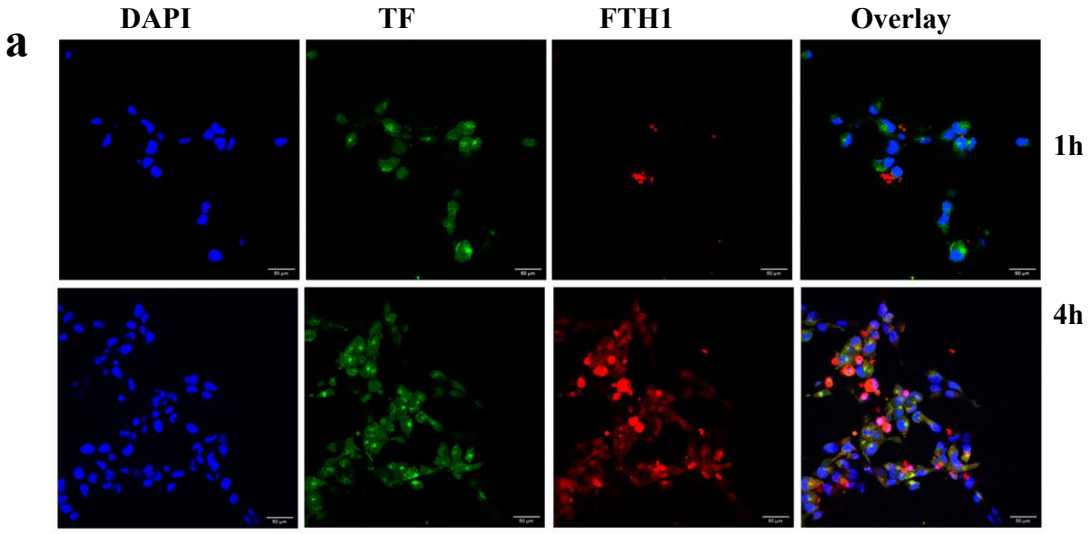
a
DAPI
TF
FTH1
Overlay
1h
4h

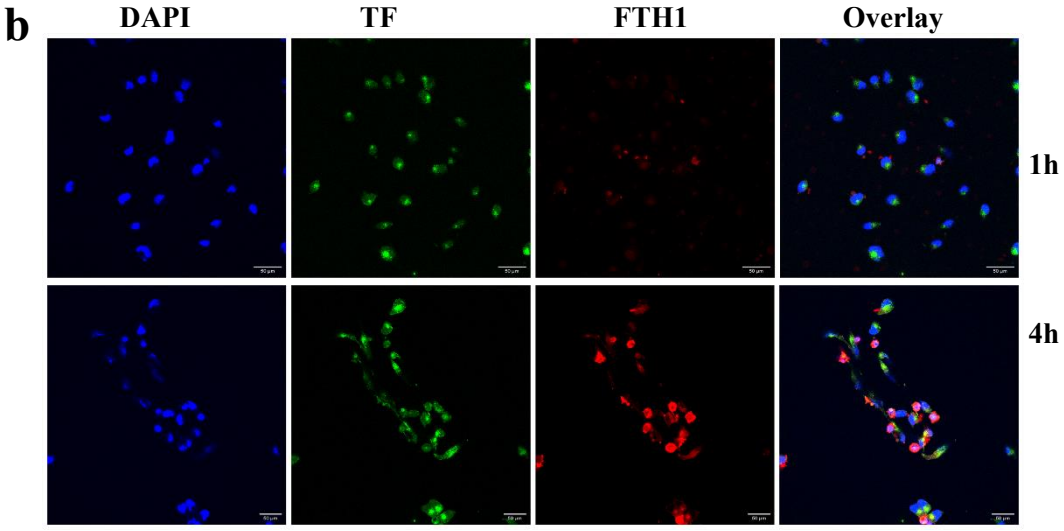
b
DAPI
TF
FTH1
Overlay
1h
4h

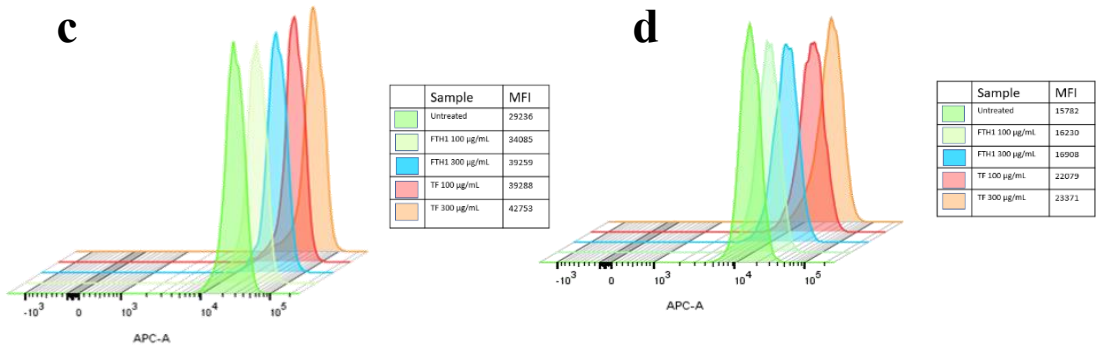

Fig. 2-2 GICs uptake exogenous H-ferritin GICs (a) T387 and (b) T3691 were plated in chamber slides and incubated with 50 µg/mL FTH1-Atto 647N (red) and 50 µg/mL Tf-Alexa488 (green) for 1h and 4h at 37°C. DAPI (blue) was used to stain the nuclei. Overlay images show all the three channels. All images were taken at 63X magnification. Labile iron pool in (c) T387 and (d) T3691 was measured using Ferrofarred probe. Cells were incubated with 0- 300 µg/mL of FTH1 or Tf for 24 hours at 37°C. FerroFarRed, which binds to Fe^{2+} labile iron ions, was added at 5µM for 1 hour at 37°C. Cells without FTH1 or Tf treatment were used as control. Images are brightened for publication purposes. Fluorescence from FerroFarRed was measured on APC filter on the BD symphony flow cytometer. MFI = Median Fluorescence Intensity from 10,000 cells analyzed per experiment. Scale bar = 50 µm

2.4.3 GICs uptake exogenous H-ferritin via TFR1

To study if the uptake of FTH1 is mediated by receptor mediated endocytosis we used CPZ to block receptor mediated endocytosis of the cells and subsequently incubated the cells with FTH1-Atto 647N. We then studied the uptake of FTH1-Atto 647N (Fig. 2-3 a, b) under the confocal microscope. FTH1-Atto 647N uptake was reduced in the T387 and T3691 that were treated with CPZ as compared to the untreated cells suggesting that FTH1 uptake is mediated by receptor mediated endocytosis. A reduction in uptake of TF-Alexa488, which is known to be taken up via receptor mediated endocytosis, confirmed the CPZ mediated blocking of the receptor mediated endocytosis process. To identify if Tim-1 or TFR1 is the receptor for FTH1 uptake we blocked these receptors using respective receptor blocking antibodies. We observed that TFR1 blocking reduced the uptake of FTH1 and TF proteins in T387 and T3691 cells whereas Tim-1 receptor blocking had no effect on the uptake of FTH1 and TF proteins (Fig.2-3 c, d). This suggests that TFR1 is the potential and predominant receptor for FTH1 uptake in these GBM cells.

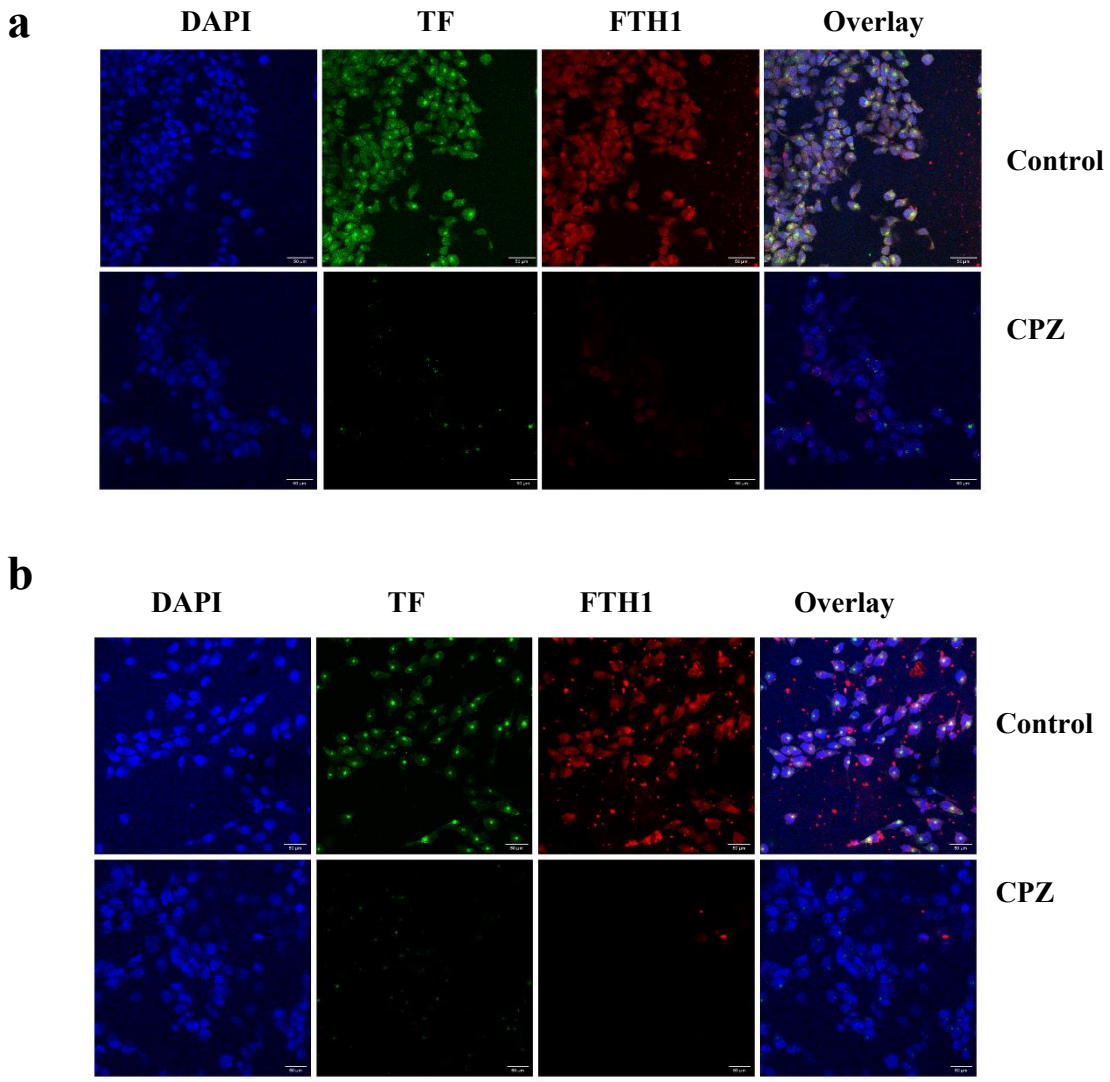

Fig. 2-3 (a, b) GICs uptake exogenous H-ferritin via TfR1 Chlorpromazine hydrochloride (CPZ) was used at 50 µM concentration to block receptor mediated endocytosis in (a) T387 and (b) T3691 cells. Following CPZ incubation for 1h at 37°C, 50 µg/mL FTH1-Atto 647N (red) and 50 µg/mL Tf-Alexa488 (green) were added and allowed to incubate for 4h at 37°C. DAPI (blue) was used to stain the nuclei. Reduced uptake of FTH1 in presence of CPZ, as compared to without CPZ, indicates that it is taken up by receptor mediated endocytosis pathway. Cells without CPZ treatment were used as control. Scale bar = 50 µm

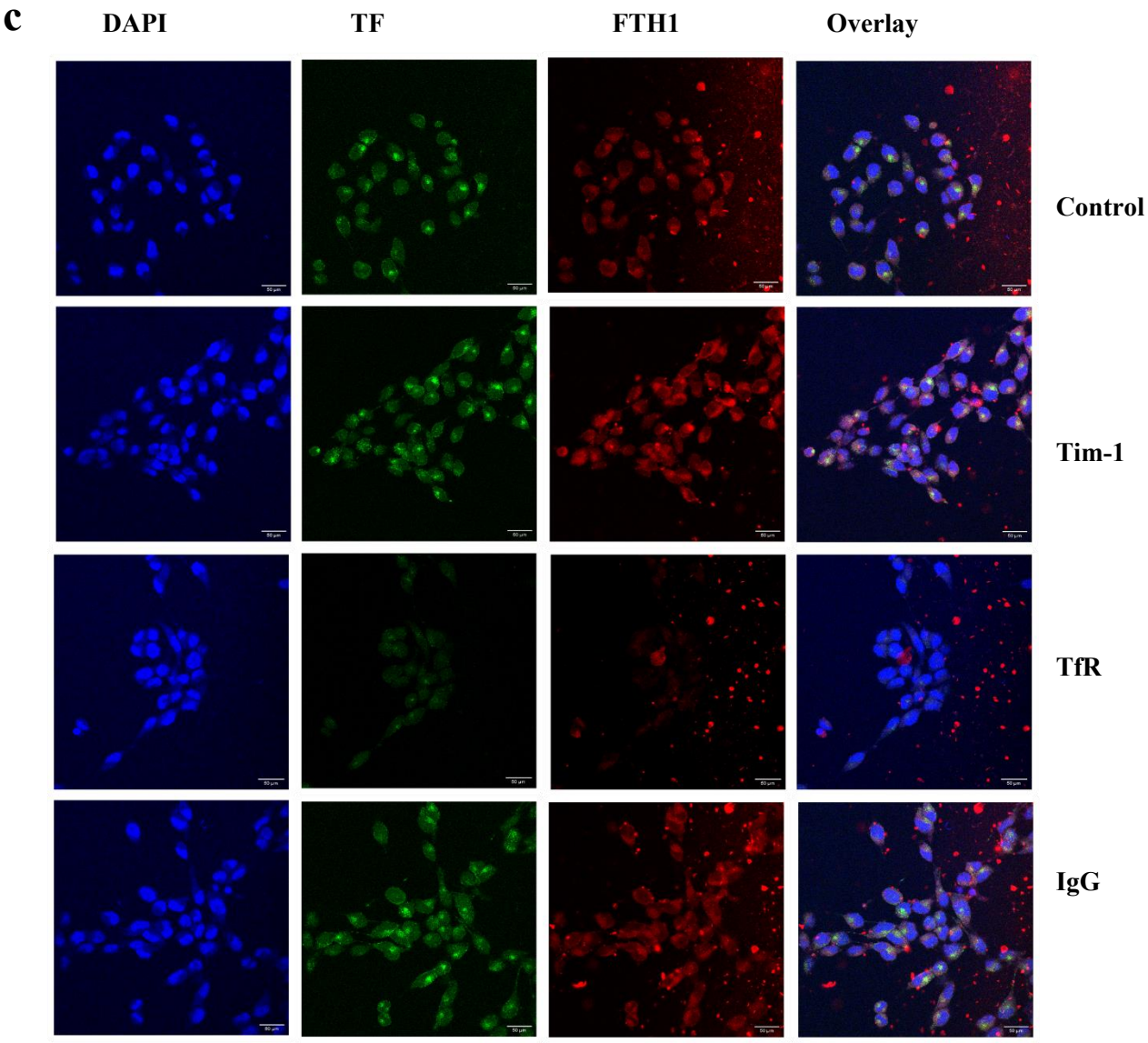
c
DAPI
TF
FTH1
Overlay
Control
Tim-1
TfR
IgG

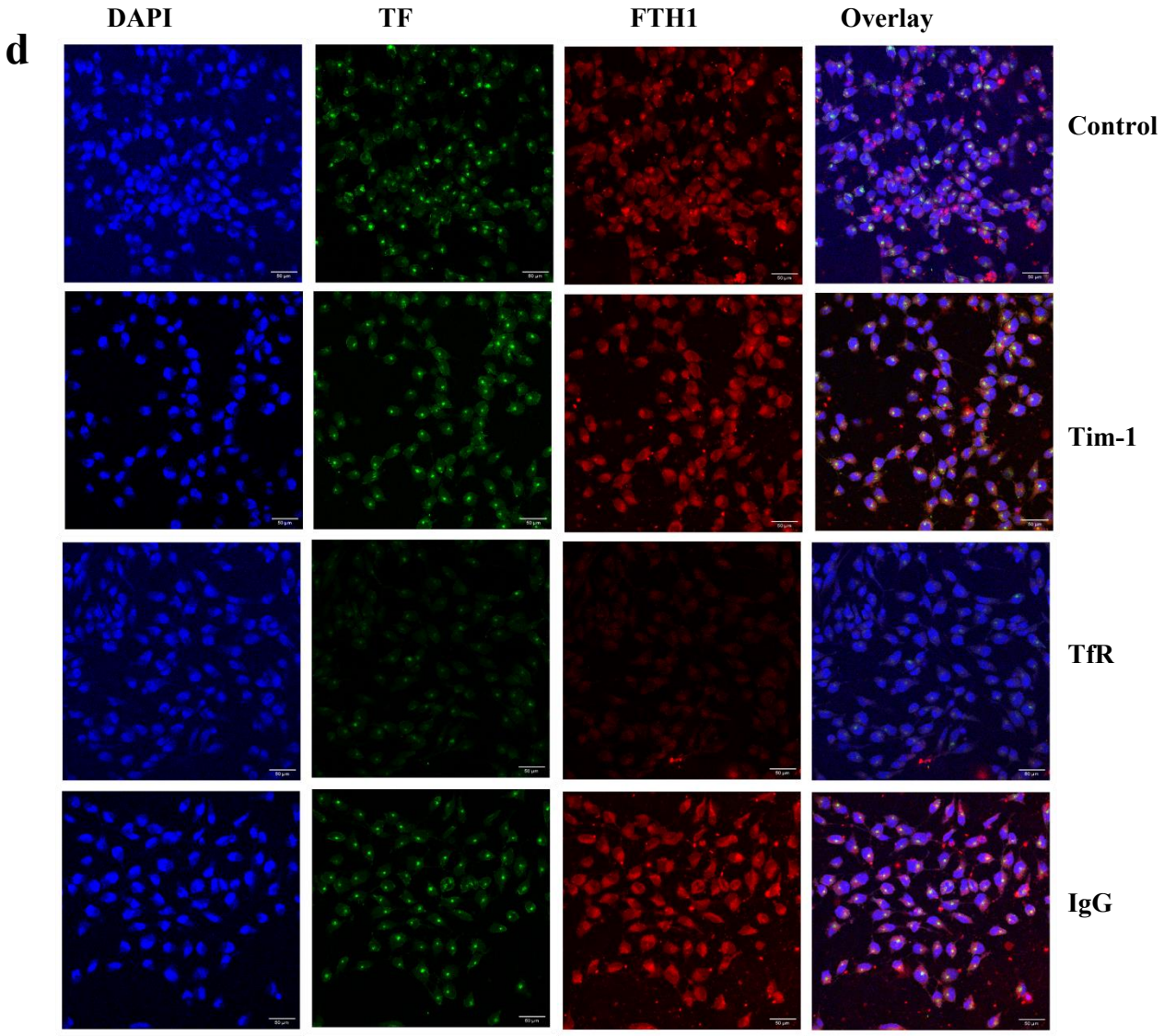

Fig. 2-3 (c, d) GICs uptake exogenous H-ferritin via TfR1 TfR1 and Tim-1 receptors were blocked using respective antibodies and uptake was studied in (b) T387 and (d) T3691 cells. IgG antibody was used as an internal antibody control and cells not treated with any antibody were used as experiment control. Following antibody incubation, 50 µg/mL FTH1-Atto 647N (red) and 50 µg/mL Tf-Alexa488 (green) were added. DAPI (blue) was used to stain the nuclei. Reduced uptake of FTH1 in presence of anti-TfR1 antibody, as compared to anti-Tim-1, indicates that it is taken up via TfR1 mediated endocytosis pathway. Overlay images show all the three channels. All images were taken at 63X magnification. Images are brightened equally for publication purposes. Scale bar = 50 µm

2.4.4 H-ferritin uptake associated with reduced invasion capacity of GICs

To investigate the functional consequences of the FTH1 uptake we investigated the invasion capacity of the cells in a 3D invasion assay using Incucyte® live-cell imaging system. Spheroid size was quantified as a function of time to assess invasive capacity of the cells. We found that FTH1 significantly reduced the invasion capacity of both T387 and T3691 cells in a concentration-dependent manner (Fig. 2-4 a, b). Next, we studied the proliferation of the cells to rule out confounding effects of proliferation on the invasion assay results. We observed that FTH1 uptake did not significantly affect the proliferation capacity of the T387 and T3691 cells as investigated using Alamar blue assay (Supplementary Fig. S1 a, b). We further evaluated compact spheroid formation capacity of GICs. FTH1 reduced spheroid formation capacity of T387 and T3691 cells. Spheroid sizes were quantitated, and sizes are inversely proportional to compact spheroid forming capacity (Fig. 2-4 c- f).

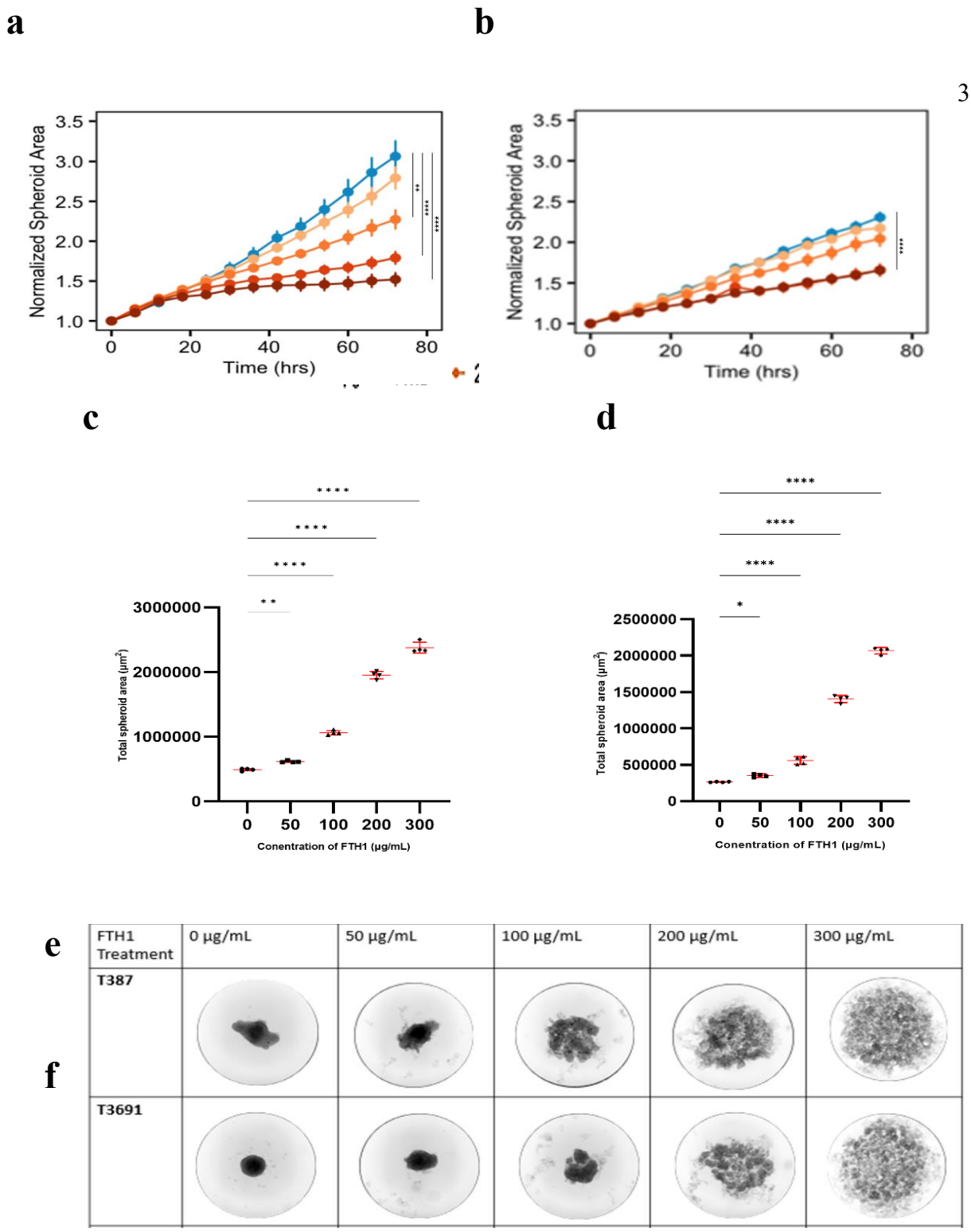

Fig. 2-4 H-ferritin uptake is associated with reduced invasion capacity of GICs. In Panel (a) T387 and (b) T3691, tumor spheroids were prepared from GBM cells. After 72 hours the spheres were embedded in Geltrex® ECM and exposed to various concentrations of recombinant FTH1 for an additional 72 hours. The cells showed a dose dependent decreased invasion capacity (decreasing spheroid size). An additional spheroid formation assay was

used (Panels c-f). In this assay both the cell lines were plated in the presence of different concentrations of FTH1 for 72 hours following which images were taken (e and f). The results are shown in graphical form in Panels c and d. There was a dose dependent reduction in compact spheroid formation in the presence of FTH1. The spheroid area was quantified using the spheroid formation assay at 72 hours for (c) T387 and (d) T3691 cells. Spheroid area is inversely related to compact spheroid formation capacity. The representative images of spheroids show reduction in formation of compact spheroid in presence of increased concentration of FTH1. Cells at lower FTH1 concentration form a compact spheroid while at higher concentrations of FTH1 the cells do not form a compact spheroid and remain as cell assemblage at the bottom of the well. Although the relationship between spheroid area and invasion capacity, and spheroid area and spheroid formation capacity are contrasting, these assays are complementary because some of the forces that are required for cell invasion are the same forces that allow cells to come together to form a compact spheroid. Hence, if FTH1 is reducing invasion capacity it must also reduce spheroid formation capacity and that is what we observed in our results. *: $p < 0.05$, **: $p < 0.01$, ***: $p < 0.001$, ****: $p < 0.0001$, one-way ANOVA with Tukey HSD

2.4.5 H-ferritin incubation associated with reduced expression of Rap1A in GICs

Next, we investigated the expression levels of Rap1A protein that has been previously identified as a protein enhancing invasion capacity of T387 and T3691 cells [226]. We observed that FTH1 incubation was significantly associated with a reduction in Rap1A protein (Fig. 2-5 a, b). Our analysis of gene expression from the sequenced patient GBM tumor tissues from TCGA database revealed that GBM tissues have higher expression of Rap1A (Supplementary Fig. S2 a) and higher expressions of Rap1A are significantly associated with reduced survival (Supplementary Fig. S2 b). To further understand how FTH1 might be regulating Rap1A levels we investigated if Rap1A mRNA has any IRE sequences (Fig. 2-5 c). We used SIRE to predict the presence of IRE in Rap1A mRNA. We found that all 6 transcripts of the Rap1A mRNA possess a non-canonical IRE, motif 18, on its 3' UTR. While the transcripts of Rap1A mRNA have a predicted IRE it remains to be determined if it is functional in-vitro and in-vivo, but our data indicate that the expression of Rap1A is responsive to FTH1 uptake by the cells.

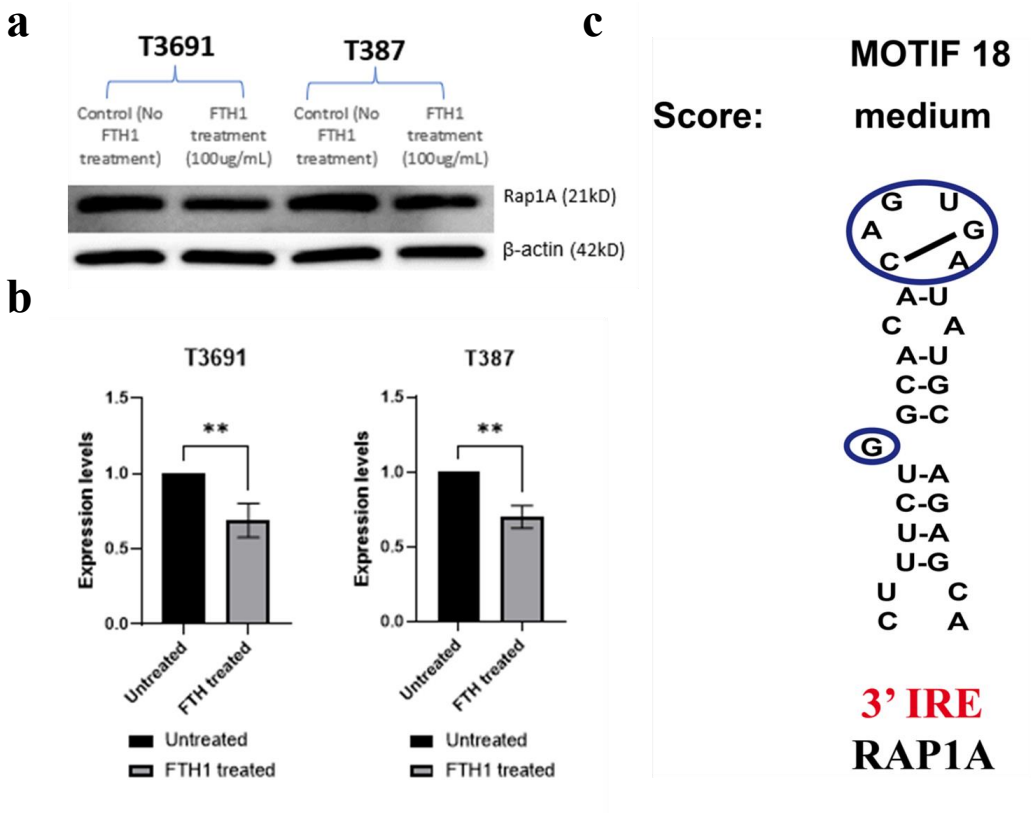

Fig. 2-5 H-ferritin incubation is associated with reduced expression of Rap1A in GICs (a) T3691 and T387 GICs were treated with 100 µg/mL FTH1 for 72h and protein expression of Rap1A was measured by immunoblotting (representative blot from triplicates). (b) Quantification of the immunoblotting experiments showed that Rap1A expression was significantly decreased in the FTH1 treated cells. Rap1A expression normalized with β-actin protein levels. Student's two-tailed t-test: *: $p < 0.05$, **: $p < 0.01$. (c) Searching for Iron Responsive Elements (SIREs) was used to identify potential iron-responsive element sequence on the 3' UTR of Rap1A mRNA transcripts. A characteristic hairpin loop and a stem structure of IRE, motif 18, sequence was identified. A UGG bulge typical of ferritin IRE sequence can also be seen in the stem of the stem-loop structure

2.5 Discussion

Intracellular ferritin levels have been shown to impact cancer cell biology by regulating proliferation, apoptosis, EMT, angiogenesis and therapeutic resistance. However, the role of extracellular ferritin in pathophysiology of GBMs has received limited study. Here we describe the uptake of exogenous/extracellular H-Ferritin protein by patient derived GICs and interrogate the functional impact on invasion capacity of the cells.

The results presented here show that exogenous FTH1 is taken up by the T387 and T3691 patient derived GICs in a receptor mediated mechanism. We further identified if FTH1 uptake occurs via Tim-1 or TFR1 receptors. Our observations of reduction in uptake of FTH1 in presence of TFR1 blocking antibodies suggest that TFR1 is the potential receptor mediating the uptake of exogenous FTH1 in T387 and T3691 cells. This finding is in agreement with previous reports that FTH1 is endocytosed, via TFR1 or Tim-1 (Tim-2 in rats) receptors (Han et al., 2011; Li et al., 2010; Todorich et al., 2011). Moreover, based on the reports that cytoplasmic ferritin enters the lysosomal compartment of the cell and replenishes the LIP by release of its iron following its degradation [232], we hypothesized that if FTH1 is taken up by the cells it should increase the LIP within the cells. Indeed, we observed an increase in LIP of T387 and T3691 cells post incubation with FTH1. These results are pertinent clinically as GBM tumors have been shown to have increased iron demands and increased expression of TFR which is correlated with poor prognosis [233,234]. Thus, our studies have demonstrated a significant and heretofore unexplored mechanism by which GBMs can obtain iron. Our binding data on the human tissues further provides evidence for clinical relevance of our observations, and even highlight sex-specificity. Because tumor cells increase iron uptake to support multiple different cellular functions such as stemness maintenance, drug resistance and metabolism, DNA synthesis and repair, cellular proliferation, invasion, and migration [235], higher binding of FTH1 on male tumor membranes suggests higher demand for iron potentially reflecting the aggressive phenotype of male tumors.

Functionally, we observed that uptake of FTH1 caused a reduction in the invasion capacity of the GICs. Because GBM tumors are highly invasive and cancer stem-like cells are known for their invasive potential and driving the metastasis we focused out attention on invasive potential of the GICs [236]. FTH1 has previously been associated negatively with invasion and expansion of ovarian cancer stem cells. FTH1 silencing in ovarian cancer stem cells, SKOV3, led to increased aggressiveness, increased 3D spheroid forming ability, and increased cell viability [237] in these cells. In another report, FTH1 was shown to interact with members of the peroxiredoxin family of proteins and reduce cell invasion and migration capacity of the lung cancer cells [238]. Here our results of reduction in the invasion capacity of GICs associated with FTH1 incubation support and expand FTH1's role as a negative regulator to brain cancer stem cell invasion. Moreover, because FTH1 incubation with GICs increases their intracellular LIP, it is possible that change in intracellular iron levels could be mediating the regulation of invasion pathways in these cells. It should be emphasized that our results on reduced invasion due to FTH1 incubation address the consequences of FTH1 uptake from extracellular milieu, and subsequent iron delivery, as opposed to previous studies on intracellular expression of FTH1. While intracellular expression of FTH1 acts to sequester intracellular iron, uptake from extracellular environments represents delivery of iron to cells.

Because reduction in proliferation of the cells could confound a reduction in invasion in the 3D invasion assay results, we investigated the effects of FTH1 on proliferation of the cells as well. We did not observe a reduction in cell proliferation with FTH1 incubation at the concentrations that were analyzed in the invasion assay thus confirming that the observed results in the invasion assay are not due to confounding reduction in cell proliferation. A positive relationship has been observed between compact spheroid formation and invasive behavior of cancer cells [239,240]. Based on this, we hypothesized that if FTH1 reduces the invasive capacity of the GICs it might also reduce the spheroid formation capacity of these cells. Our results confirm this relationship in T387 and T3691 GICs. Incubation of the GICs with FTH1 had a dose dependent effect on the compact spheroid formation capacity of the cells. At higher concentration of the FTH1, cells were spread out at the bottom of the well as cell assemblages instead of compact spheroids. This suggests that FTH1 might play a role in the pathways modulating contractility as these are essentially activated during both invasion and spheroid formation [239,241].

Mechanistically, we focused our attention on Rap1A, a highly conserved member of the Ras family of small GTPases. Rap1A signaling has been associated with invasion capacity of several types of cancer cells [226,242–245]. Importantly, Rap1A has previously been identified as a protein supporting invasion capacity of the T387 and T3691 GICs [226]. Our analysis of the Rap1A expression in TCGA datasets revealed that it is highly expressed in aggressive tumors as compared to non-tumors. We also found that higher Rap1A expression is significantly associated with poor survival as compared to low Rap1A levels. This suggests a critical role of Rap1A in GBM survival. Further, our observations in the T387 and T3691 GICs, following FTH1 uptake, revealed a reduced expression of the Rap1A protein. To understand the possible mode of regulation of Rap1A by FTH1 we investigated the IRE-IRP system. Iron regulatory proteins (IRPs) bind to the IREs on the target mRNAs to regulate them. During low iron conditions in the cells for example, IRP1 and IRP2 bind to the IRE sequence on the 5'UTR of FTH1 (and L-ferritin) mRNA to prevent its translation. While IRP1/2 binding on the 3'UTR of the TF mRNA, under similar cell conditions, stabilizes it for translation [18,39]. IREs are highly conserved, 25–30 nucleotides, sequences with hairpin structures containing a base pair stabilized stem and a loop with sequence 5′-CAGUGH-3′ (H denotes A, C or U) [246]. Our bioinformatic analysis of Rap1A mRNA using SIRE predicted the presence of one non-canonical IRE, motif 18, on the 3' UTR of all 6 Rap1A transcripts. Prediction of IRE on Rap1A transcripts supports the possibility of regulation by increased Fe^{2+} (LIP) due to uptake of exogenous FTH1. Rap1A mRNA has the 5′-CAGUG**A**-3′ conserved loop and a UGG bulge typically known as the 'UGC/C8 bulge' [246]. However, these are bioinformatic predictions and it thus remains to be determined if the IRE on Rap1A mRNA transcripts is functional in vivo. Interestingly, however, all the 6 transcripts of the Rap1B mRNA, which shares 95% amino acid sequence identity with Rap1A and potentially has an

overlapping role in invasion [243], were also predicted (in our SIRE analysis) to have an IRE, motif 16, on their 3' UTR (Supplementary Fig. S3). Moreover, some of the downstream effectors in the Rap1A/B signaling pathway such as CDC42 and CDC42BPA have also been identified to have IRE sequences suggesting that the invasive pathway for GICs could be regulated through iron dependent mechanisms [247,248].

A possible explanation for FTH1 driving reduction in invasion can be made from the go or grow hypothesis (invade/proliferate dichotomy) in cancer. Numerous experimental and mathematical models have supported the mutual exclusivity between the invasive and proliferative processes in cancer cells driven by nutrient availability, hypoxia, and stromal resistance amongst others [249–251]. Our observations presented here along with previous reports of increased H-ferritin expression associated with increased ovarian cancer stem cell expansion and reduced invasion [237] support the invade/proliferate dichotomy. FTH1 uptake could represent a nutrient rich (iron) environment driving the switch between invasion, proliferation, and cancer stem cell expansion. Additionally, previous studies have shown that macrophages secrete ferritin, including H-ferritin that can potentially contain higher amounts of iron as compared to serum ferritin [109]. Given that macrophages comprise 50% of non-tumor cell population in GBM there is a higher probability that macrophages could be a source of iron rich H-ferritin in the tumor microenvironment [252,253].

2.6 Conclusions

We identified FTH1 as a novel iron delivery protein for GBMs and GICs in culture and show that the uptake is primarily mediated by TFR1. That FTH1 delivers iron is demonstrated by the measurable increase in LIP. Functionally, uptake of FTH1 reduces the invasive potential of the GICs. Consistent with the reduced invasive potential RAP1A, a protein intricately involved in the invasion capacity of GICs is reduced following uptake of FTH1. These data demonstrate the FTH1 is part of the iron delivery and acquisition mechanism of GBMs.

Chapter 3: Effect of Sex and HFE on H-ferritin and Transferrin Uptake in Mouse Tumors

3.1 Abstract

Purpose: Iron acquisition is frequently upregulated in cancer cells to support their proliferation and growth needs. Glioblastoma (GBM) cells have been shown to modulate iron-associated genes to enhance their iron uptake from the tumor microenvironment (TME). Significant sex differences were observed in the binding of iron-carrying H-ferritin (FTH1) and Transferrin (TF) proteins in our previous reports. However, the binding of the proteins is followed by their uptake, and it is not known if the uptake of the proteins is also sex-specific. Homeostatic Iron Regulator (HFE) is known to regulate the Transferrin receptor (TfR) at the cell surface and has been shown to play a sex-specific role in human GBMs. This leads to questions, answered herein, of whether the HFE regulates FTH1 uptake as well in a sex-specific manner. **Methods:** We developed male and female mice models of GBM to study the radioactive uptake of FTH1 and TF proteins. We further developed mice models with tumor intrinsic downregulation of HFE by orthotopic injection of HFE knockdown cell lines. **Results:** The uptake of FTH1 and TF did not show any significant difference between the male and female mice. Furthermore, HFE knockdown did not influence the uptake of FTH1 and TF proteins in the mice tumors. However, HFE knockdown significantly improved overall survival in the female mice. **Conclusion:** Our findings demonstrate that both FTH1 and TF are taken up by mouse tumors but there is no sex bias in the uptake. Furthermore, although HFE expression levels are associated with differences in survival, decreasing expression of HFE in the tumor did not significantly alter FTH1 or TF uptake.

3.2 Introduction

Sex disparities in cancer incidence, mortality, and therapeutic responses have been observed in many cancers including GBMs[254,255]. Males have a 1.6 times higher incidence of GBM tumors than females. Sex differences in specific subtypes of GBM have also been noted with males having a higher incidence of primary tumors while females having a higher incidence of secondary tumors[256]. Although recurrence in GBM tumors is inevitable the treatment for recurrence differs drastically by sex[256]. Sex differences in GBM are not limited to overall incidence and survival but are observed at molecular levels as well. For example, methylation of O[6]-methylguanine-DNA methyltransferase (MGMT) promoter and increased presence of mutations in the Isocitrate Dehydrogenase (IDH) gene exhibit a favorable

prognosis based on sex. Females with MGMT-methylated GBM tumors have improved survival rates compared to males. Whereas it is males who have improved survival with IDH-mutant GBM tumors[257–259]. In the previous chapter, we showed that GBM cells uptake exogenous H-ferritin (FTH1) and its functional impact on GBM cells as an iron delivery protein.

FTH1 is an iron-delivery protein and ferritin has been utilized to deliver theranostics to GBMs. The canonical iron transport protein for brain tumors and most cells is transferrin. The uptake of transferrin is modulated by the Homeostatic Iron regulatory (HFE) protein, and we have shown that HFE significantly influences survival of GBM patients[260]. Moreover, this survival is sex-biased. Whether FTH1 iron delivery is also influenced by HFE is not known. In this chapter, we further investigate whether factors such as sex and HFE levels influence FTH1 uptake by GBM cells.

Intracellular iron homeostasis is maintained via a careful balance between iron uptake, storage, and release. One of the ways cells regulate iron uptake and release is via HFE protein. HFE functions as an iron sensor in the cells, mediating iron uptake and release via direct or indirect interactions with other iron-associated proteins[261]. A direct way for HFE to maintain intracellular iron flux is via direct binding to (transferrin receptor 1) TFR1. An increase in serum transferrin iron saturation then triggers the release of HFE from TFR1 subsequently making TFR accessible to holo-transferrin for binding and endocytosis[262,263]. HFE has also been shown to regulate iron homeostasis indirectly by associating with an iron complex consisting of Smad and BMP proteins in hepatocytes[262,264]. Mutations in HFE gene have been shown to cause diseases like hereditary hemochromatosis (HH), an iron overload disease. Dysregulated iron absorption in HH causes high amounts of tissue iron accumulation, culminating cell death due to oxidative damage[265]. Currently there is a gap in our understanding of the role of HFE in cancers. The existing literature is very limited and has identified contrasting roles. For example, in a study on HT29 human colon carcinoma cells, HFE inhibited release of iron from the cells subsequently causing an iron overload phenotype but without affecting iron uptake. In contrast, in HeLa, and hepatocellular carcinoma, HepG2 cells, HFE overexpression decreased iron loading[264,266,267]. These contradictory results indicate that HFE might be involved in context-specific iron-regulatory mechanisms depending on its site of expression. Understanding these complex regulatory mechanisms in cancers is crucial for understanding iron homeostasis and regulation at molecular level and could provide better therapeutic targets in the future. In GBMs, we had reported that high HFE levels abrogated survival benefits in female patients[268]. Another report from our collaborators further demonstrated that knockdown in HFE expression caused alterations in the expression levels of several iron-associated genes, suggesting a global disruption of intracellular iron homeostasis[269].

In this study, we characterize whether sex and HFE status have any impact on FTH1 and TF

uptake. We show that there is no statistically significant difference in uptake of FTH1 and TF protein between male and female mice models. We further show that HFE loss in glioma cells enhances radioactive iron uptake, extends sex-specific survival in mice, and reverses the trend of FTH1 and TF uptake in male and female mice models (non-significant). Our results emphasize the molecular mechanisms of HFE in iron homeostatic maintenance and its potential as a target for therapeutic management of GBM.

3.3 Materials and Methods

3.3.1 Cell culture

Syngeneic mouse GBM cell lines, CT2A and KR158, were transfected to overexpress or knockdown expression of HFE respectively. The cell lines were grown in adherent conditions in RPMI 1640 media with 10% fetal bovine serum (FBS) and 1% penicillin-streptomycin. Media was replaced every other day and sub-confluent cells were passaged with trypsin-EDTA and phosphate buffered saline. Cells were maintained in cell culture incubator at 37°C and 5% CO_2. Mice cell line, GL261, were grown as adherent cultures in RPMI 1640 media with 10% fetal bovine serum (FBS) and 1% penicillin-streptomycin. Media was replaced every other day and sub-confluent cells were passaged with trypsin-EDTA and phosphate buffered saline. Cells were maintained in cell culture incubator at 37°C and 5% CO_2.

3.3.2 HFE knockdown and overexpression in mice cell lines

HFE overexpressed (OE) and knockdown (KD) cell lines were a gift from Dr. Justin Lathia, Cleveland Clinic, Ohio. A summary of the protocol for generating these modified cell lines is as follows: MISSION® pLKO.1-puro non-mammalian shRNA control plasmid (SHC002, Sigma) and HFE shRNA plasmids TRCN0000105419 (KD2, Sigma) were used to generate HFE OE and KD conditions. Lentiviral vectors psPAX2 and pMD2G were used to package the lentivirus in 293T cells via calcium phosphate transfection. Following transfection, lentiviral particles were collected from the supernatant media and concentrated using a PEGit virus precipitation solution. For transfection in KR158 and CT2A cells, concentrated lentivirus was added to the cells grown in 10 cm tissue culture plates. Post 24 hours of incubation, at 37°C, media was changed followed by an additional incubation of 24 hours prior to selection with puromycin (5μg/mL)[269].

3.3.3 FTH1 and TF uptake in mice model

GL261 ($1*10^4$) cells were injected orthotopically in, 6 weeks old, C57bl/6 male (FTH1 uptake (n = 6), TF uptake (n=9)) and female (FTH1 uptake (n = 6), TF uptake (n = 10)) mice. Mice were weighed every week after injection. Post 3 weeks of injection, ^{125}I labeled FTH1 or TF were injected retro-orbitally in mice. After 24 hours, mice were sacrificed followed with perfusions using 0.1 M filtered PBS. Matched tumor and non-tumor portions from their brains were collected and radioactivity read on a Beckman Gamma 4000 Analyzer.

3.3.4 55Fe iron labeling and uptake study

The ^{55}Fe labeling of iron was performed as previously described[270]. Briefly, a complex of ^{55}Fe (Perkin Elmer) nitrilotriacetic acid (NTA), ferric chloride ($FeCl_3$), and sodium bicarbonate ($NaHCO_3$) was generated at a ratio of 100 µL NTA: 6.7 µL $FeCl_3$: 23.3 µL NaHCO3: 50 µCi $^{55}FeCl_3$. Free iron separation from the complex was carried out using PD midiTrap-G25 columns following the manufacturer's instructions (GE Healthcare Biosciences). Radiolabeled iron was then added to CT2A and KR158 cells, in 6 well plates, for 0.5, 1, and 2 hours at 37°C. Post incubation, cells were washed twice with ice-cold PBS for 5 minutes. After PBS washing, Hionic-Fluor scintillation cocktail (Perkin Elmer), 10 mL, was added to the cells and radioactivity was measured on Hidex 300 SL (LabLogic) scintillation counter for three minutes each. Background counts were corrected by subtracting the blank tube values from final counts.

3.3.5 HFE KD mice model and survival

KR158 ($1*10^5$) cells with HFE KD or HFE control (containing control vector, C) were injected orthotopically in, 6 weeks old, C57bl/6 male (KD n = 5, C n = 3) and female (KD n = 5, C n = 3) mice. Post injection mice were monitored and weighed periodically. Log-rank tests were used for in vivo survival analysis.

3.3.6 HFE KD mice model and protein uptake

KR158 ($1*10^5$) cells with HFE KD or control (containing control vector, C) were injected orthotopically in, 6 weeks old, C57bl/6 male (KD n = 4, C n = 5) and female (KD n = 5, C n = 5) mice. Mice were weighed every week after injection. Post 3 weeks of injection, ^{125}I labeled H-ferritin or TF were injected retro-orbitally in mice. After 24 hours, mice were sacrificed followed with perfusions using 0.1 M filtered PBS. Matched tumor and non-tumor portions from their brains were collected and radioactivity read on a Beckman Gamma 4000 Analyzer.

3.3.7 Statistical analysis

Relevant statistical analyses were performed using GraphPad Prism 9.5 (GraphPad Software Inc., San Diego, CA). TCGA_GBM and GEPIA databases were accessed on 09 February 2023 for HFE survival and expression analysis.

3.4 Results

3.4.1 Sexual differences in uptake of H-ferritin in mice model

To investigate the uptake of FTH1 in vivo we used a syngeneic mice GBM model. GL261 mice cells were injected orthotopically in C57bl/6 mice brains and GBM tumors were assessed for uptake of the radiolabeled proteins. We observed that tumor and matched non-tumor control tissues take up the radiolabeled FTH1, but we did not observe any significant differences in uptake between the different (male tumor, male non-tumor, female tumor, female non-tumor) groups (Fig. 3-1 a). Similarly, for TF uptake, we did not observe significant differences between the four groups (Fig. 3-1 b). While the differences between males and females and tumor and matched non-tumor controls were not obvious our analysis on identifying which protein, between FTH1 and TF, is preferred by the tissues revealed that TF uptake was significantly higher than FTH1 uptake in all the four groups (Fig. 3-1 c, d).

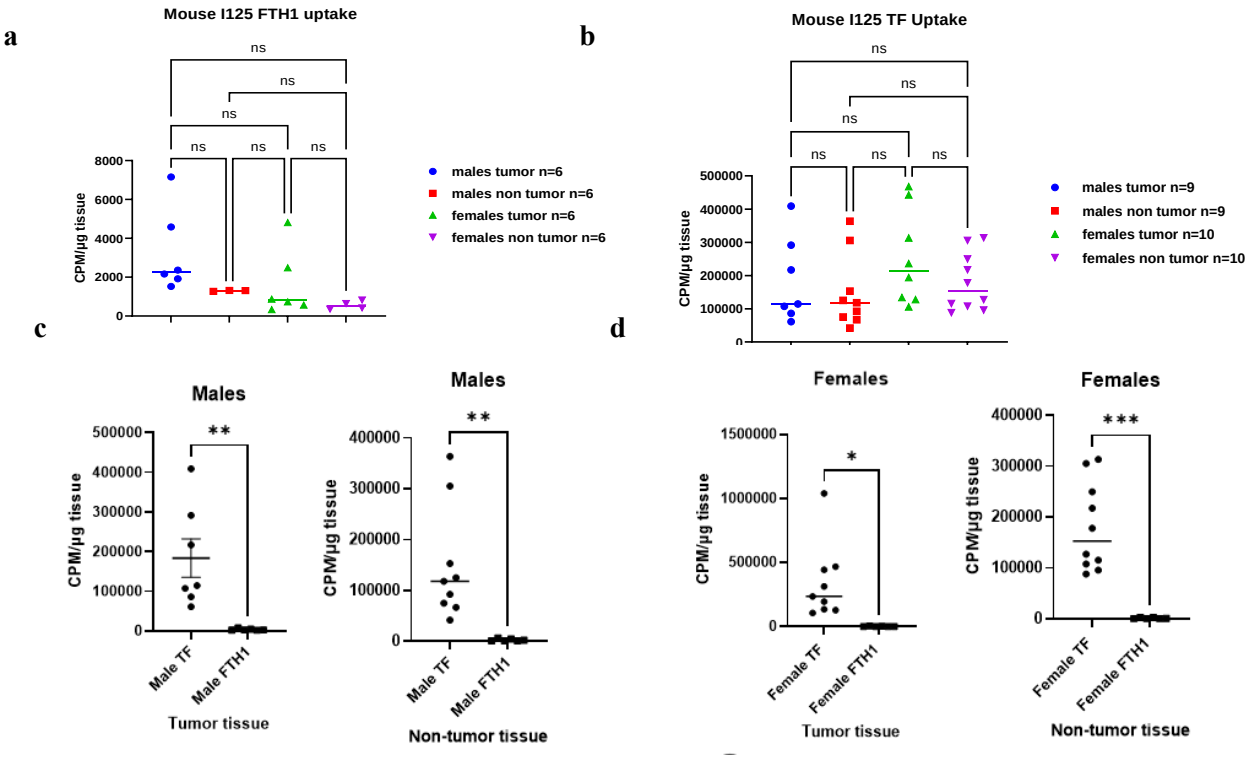

Fig. 3-1 Uptake of H-ferritin in male and female mice models (a) Increased ^{125}I-FTH1 uptake was observed in the male mice tumor (n = 6) samples as compared to the female mice tumor (n = 6) samples. Higher H-ferritin uptake was observed in the male and female tumor samples compared to their respective, matched, non-tumor control samples. (b) Increased ^{125}I-TF uptake was observed in the female mice tumor (n = 10) samples as compared to the male mice tumor (n = 9) samples. Increased Transferrin uptake was observed in the male and female tumor samples as compared to their respective, matched, non-tumor samples. (c) TF uptake was higher as compared to FTH1 in male tumor and non-tumor tissues. (d) TF uptake was higher as compared to FTH1 in female tumor and non-tumor tissues. The data were analyzed for statistical significance by one-way ANOVA, followed by Tukey's post – hoc multiple comparisons, and the differences were found to be not significant.

3.4.2 Upregulation of HFE and its association with survival in human female GBM patients

HFE has previously been shown by our lab to be correlated with survival although the mechanism behind this effect remains yet to be uncovered. We therefore investigated the role of HFE in GBM, in context of iron uptake, by first determining if HFE levels in GBM patient tumors differ from those in non-tumor brain tissue. We used Gene Expression Profiling Interactive Analysis (GEPIA) database (http://gepia.cancer-pku.cn/) and observed a significantly elevated HFE expression in GBM compared to non-tumor brain tissue (Fig. 3-2 a, b). Next, we used The Cancer Genome Atlas (TCGA) dataset to identify if there is a direct correlation between HFE and tumor grade. Our analysis revealed that GBM tumors, grade IV, had the highest expression of HFE as compared to lower grades (Fig. 3-2 c). We further assessed if HFE levels had any correlation with patient survival by using TCGA database. We defined high and low HFE as the top and bottom 50% of gene expression. Our data analysis revealed that while male patients had no significant survival differences females had a significantly better survival outcome with low HFE levels. (Fig. 3-2 d). High and low HFE levels were comparable in males and females eliminating the confounding factor of inherent sex-specific variation in HFE levels (Fig. 3-2 e).

a

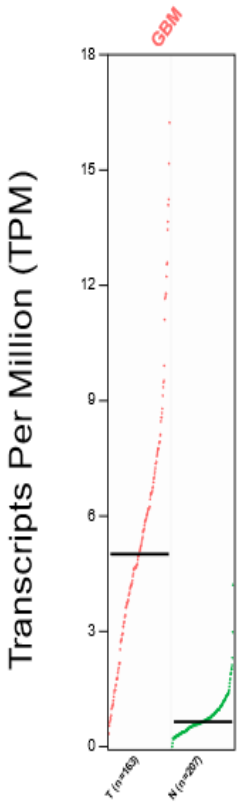

b

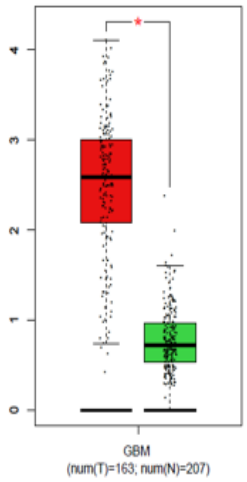

c

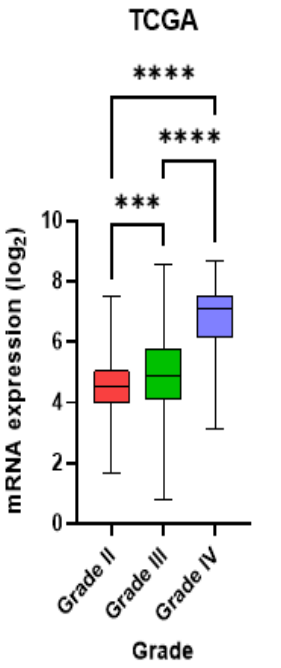

Grade II (n = 226)
Grade III (n = 244)
Grade IV (n = 150)

d

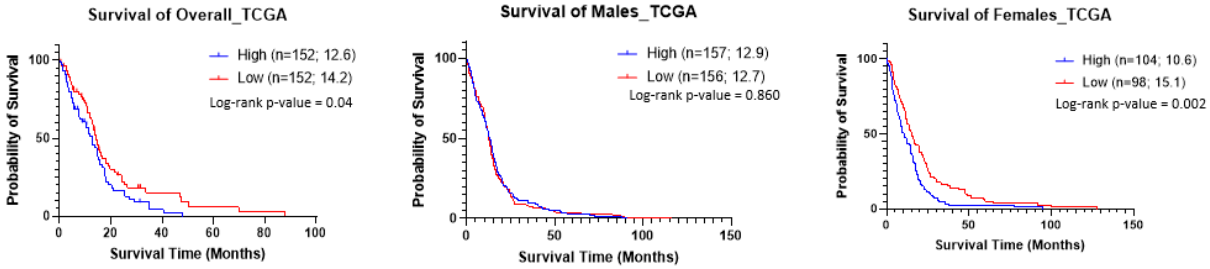

e

HFE expression (log_2)	**High**	**Low**

Male	8.67	3.12
Female	8.56	3.97

Fig. 3-2 Upregulation of HFE and its association with survival in human female GBM patients HFE expression analysis from GEPIA. Higher gene expression was observed in the tumors as compared to non-tumor tissue. Gene expression profile (a) in GBM tumor (n = 163) and non-tumor (n = 207) brain tissue (b) boxplot of the gene expression profile in log-scale. (c) HFE expression increases with increasing grade of the tumors, comparisons of grades II-IV in TCGA database. (d) Survival data from TCGA databases comparing overall survival based on high and low HFE expression (top and bottom 50% of expression) in male and female human GBM tissues. (e) High and low mRNA expression (log_2) levels in males and females. *$p<0.05$; **$p<0.01$; ***$p<0.001$ determined by one-way ANOVA with Dunnett's multiple comparisons test. Survival analysis was carried out using a log-rank test for survival data.

3.4.3 Low HFE levels provide survival benefit in female mice model

To investigate the role of HFE in FTH1 uptake we used KR158 and CT2A mice cell lines with HFE knockdown and upregulation respectively. HFE knockdown and overexpression were confirmed with both qPCR and western blot by our collaborators and are presented without further modifications (Fig. 3-3 a, b). A known function of HFE is to limit iron uptake via binding to TFR receptor. We thus investigated iron uptake, using ^{55}Fe uptake assays, in the KR158 HFE knockdown and CT2A HFE overexpression cell lines. Our observations revealed a significantly increased uptake of ^{55}Fe-iron in HFE knockdown cells compared to control (Fig. 3-3 c). This is consistent with the previously mentioned known function of HFE. HFE overexpression on the other hand had no effect on iron uptake (Fig. 3-3 d). We next developed the HFE knockdown mice model and studied the effects of HFE knockdown on survival of mice (Fig. 3-3 e). We observed that female mice with tumors developed from KR158 cells (that had low HFE levels; aka KR158 HFE knockdown cells) had significantly better median survival as compared to the females with the KR158 cells containing wild type levels of HFE (aka HFE control/empty vector). We find the differences in median survival consistent with previous reports which have shown that GBM tumors with low HFE expression in females have a significant survival benefit[269]. Males with HFE KD also had a significant survival benefit as compared to males GBM with control vector.

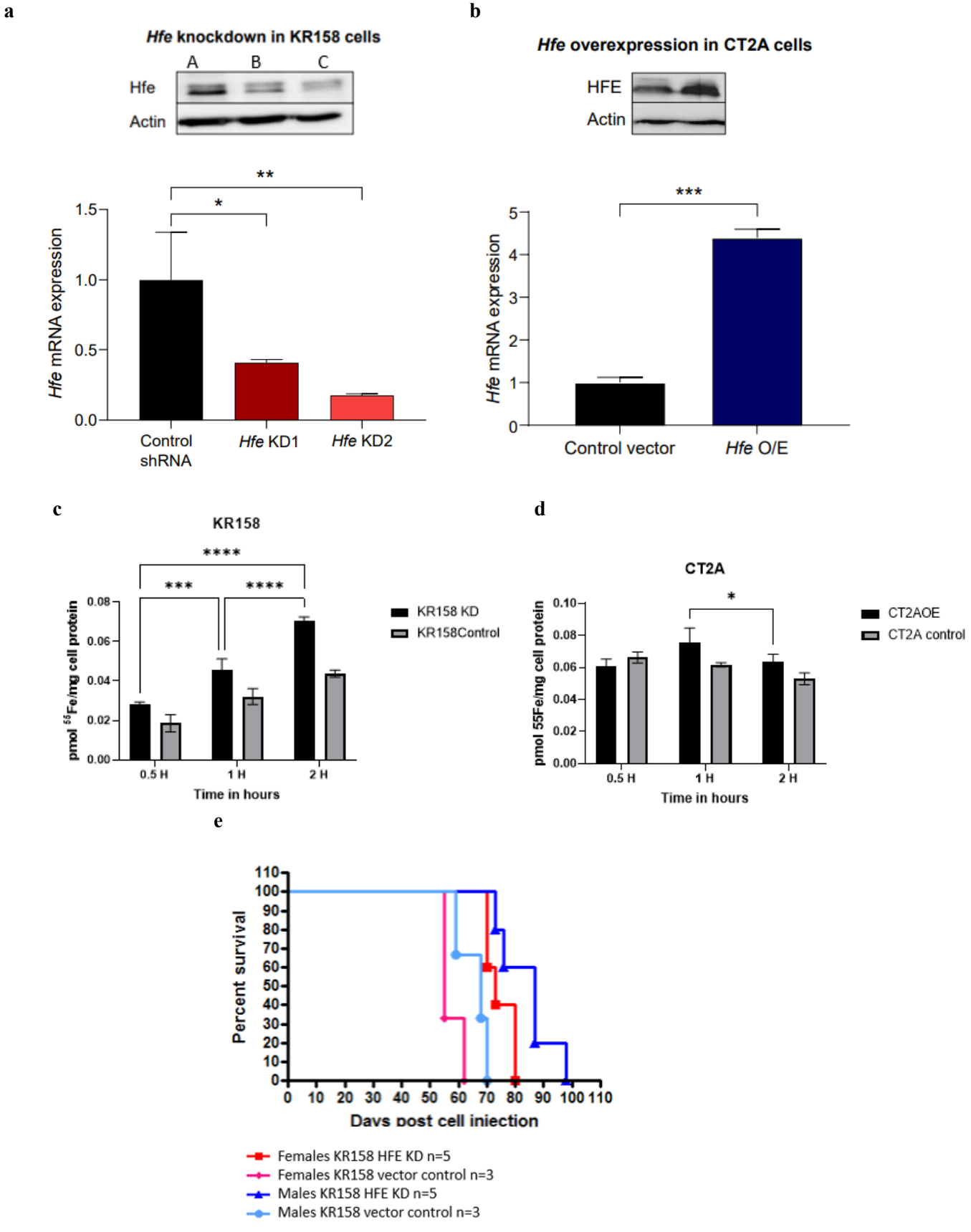
a
Hfe knockdown in KR158 cells
A
B
C
Hfe
Actin
**
*
Hfe mRNA expression
1.5
1.0
0.5
0.0
Control shRNA
Hfe KD1
Hfe KD2
b
Hfe overexpression in CT2A cells
HFE
Actin
***
Hfe mRNA expression
5
4
3
2
1
0
Control vector
Hfe O/E
c
KR158
****
***
****
pmol 55Fe/mg cell protein
0.08
0.06
0.04
0.02
0.00
0.5 H
1 H
2 H
Time in hours
KR158 KD
KR158Control
d
CT2A
*
pmol 55Fe/mg cell protein
0.10
0.08
0.06
0.04
0.02
0.00
0.5 H
1 H
2 H
Time in hours
CT2AOE
CT2A control
e
Percent survival
110
100
90
80
70
60
50
40
30
20
10
0
0 10 20 30 40 50 60 70 80 90 100 110
Days post cell injection
Females KR158 HFE KD n=5
Females KR158 vector control n=3
Males KR158 HFE KD n=5
Males KR158 vector control n=3

Fig. 3-3 Low HFE levels provide a survival benefit in female mice model (a) HFE knockdown validation in KR158 cell line as confirmed by western blot and qPCR. (b) Hfe overexpression validation in CT2A cell line as confirmed by western blot and qPCR. Data reproduced from Dr. Justin Lathi lab. (c) ^{55}Fe-iron uptake by KR158 HFE knockdown cells. (d) ^{55}Fe-iron uptake by CT2A HFE overexpressing cells. Cell-associated ^{55}Fe was determined by liquid scintillation counting. DPM counts were converted to pmoles of ^{55}Fe (at ^{55}Fe Specific Activity of 2466.81Ci/mmol). pmol uptake was then normalized to total cell protein content to obtain pmol ^{55}Fe/mg cell protein. Data were statistically analyzed by two-way ANOVA. Outliers removed by ROUT method at Q = 1%. $p < 0.05$, **: $p < 0.01$, ***: $p < 0.001$, ****: $p < 0.0001$. Experiments performed in triplicates. (e) Survival analysis of mice with GBM tumors developed by orthotopic injection of KR158 cells with HFE knockdown (males n = 5, females n = 5) and control (males n = 3, females n = 3) vectors. Male and female mice with low HFE levels had a survival advantage as compared to their control HFE levels' counterparts. Survival analysis was performed using the log-rank (Mantel-Cox) test and the survival differences were found to be non-significant. Data were statistically analyzed by Log-rank (Mantel-Cox) test. Outliers were removed by ROUT method at Q = 1%. $p < 0.05$, **: $p < 0.01$, ***: $p < 0.001$, ****: $p < 0.0001$.

3.4.4 Uptake of FTH1 and TF in presence of HFE knockdown tumors

To study the effect of HFE levels on FTH1 uptake we utilized the HFE KD mice model with GBM tumors that was described in the previous section. Male and female mice were injected with KR158 cells containing HFE KD or a control vector. ^{125}I-FTH1 uptake analysis revealed that there were no significant differences in uptake between GBM tumors with the HFE KD versus HFE normal/control levels. We observed a high amount of variability in the female HFE KD groups (Fig. 3-4 a). This suggests that there might be confounding variables in the female tumors contributing to the observed results. Similarly, we observed no significant differences in TF uptake in tumors with HFE KD versus HFE control (Fig. 3-4 b). However, there was increased variability in the uptake of TF by female tumors with HFE KD (CV = 129%) as compared to the rest of the female groups (tumor HFE control, CV = 104%, non-tumor HFE KD, CV = 14%, non-tumor HFE control, CV = 54%). In males, we observed a similar trend of increased variability in the uptake of TF in tumors with HFE KD (CV = 174%) as compared to the rest of the male groups (tumor HFE control, CV = 114%, non-tumor HFE KD, CV = 69%, non-tumor HFE control, CV = 121%). Overall, we observed that HFE KD caused an increase in the uptake of H-ferritin in female tumors and Transferrin in both male and female tumors.

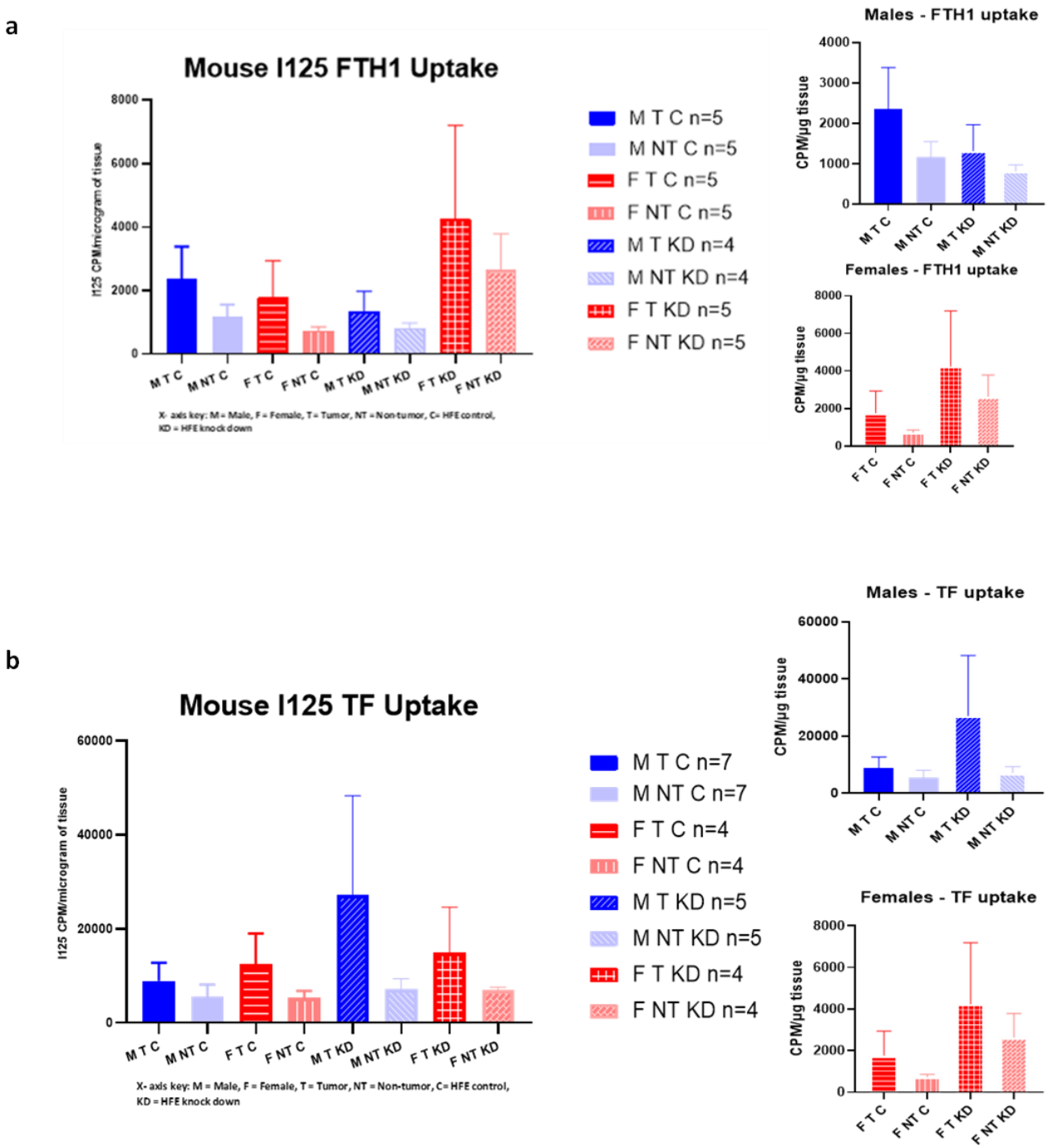

Fig. 3-4 HFE KD reduces FTH1 uptake female tumors ^{125}I FTH1 uptake was performed in vivo HFE KD mice model. (a) Increased ^{125}I FTH1 uptake was observed in female tumors with HFE KD as compared to the corresponding male tumors with HFE KD. Female tumors with HFE KD had an increased ^{125}I FTH1 uptake as compared to female tumors with normal HFE levels. Female tumors in both KD and control HFE levels had higher

uptake as compared to their matched non-tumor counterparts. (b) Increased ^{125}I TF uptake was observed in male tumors with HFE KD as compared to the corresponding female tumors with HFE KD. Male tumors with HFE KD had an increased ^{125}I FTH1 uptake as compared to male tumors with normal HFE levels. Male tumors in both KD and control HFE levels had higher uptake as compared to their matched non-tumor counterparts. Data were statistically analyzed by two-way ANOVA. Outliers removed by the ROUT method at Q = 1%. $p < 0.05$, **: $p < 0.01$, ***: $p < 0.001$, ****: $p < 0.0001$.

3.5 Discussion

In this study, we investigated the effect of known iron metabolism modulators, sex, and HFE, in the context of iron acquisition in tumors. We observed no significant differences in the uptake of FTH1 and TF between male and female groups. HFE knockdown in the mice tumors did not further affect the uptake of the two proteins. However, we observed that HFE KD significantly affected the survival of male and female GBM mice suggesting that survival in this mice model may be associated with HFE functions other than directly impacting the uptake of these proteins. For example, as mentioned earlier, HFE levels could be impacting the iron metabolism associated genes or could be impacting the gene signatures of infiltrating immune cells. proteins.

FTH1 and TF are iron-delivery proteins. Our lab has previously shown that FTH1 and TF bind to human GBM tissues and that this binding is sexually biased with males having significantly increased binding as compared to females. The binding of FTH1 and TF to tissues signifies the presence of specific receptors and subsequent uptake of the protein with the help of these receptors[271]. An increase in uptake of these proteins in turn signifies the increased need of cancer cells to acquire iron, from the tumor microenvironment, for sustaining a variety of functions. The uptake of TF, post its binding to the Transferrin receptor (TfR), is very well known[246,272]. FTH1 uptake however, is not well studied and has been reported in a very few cells such as K562 (erythroleukemia), and HeLa (ovarian cancer)[28]. FTH1 can bind to receptors such as Tim-1 (human)[193], Tim-2 (mice)[273], and TfR[28]. Our report (chapter 2 of this thesis) was the first to report FTH1 uptake, via the TfR receptor, by GBM cancer stem cells. All in all, these data suggest a possibility that the uptake of FTH1 and TF in GBM tumors might be sex-specific further indicating differences in underlying mechanisms of iron acquisition and metabolism between males and females. To investigate the possibility of whether FTH1 and TF uptake is sexually dimorphic we performed uptake analysis in male and female mice models in this study. Our data did not reveal any significant differences in the uptake of the two proteins. The number of animals included in the study is adequately powered. A sample size calculation analysis conducted before the study for a one-way

ANOVA (with a number of groups (κ) = 4, requiring the sacrifice of the animal for end analysis) indicated that the minimum sample size to yield a statistical power of at least 0.8 with an alpha of 0.05 is 4 in each group. We have used more than 4 animals in each group which suggests that the number of animals is not a potential issue in detecting significant differences in the uptake of the proteins. A potential explanation behind the observed results could be that the binding analyses were performed on human GBM tissues whereas in the mice we performed uptake experiments. The differences observed between human and mice studies could arise from the orthotropic implantation of GBM cancer cells in mice as it does not reproduce the conditions of the tumor microenvironment (TME) seen in the human GBM tissues[274,275]. For example, studies have shown that markers such as Cst, Hexb, and Sparc are highly differentially expressed between microglia and tumor associated macrophages (TAMs) in mouse GBM but not in human GBMs. In contrast, APOC2, TMIGD3, and SCIN are microglia-specific markers restricted to human GBMs[276]. TAMs comprise 30-40%[277] of the GBM TME in both mice and humans and are also major cells in the TME that regulate iron metabolism within the tumors[278]. Phenotypic heterogeneity between the human and mouse TAMs could thus drive the differences between iron metabolism in tumors reflected in form of differences in uptake and binding of the H-ferritin observed in the mice and human models respectively.

HFE is a known modulator of iron uptake in normal cells. High HFE expression in GBM has been previously associated with poor survival outcomes[268]. Here we investigated HFE expression in human TCGA and GEPIA database and found that HFE is upregulated in GBM tumors compared to non-tumor brain tissue. Furthermore, below median levels of HFE exerted a significant survival benefit in females but not males, consistent with existing literature utilizing separate databases. Because of HFE's role in iron acquisition by cells we hypothesized that HFE modulates iron acquisition in the GBM tissues in a sex specific manner contributing to the observed survival differences between males and females. We started testing this hypothesis by first confirming the known function of HFE in iron uptake. We performed radioactive iron uptake studies on the HFE knockdown, overexpression, and control cells. Our findings from the radioactive experiments in these cell lines demonstrated an increased iron uptake with HFE knockdown as compared to control cells. While overexpression of HFE had no effect on iron uptake as compared to control cells. These results support the existing literature on HFE and its role in iron uptake in the knockdown and overexpression conditions[269]. Lack of effect in the overexpression model could be attributed to the saturable binding of HFE to TfR in control and overexpressing cells. During under expression, there are less HFE molecules binding to TfR thus increasing influx of holotransferrin.. But during overexpression, the number of TfR receptors may not change, thus the additional HFE

expression has no additional TfR to bind to and cause an impact on iron uptake. This overexpression effect is also consistent with the literature[269]. These results confirmed that our knockdown and overexpression cell models are efficient.

We next tested the survival effects of low HFE in mice model. Our observations about low HFE exerting a significant survival benefit in female mice are again consistent with the existing literature[268,269]. We further observed that the male mice with HFE knockdown cancer cells also had a significant survival benefit. These observations, although consistent with existing literature in the mice models, are different from what has been observed in the human dataset analyses. In humans, low HFE has been shown to exert sex-specific survival benefit to females but not males.

A part of this survival benefit could be contributed by a reduction in the migration and invasion capacity of the KR158 cells upon HFE knockdown. KR158 cells grow highly aggressively when injected orthotopically in C57bl/6 mice[279]. However, a cell culture report from our lab has previously shown that KR158 cells with HFE knockdown have reduced migratory capacity[280]. Combining these two reports we can suspect that reduced migratory capacity of the KR158 cells could be contributing to the overall survival in both the mice sexes. However, as mentioned earlier, HFE's impact on the iron metabolism genes and genes of the infiltrating immune cells as well as differences in the phenotype of myeloid cells such as macrophages[281], which further regulate immune cell type, infiltration in the TME could contribute to the observed differences in survival between human and mice. Further evaluation of the mice GBM tumors with low HFE may reveal factors that contribute to survival in males that can further be exploited for therapeutic purposes in human GBM males.

To understand if the observed differences in the mice survival are mediated by HFE's role in iron acquisition we studied FTH1 and TF uptake in the HFE knockdown mice model. We did not find significant differences in uptake of FTH1 and TF proteins between the HFE KD and HFE control groups. We observed that HFE knockdown reversed the mode of iron uptake, in a sex specific manner, in the tumors in mice. In control HFE models of uptake, male tumors had a higher uptake of FTH1 while female tumors had high TF uptake. However, this mode of uptake was reversed upon HFE knockdown: male tumors with HFE knockdown had higher uptake of TF while female tumors with HFE knockdown had higher uptake of FTH1. Again, these observed differences were not statistically significant and there was a high amount of variability seen in the uptake. Although not significant, these data reveal that uptake of the FTH1 and TF proteins in the HFE knockdown tumor models might still potentially contribute to the overall survival of the mice. For example, subtle increase in labile iron pool (due to increased iron uptake or FTH1 uptake) in the tumor cells has been shown in the past to contribute to reduction in the invasion

and migration capacity of the cells[282,283]. Differences in survival between human and mice males in presence of HFE downregulation further provide an opportunity to investigate these mice models further and identify the differentiating factors which can be modulated and hold a translational potential in modulating survival in human GBM males.

3.6 Conclusions

This study shows that GBM tumors uptake FTH1 and TF proteins. This is a novel finding for FTh1 and expands our findings for FTH1 from humans to mice. We did not find any statistical differences in the uptake of the proteins between the male and female mice groups suggesting there might not be a sexually biased uptake of these proteins in this experimental model. We also show that TF is potentially the major iron delivery protein for these tumors. Our study further showed that low HFE levels do not significantly impact the uptake of these proteins, but they do reverse the apparent primary source of iron. Moreover, the decreased expression of HFE significantly impacts the survival in both male and female mice but the survival effect is limited to females with human GBM tumors.

Chapter 4: Sexually dimorphic effect of H-ferritin genetic manipulation on survival and tumor microenvironment in a mouse model of Glioblastoma

This work has been previously submitted as:
Bhavyata (Pandya) Shesh, Vonn Walter, Kondaiah Palsa, Becky Slagle-Webb, Elizabeth Neely, Todd Schell, James R. Connor, Sexually dimorphic effect of H-ferritin genetic manipulation on survival and tumor microenvironment in a mouse model of Glioblastoma, Journal of Neuro- Oncology, 2023

4.1 Abstract

Purpose: Iron plays a crucial role in various biological mechanisms and has been found to promote tumor growth. Recent research has shown that the H-ferritin (FTH1) protein, traditionally recognized as an essential iron storage protein, can transport iron to GBM cancer stem cells, reducing their invasion activity. Moreover, the binding of extracellular FTH1 to human GBM tissues, and brain iron delivery in general, has been found to have a sex bias. These observations raise questions, addressed in this study, about whether H-ferritin levels extrinsic to the tumor can affect tumor cell pathways and if this impact is sex-specific. **Methods:** To interrogate the role of systemic H-ferritin in GBM we introduce a mouse model in which H-ferritin levels are genetically manipulated. Mice that were genetically manipulated to be heterozygous for H-ferritin (*Fth1*+/-) gene expression were orthotopically implanted with a mouse GBM cell line (GL261). Littermate *Fth1* +/+ mice were used as controls. The animals were evaluated for survival and the tumors were subjected to RNA sequencing protocols. We analyzed the resulting data utilizing the murine Microenvironment Cell Population (mMCP) method for in silico immune deconvolution. mMCP analysis estimates the abundance of tissue infiltrating immune and stromal populations based on cell-specific gene expression signatures. **Results:** There was a clear sex bias in survival. Female *Fth1*+/- mice had significantly poorer survival than control females (*Fth1*+/+). The *Fth1* genetic status did not affect survival in males. The mMCP analysis revealed a significant reduction in T cells and CD8+ T cell infiltration in the tumors of females with *Fth1*+/- background as compared to the *Fth1*+/+. Mast and fibroblast cell infiltration was increased in females and males with *Fth1*+/- background, respectively, compared to *Fth1*+/+ mice. **Conclusion:** Genetic manipulation of *Fth1* which leads to reduced systemic levels of FTH1 protein had a sexually dimorphic impact on survival. *Fth1* heterozygosity significantly worsened survival in females but did not affect survival in male GBMs. Furthermore, the genetic manipulation of *Fth1* significantly affected tumor infiltration of T-cells, CD8+ T cells, fibroblasts, and mast cells in a sexually dimorphic manner. These results demonstrate a role for

FTH1 and presumably iron status in establishing the tumor cellular landscape that ultimately impacts survival and further reveals a sex bias that may inform the population studies showing a sex effect on the prevalence of brain tumors.

4.2 Introduction

Glioblastoma (GBM) is one of the most devastating and most common primary brain tumors, with only 15 months of median overall survival post-diagnosis [211]. The 5-year survival rate of 4-5% for GBMs is the lowest among all cancer types [284,285]. Sex-based dimorphism in cancer incidence, mortality, and therapeutic responses have been observed in many cancers, including GBMs [254,286]. GBM incidence is not only less common in females, but females also have a better survival outlook than males. Sex-based differences in GBMs are not limited to overall survival and incidence but are also observed at molecular levels. For example, methylation of O [6]-methylguanine-DNA methyltransferase (MGMT) promoter and increased presence of mutations in the isocitrate dehydrogenase (IDH) gene exhibit a favorable prognosis based on sex. Females with MGMT-methylated GBM tumors have better survival rates than males. Whereas it is males who have improved survival with IDH-mutant GBM tumors [257–259]. At the cellular level, sex-biased differences have been seen in the immune infiltration of tumors. Stronger innate and adaptive immune responses to cancer are considered one of the major reasons behind the reduced risk of cancer mortality in females. Immune infiltration of tumors is more abundant in females than males. Enrichment of T-cell subpopulations is also usually seen in female tumors as compared to male tumors [287–289]. Although sex hormones, genetic and epigenetic factors, and environmental/psychosocial factors are believed to be the underpinnings of such sex-based differences, the exact molecular mechanisms and pathways driving these differences are yet to be clearly understood.

Iron metabolism and its homeostasis are important for cellular processes such as DNA synthesis and energy production and thus play a critical role in cancer development, maintenance, and progression [224,290]. Cancer cells are known to be ‘iron addicted’ [115,116,235]. They scavenge iron and its sources from the tumor microenvironment and modulate gene expression reflecting increased iron uptake and metabolism. For example, an increase in expression of genes such as transferrin receptor (TfR1), and divalent metal transporter (DMT1), proteins involved in iron uptake, provide evidence for increased iron uptake by multiple different cancer cell types [58,291]. TfR1-Transferrin-mediated iron uptake is the canonical mechanism for iron uptake by normal and cancer cells. However, we recently reported that the extracellular form of H-ferritin (FTH1), a canonical iron storage molecule, could also act as a source of iron for GBM cancer stem cells (GSCs) [282]. Moreover, we reported that human male GBM tumors bind to

significantly higher levels of extracellular ferritin as compared to female GBM tumors. Higher binding of FTH1 on male tumors suggests higher demand for iron potentially reflecting the aggressive phenotype of male tumors. In another report, serum FTH1 was also shown to impact circulating regulatory T cells (Treg) cells and support their immune functions in melanoma patients [292]. These reports suggest that FTH1 levels outside the tumor cells might play an important role in modulating cancer cell pathways, anti-cancer immunity, and influencing cancer cell survival and growth. More importantly, FTH1's effect on cancer cell pathways seems to be sexually biased. However, not much is known regarding tumor extrinsic ferritin and its role in GBMs, including its impact on survival, tumor microenvironment modulation, and influence on cancer cell pathways.

Hence, with this report, we intend to study the role of tumor extrinsic FTH1 on GBM and further investigate the extent of sexual dimorphism in its impact on GBMs by introducing a novel animal model in which one copy of the *Fth1* gene has been deleted. Homozygous deletion of *Fth1* is known to be embryonically lethal [293]. The *Fth1* heterozygous knockout mice model used here has a 2-fold reduction in systemic H-ferritin levels [293]. However, the *Fth1* in tumor cells that are injected in these mice is not manipulated/modified in any other manner. To identify the pathways that are modulated by the decrease in tumor extrinsic *Fth1*, we employed RNA sequencing techniques on the mice GBM tumors isolated from *Fth1* heterozygous knockout and *Fth1*+/+ littermate controls. This study thus provides a unique opportunity to analyze the genetic modulation of systemic *Fth1* extrinsic to the tumor and its sex-specific role in GBMs.

We present data revealing significant sex differences in overall survival associated with *Fth1* heterozygous knockout in mice. We show that in the *Fth1*+/- mice, there is a significant reduction in the overall survival in female GBM mice as compared to *Fth1* +/+ control females but no survival effect on male mice. Our RNA sequencing analyses on the orthotopic GBM tumors in mice with *Fth1*+/- background show differences in gene expression between male and female tumors as compared to tumors in *Fth1*+/+ mice. Deconvolution analyses based on immune and stromal cell infiltrating gene expression signatures further suggested that *Fth1* has significant sex-biased effects on tumor-infiltrating T, CD8+ T, mast, and fibroblast cell populations in mice GBM tumors.

4.3 Materials and Methods

4.3.1 Cell culture

Mice cell line, GL261, was grown as adherent cultures in RPMI 1640 media with 10% fetal bovine serum (FBS) and 1% penicillin-streptomycin. Media was replaced every other day, and sub-confluent cells were passaged with trypsin-EDTA and phosphate-buffered saline. Cells were maintained in a cell culture incubator at 37°C and 5% CO_2.

4.3.2 Fth1+/- mice model

Since *Fth1* double knockout is embryonically lethal in mice, a heterozygous mouse model which has more than two-fold reduction in *Fth1* protein concentration in serum was developed [22]. *Fth1*+/- mice were injected intracranially with GL261 mouse GBM cells. H-ferritin heterozygote mice of mixed C57BL6/J X 129SvEv genetic background were used. *Fth1*+/- knockout was generated as previously described [294]. Briefly, a modified PBS [sk]II vector targeting a 770 bp promoter region of the *Fth1* gene was introduced into the 129SvEv CCE embryonic stem (ES) cells by electroporation. Successful clones were selected for G418 and ganciclovir resistance. Positive ES clones were then injected into the C57BL6/J blastocysts and resulting chimeric males were bred to C57BL6/J females to produce F1 heterozygous mice. The heterozygous (*Fth1*+/-) mouse colonies were maintained under normal housing conditions. The mouse genotype was confirmed by using PCR.

4.3.3 Intracranial injections for generating GBM mouse model

To generate the *Fth1*+/- mice GBM model, GL261 ($2*10^4$) mouse GBM cells were injected orthotopically in 6-week-old, *Fth1*+/- and control (*Fth1*+/+) male and female mice. The tumor implantation was performed as previously described [295]. Briefly, mice were anesthetized via the inhaled form of isoflurane. Mice heads were shaved and topically disinfected to receive the tumor cells intracranially. For the tumor cell injection, Hamilton syringes filled with 3µL of RPMI 1640 containing GL261 cells were fitted onto the stereotaxic apparatus. The apparatus was guided into the right hemisphere of the brain (mice shaved and ready for receiving the cells) at a depth of approximately 3.5 mm and GL261 cells suspended in 3µL of null RPMI 1640 media were injected. Post injection, animals were monitored daily and weighed weekly for neurological and behavioral symptoms. All animal experiments were performed in compliance

with institutional guidelines and were approved by the Institutional Animal Care and Use Committee of the Penn State College of Medicine (Penn State Hershey College of Medicine IACUC # PROTO202001393 approved).

4.3.4 Survival study

GBM male *Fth1*+/- (n = 12), male *Fth1*+/+ (n=13), female *Fth1*+/- (n=14), female *Fth1*+/+ (n=12) mice were orthotopically implanted with GL261 cells as described above. Post implantation, mice were provided food and water ad libitum and monitored daily for signs of tumor growth and progression. Survival continued until humane endpoints including loss of locomotor activity and weight loss (up to 20%). The survival time was measured from the day of tumor cell implantation to the day of euthanasia or death and mice not showing palpable tumors and other clinical signs of progressive tumor growth by 3 months post-implantation were euthanized. Log-rank tests were used for in vivo survival analysis.

4.3.5 GBM tumor harvesting for RNA sequencing

GBM male *Fth1*+/- (n = 5), male *Fth1*+/+ (n=4), female *Fth1*+/- (n=7), female *Fth1*+/+ (n=5) mice were orthotopically implanted with GL261 cells as described above. Post 3 weeks of injection, mice were euthanized, and tumors were harvested immediately and flash frozen using Isopentane (Sigma-Aldrich) chilled with dry ice [296]. The frozen tumors were subsequently homogenized for RNA sequencing.

4.3.6 Tissue homogenization and RNA isolation

A bead mill homogenizer (Bullet Blender, Next Advance) was used to homogenize each mouse's GBM tumor tissue. Approximately 30 mg of tissue sample was transferred to a safe-lock microcentrifuge tube (Eppendorf). A mass of stainless-steel beads (Next Advance, cat# SSB14B) equal to the mass of the tissue was added to the tube. Half volume of the mass of the tissue of the NucleoZol reagent (Macherey-Nagel) was added to the tube and samples were immediately mixed in the Bullet Blender (Next Advance) for 1 min at a speed of seven. Samples were visually inspected to confirm the desired homogenization and then incubated at 37 °C for 5 min. Another half volume of the NucleoZol reagent was added and homogenization was repeated, if needed. Total RNA was extracted using Macherey-Nagel NucleoSpin RNA Kit. RNA integrity number (RIN) was measured using BioAnalyzer (Agilent Technologies) RNA 6000 Nano Kit.

4.3.7 Library preparation and mRNA sequencing

RNA-sequencing libraries were prepared in the Penn State College of Medicine Genome Sciences Core (RRID: SCR_021123) using the Illumina Stranded mRNA Prep, Ligation kit (Illumina) as per the manufacturer's instructions. Briefly, polyA RNA was purified from 200 ng of total RNA using oligo (dT) beads. The extracted mRNA fraction was subjected to fragmentation, reverse transcription, end repair, 3' end adenylation, and adaptor ligation, followed by PCR amplification and magnetic bead purification (Omega Bio-Tek). The unique dual index sequences (IDT for Illumina RNA UD Indexes Set B, Ligation, Illumina) were incorporated in the adaptors for multiplexed high-throughput sequencing. The final product was assessed for its size distribution and concentration using BioAnalyzer High Sensitivity DNA Kit (Agilent Technologies). The libraries were pooled and sequenced on Illumina NovaSeq 6000 (Illumina), to get on average 25 million, paired-end 59 bp reads, according to the manufacturer's instructions.

4.3.8 Sequencing analysis

RNA sequencing analyses were performed using gene-level read counts. Ensembl gene identifiers were converted to gene symbols, then all Ensembl identifiers corresponding to repeated gene symbols were removed. Immune deconvolution analyses were executed using the mMCP-counter R package [297,298] and log2 (TPM + 1) expression values. Differential expression analyses were performed for female and male mice separately. In brief, lowly expressed genes were removed, then the RUVSeq R package [299] was applied to normalize the expression data using a set of mouse housekeeping genes [300]. Differentially expressed genes in *Fth1*+/- vs. *Fth1*+/+ mice were identified using the edgeR R package [301] and a false discovery rate q-value threshold of 0.05. The design matrix controlled for sequencing batch and a single covariate (k = 1) from the RUVSeq analysis. The gene set enrichment analysis (GSEA) software [302] was applied to perform pathway analyses using the GSEA pre-ranked approach and 102 select gene sets of interest. For each comparison in the differential expression analysis, genes were ranked using a signed version of the likelihood ratio statistic in the edgeR output. The signed likelihood ratio statistic was computed by multiplying the likelihood ratio statistic by the sign of the log fold change, thus providing a single statistic that was used to rank both up-and down-regulated genes. Gene ontology analyses were performed with the topGO R package [303].

4.3.9 Statistical analysis

Log-rank (Mantel-Cox) test for survival curve comparisons and Mann Whitney test for mMCP score comparisons were performed using GraphPad Prism 9.5 (GraphPad Software Inc., San Diego, CA).

4.4 Results

4.4.1 Heterozygous Fth1 knockout abrogates survival benefit of the female sex in GBM mice model

To investigate whether tumor extrinsic FTH1 expression has any role in GBM survival we used an *Fth1* heterozygous knockout mouse model. GBMs were developed by injecting GL261 cells orthotopically in mice with *Fth1*+/- and *Fth1*+/+ genetic backgrounds. In our survival analysis, we did not find significant differences between the 4 groups: *Fth1*+/- males, *Fth1*+/+ males, *Fth1*+/- females, *Fth1*+/+ females (p-value = 0.13) (Fig. 4-1 a). We next performed the survival analysis separately on male and female groups and observed that there were no significant differences in survival between *Fth1*+/- and *Fth1*+/+ male groups (p-value = 0.73) (Fig. 4-1 b) but female *Fth1*+/- mice had a significantly worse survival rate as compared to *Fth1* +/+ background (p-value = 0.02) (Fig. 4-1 c). We also compared survival of the *Fth1*+/+ mice in male versus female and the *Fth1*+/- mice in males versus females (Supplementary Fig. S1 a, b) and did not find any statistically significant differences in survival between them.

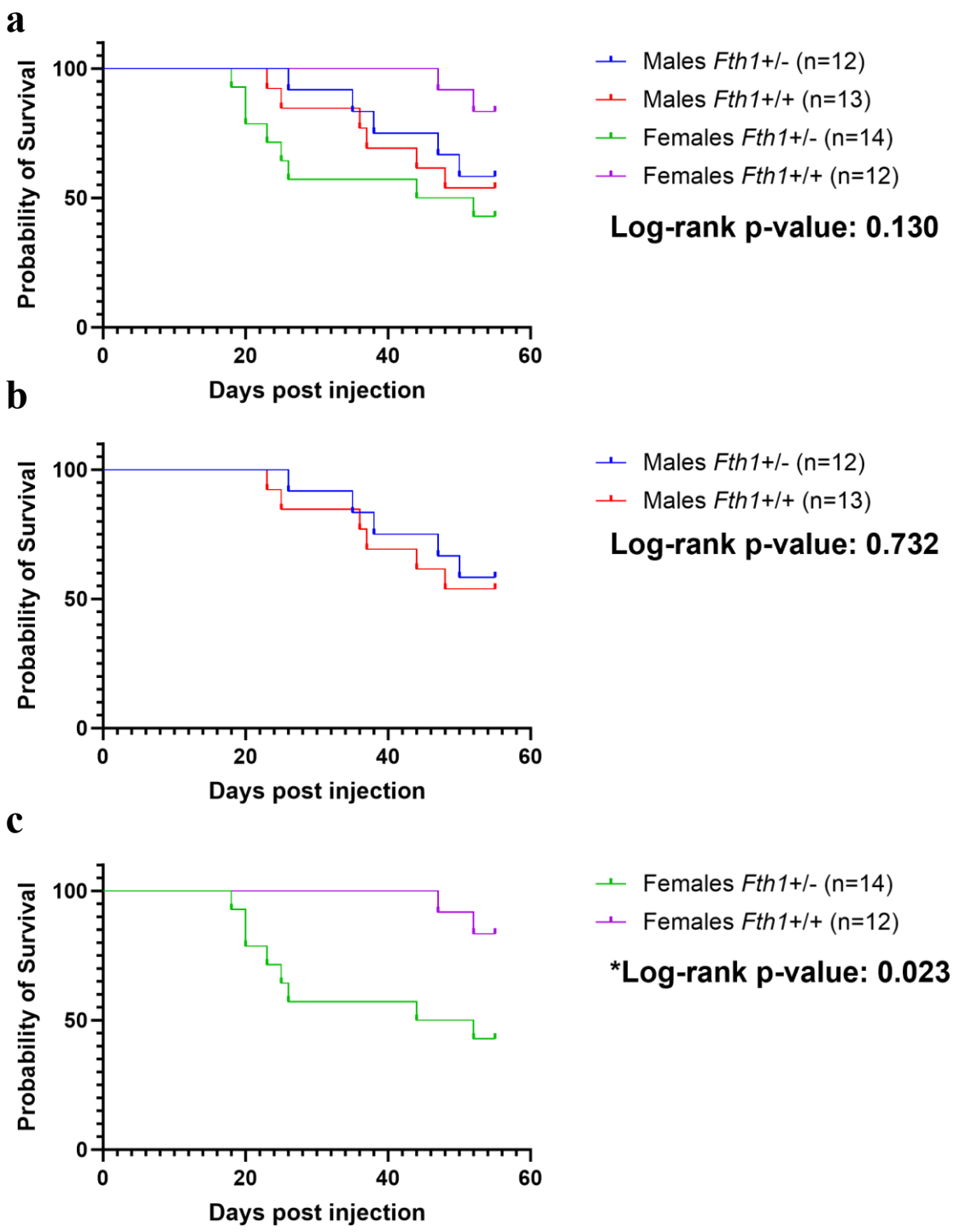

Fig. 4-1 Heterozygous *Fth1* knockout abrogates survival benefit of the female sex in GBM mice model (a) Survival outcomes in the mice GBM model, (b) there was no survival difference between the male mice with *Fth1*+/- and *Fth1*+/+ genetic backgrounds, (c) female mice with heterozygous knockdown of *Fth1* had worse

survival outcome as compared to the female *Fth1*+/+ mice, Kaplan–Meier survival curves were compared by log-rank test. Not significant (ns), * $p < 0.05$, *** $p < 0.001$, **** $p < 0.0001$.

4.4.2 Fth1 +/- mice have altered tumor gene expression profiles

A total of 47 and 1265 genes exhibited altered expression in the *Fth1*+/- group versus the *Fth1*+/+ group in males and females respectively (Fig. 4-2 a, b). Among these DEGs, 46 (97%) and 1078 (85%) genes were upregulated in the *Fth1*+/- compared to *Fth1*+/+ male and female groups respectively (Figure 2, red dots) and 1 (3%) and 187 (15%) genes were downregulated in the *Fth1*+/- compared to *Fth1*+/+ male and female groups respectively (Figure 4-2, a, b; blue dots).

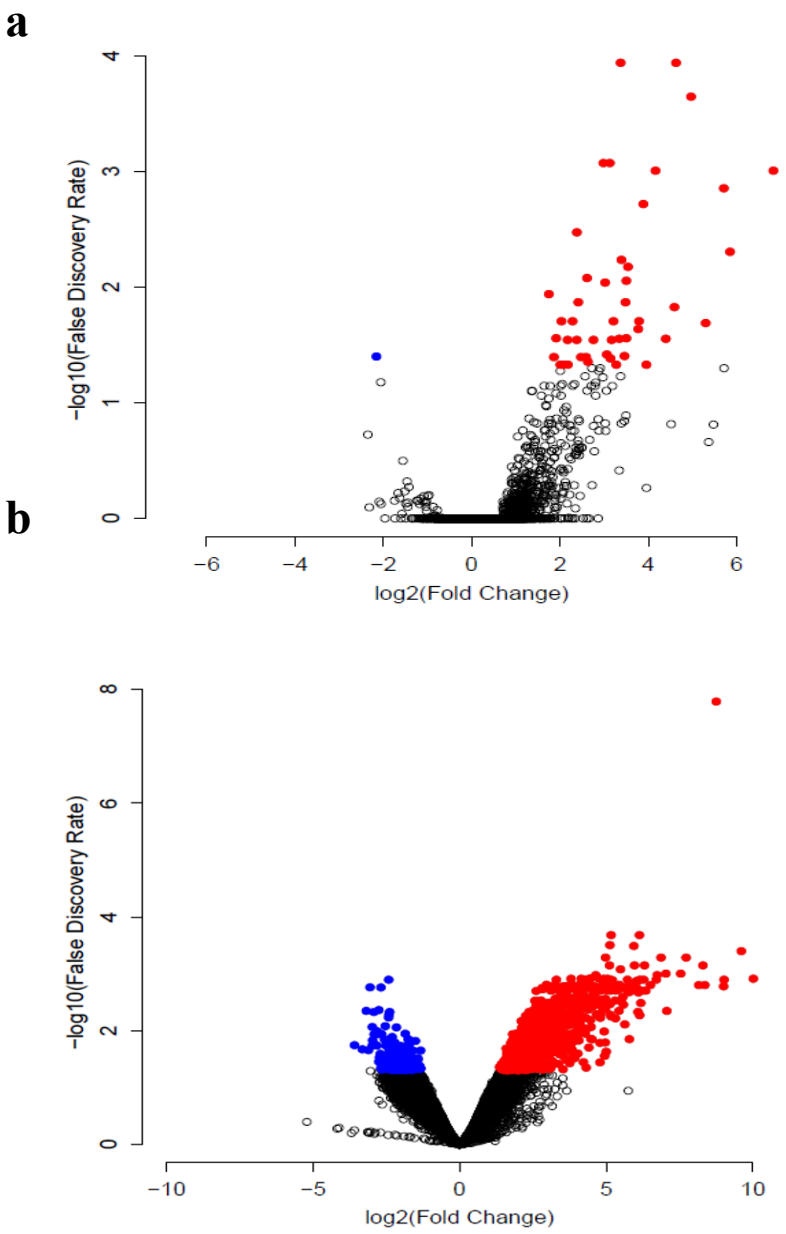

Fig. 4-2 *Fth1* +/- mice have altered tumor gene expression profiles

Volcano plot of the upregulated and downregulated DEGs. The volcano plot shows the upregulated and downregulated differentially expressed genes (DEGs) of the (a) male tumors and (b) female tumors, in the *Fth1*+/- and *Fth1*+/+ groups. For each plot, the x-axis represents the $\log_2$-fold change (FC), and the y-axis represents $\log_{10}$(False Discovery Rate FDR, q-value < 0.05). Genes with an adjusted p-value of less than 0.05 found with edgeR were classified as differentially expressed.

4.4.3 Pathway analysis: topGO and Gene Set Enrichment Analysis (GSEA)

We performed Gene Set Enrichment Analysis using a ranked list of all genes from GBM tumors in the males (Fig. 4-3 a) and females (Fig. 4-3 b) with *Fth1*+/- and *Fth1*+/+ genetic backgrounds. We observed that females with *Fth1*+/- had upregulation of genes involved in the activation of immune response including adaptive immune response, T cell-mediated cytotoxicity, and T cell proliferation as compared to females with *Fth1*+/+ background. Females with *Fth1*+/- also had gene signatures showing downregulation of GPCR signaling, miR-124-5p, miR-181-5p, hedgehog signaling, and fibroblast growth factor receptor signaling as compared to females with *Fth1*+/+. Males with *Fth1*+/- had upregulation of genes in the GPCR signaling, EMT pathway, hedgehog signaling, fibroblast growth factor receptor signaling, and angiogenesis pathways as compared to males with *Fth1*+/+ background. miR-124-5p and miR-181-5p are shown to inhibit proliferation and invasion in GBM cells [304–307]. Their downregulation in females and not in males highlights the heterogeneity in pathways impacted, due to heterozygous *Fth1* knockout, between males and females. Almost opposite gene signatures for GPCR signaling, hedgehog signaling, and fibroblast growth factor receptor signaling pathways which are implicated in evasion of growth suppressors, resistance to apoptosis, initiation of angiogenesis, and activation of invasion and metastasis of cancers, in both the sexes further signifies the sexual differences in modes of growth, survival, and progression in GBMs.

a

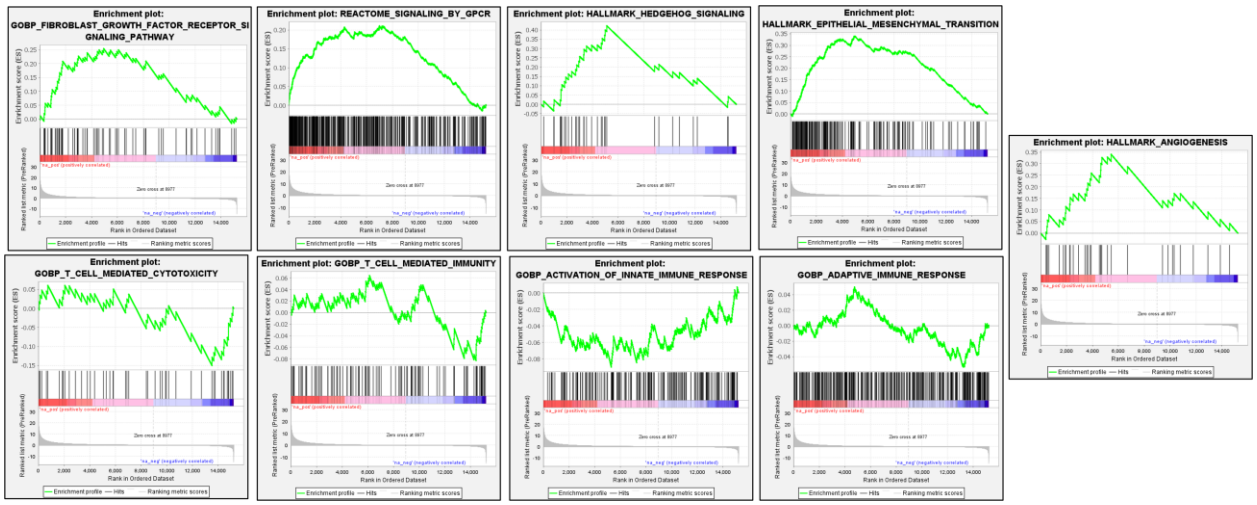

b

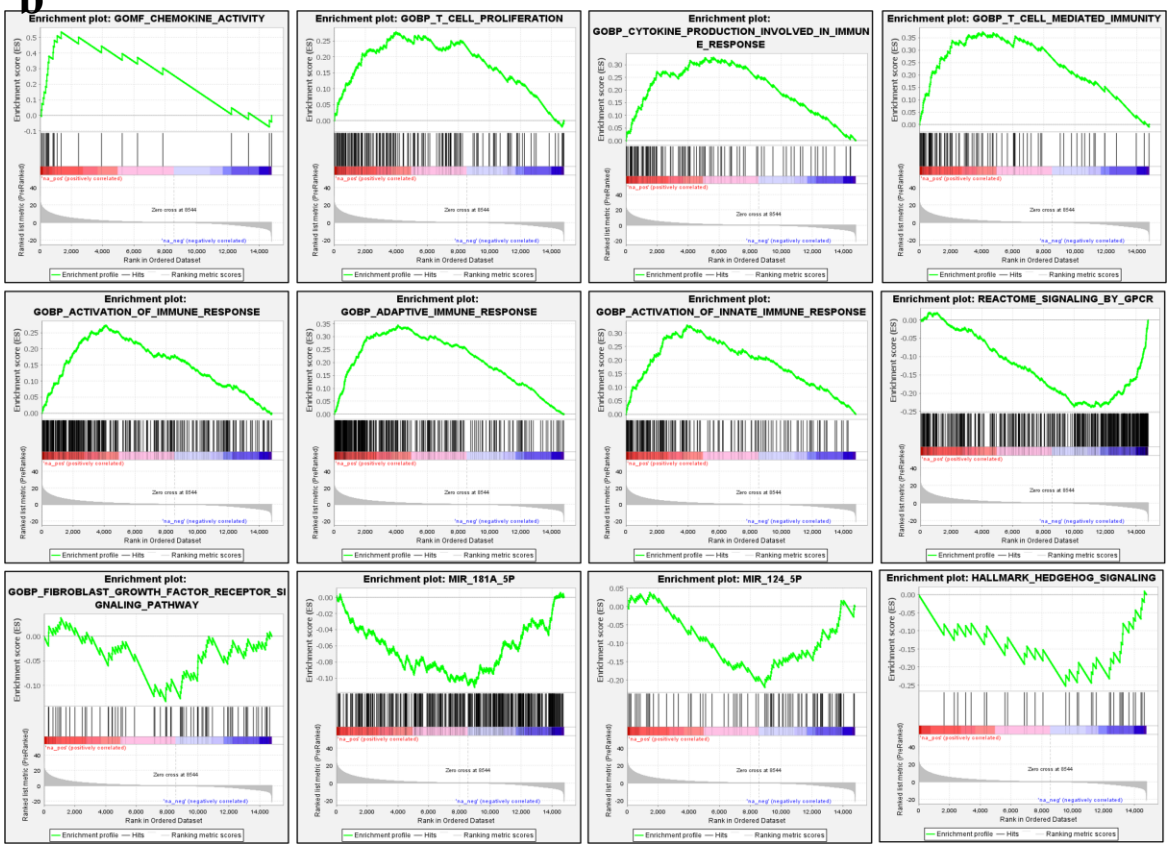

Fig. 4-3 Pre-ranked gene set enrichment analysis (GSEA) reports in males (a) In males GPCR signaling, EMT, fibroblast growth factor receptor signaling pathway, hedgehog signaling, and angiogenesis processes were found to be enriched in the upregulated genes between males *Fth1*+/- vs. males *Fth1*+/+. T-cell mediated cytotoxicity and immunity, and innate and adaptive immune response genes were found to be enriched in downregulated genes between males *Fth1*+/- vs. males *Fth1*+/+. (b) In females, immune response, adaptive and innate immune response, T cell activation proliferation and cytotoxicity along with chemokine and cytokine production processes were enriched in the upregulated DEGs between *Fth1*+/- vs. *Fth1*+/+. GPCR signaling, miR-124-5p, miR-181A-5p, hedgehog signaling, and fibroblast growth factor receptor signaling processes were enriched in the downregulated DEGs between *Fth1*+/- and *Fth1*+/+ groups.

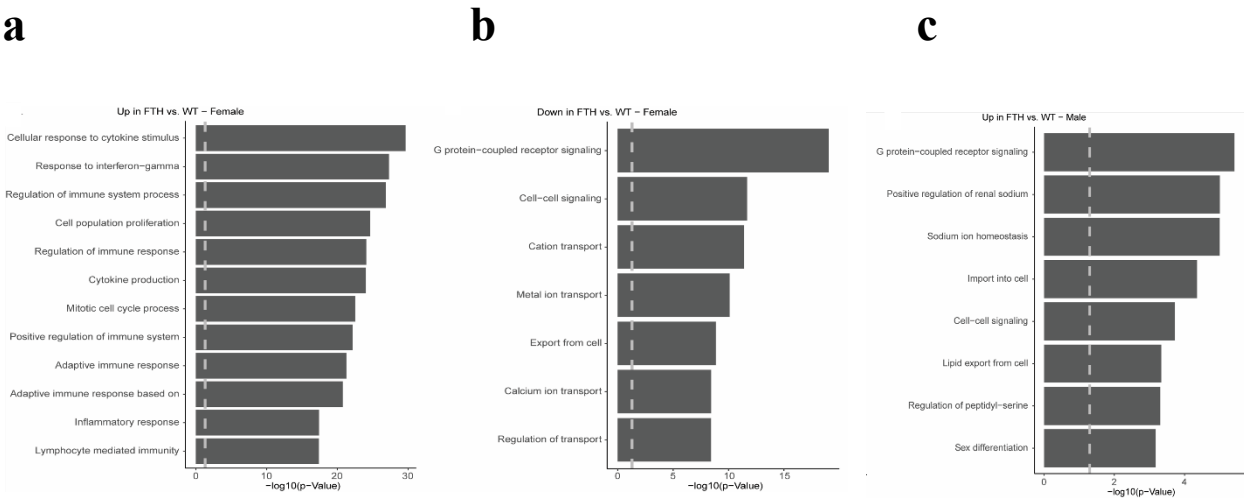

Fig. 4-4 TopGO analysis of differentially upregulated genes (a-c) TopGO Enrichment results of genes differentially upregulated in *Fth1*+/- vs *Fth1*+/+, observed separately in males and females. The bar plots show the top biological processes based on fold enrichment value (converted to log 2 scales). In female *Fth1*+/- vs. *Fth1*+/+, cellular response to cytokine stimulus, response to Interferon-gamma, regulation of immune system process, cell population proliferation, and regulation of immune response are the top 5 up-regulated processes. The top-downregulated processes in the same groups are GPCR signaling, cell-cell signaling, cation, and metal ion transport. In male *Fth1*+/- vs. *Fth1*+/+, GPCR signaling, cell-cell signaling, and cell import were some of the processes that were found to be upregulated. There were no significant down-regulated genes in males. For simplicity, *Fth1*+/+ are labeled as WT in the figures.

A complimentary topGO analysis (Fig. 4-4 a - c) on the differentially expressed genes (DEGs) further revealed that there was an upregulation of immune system-related genes in the female groups with *Fth1*+/- as compared to females with *Fth1*+/+ background. And the males with *Fth1*+/- had upregulation of GPCR signaling as one of the top pathways identified by the topGO algorithm as compared to males with *Fth1*+/+ background.

4.4.4 GBM in Fth1+/- females have significantly lower CD8+ T cell and higher mast cell infiltration

To determine whether *Fth1* +/- influenced the immune cell infiltration in the tumor, we used mMCP-counter analysis on the gene expression data obtained via RNA sequencing from the male and female mice with *Fth1*+/- and *Fth1*+/+ background. mMCP-counter analysis is based on the identification of highly specific transcriptomic signatures for each of the cell populations considered. We observed that there was a total of 4 cell types, out of the total of 15 that were analyzed, that had a significant difference between *Fth1*+/- and *Fth1*+/+ groups (Fig. 4-5 a, b).

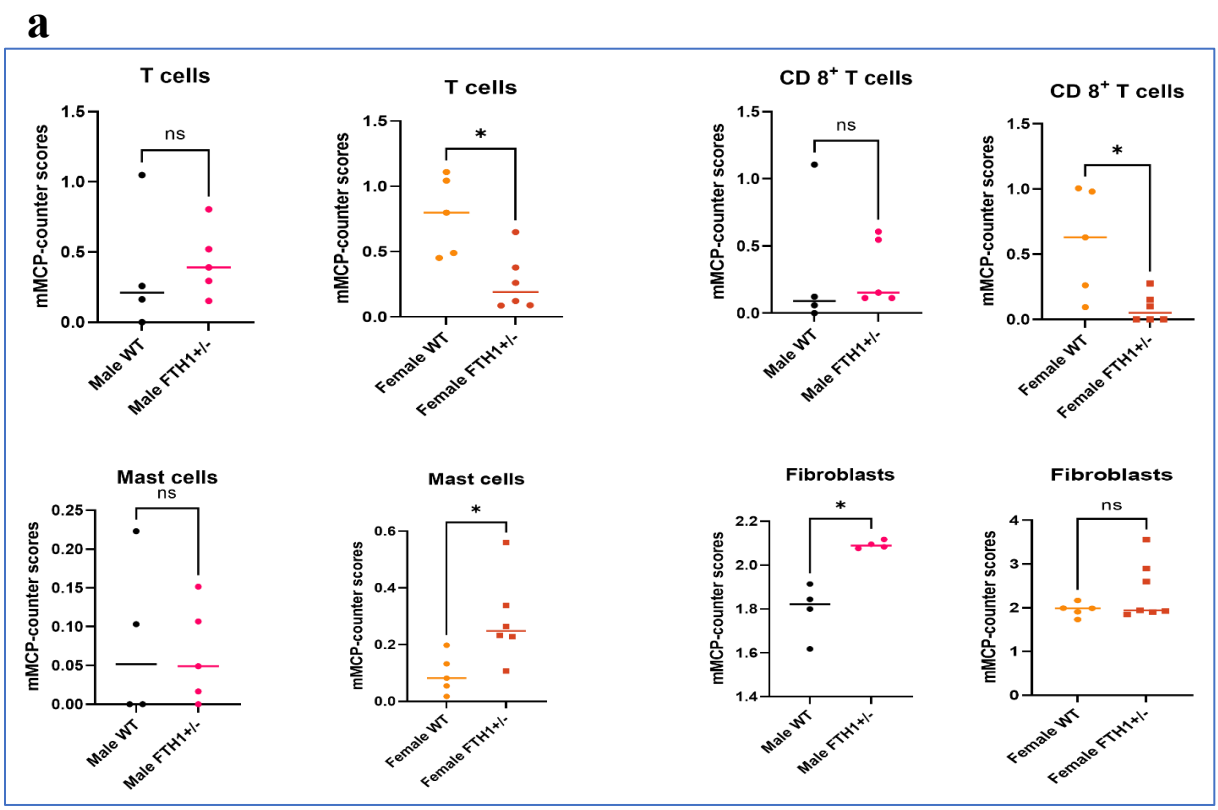

Fig. 4-5 GBM in *Fth1*+/- females have significantly lower CD8+ T cell and high mast cell tumor infiltration

The four groups of mice that were analyzed were male *Fth1*+/+, background (*Fth1*+/+, n = 4), male *Fth1*+/- heterozygous background (*Fth1*+/- n = 5), female *Fth1*+/+ background (*Fth1*+/+, n = 5), female *Fth1*+/- heterozygous background (*Fth1*+/- n = 7). mMCP Immune Scores were compared using the Mann-Whitney test. (a) Significant differences were observed between *Fth1*+/- and *Fth1*+/+, groups in female infiltration of T cells, CD 8+ T cells, and mast cells. In males, significant differences were observed between the *Fth1*+/- and *Fth1*+/+ groups in the fibroblast infiltration. (b) The other cell types had no significant differences between the groups. For simplicity, *Fth1*+/+ are labeled as WT in the figures. Not significant (ns), * $p < 0.05$, *** $p < 0.001$, **** $p < 0.0001$.

b

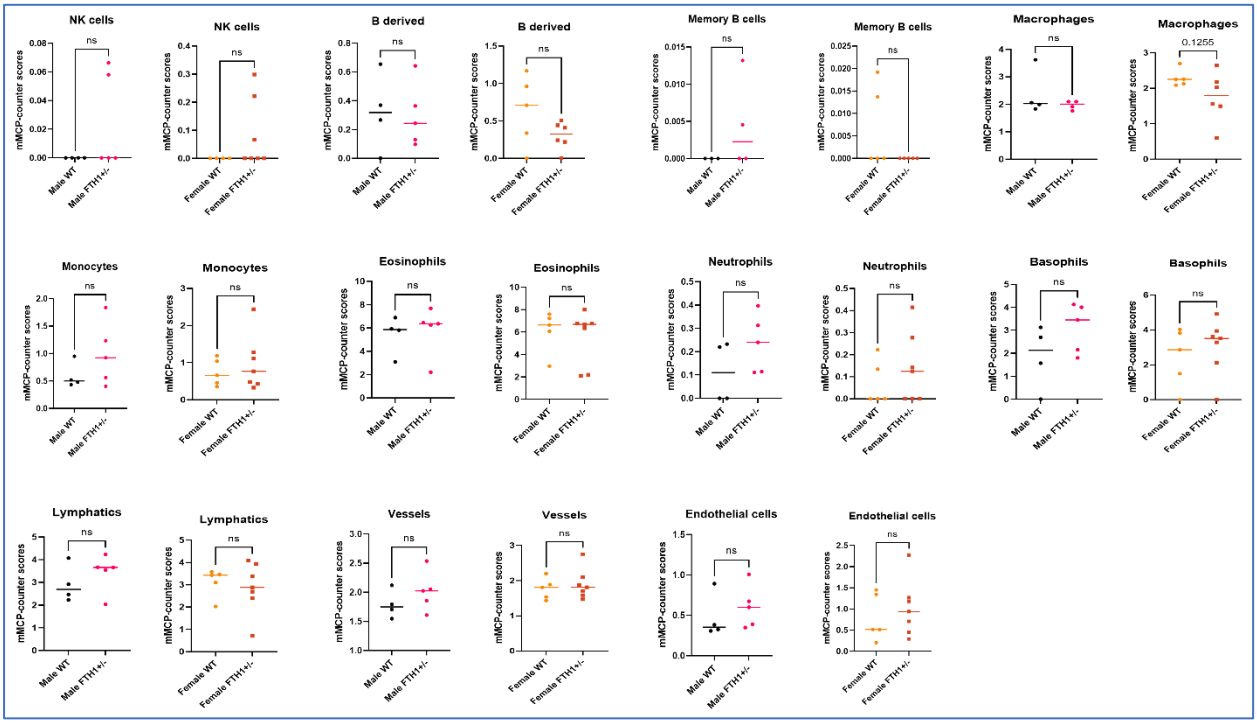

Female *Fth1*+/- mice had a significant reduction in tumor-infiltrating T cell and CD8+ T cell populations as compared to females with *Fth1*+/+ background. However, there was no significant difference in these two cell populations between male *Fth1*+/- and *Fth1*+/+ groups. Additionally, we observed that female *Fth1*+/- group had a significant increase in stromal cell population of mast cells as compared to the control groups. Whereas there was no difference in mast cell population between the male *Fth1*+/- and control groups. We also observed that male *Fth1*+/- group had a significantly higher population of the fibroblasts as compared to the male control group. There was no significant increase in fibroblast population between the female *Fth1*+/- and *Fth1*+/+ groups. To confirm that a reduction in the infiltrating T and CD8+ T cell profile is not due to the inherent reduction in the circulating T cells and CD8+ T cells due to *Fth1* +/- we performed flow cytometry analysis on the blood from the tumor-free mice (Supplementary Fig. S2 a-e). We did not observe any significant differences in the circulating T and CD8+ T cell populations in the blood of the mice suggesting that *Fth1* manipulation in the mice did not significantly reduce these cell types.

4.5 Discussion

The results of this study demonstrate that genetic manipulation of *Fth1* which alters FTH1 protein expression (two-fold reduction of protein in blood [293]) impacts survival in female mice but not in male mice with GBMs. Furthermore, we show that this genetic manipulation is associated with altered tumor infiltration of immune cells such as T-cells, and CD8+ T cells, and stromal cells such as mast cells and fibroblasts. More importantly, the influence on tumor infiltration of immune cells is sex biased.

FTH1 expression in tumor cells has been studied in multiple cancers, including GBM, and has been shown to be associated with GBM survival [116]. However, there are very few studies on the impact of FTH1 extrinsic to the tumor and its potential role in GBMs. Extracellular FTH1 has been shown to impact cellular invasion activity of GBM stem cells, thus suggesting a potential role of tumor extrinsic FTH1 levels in modulating tumor cell pathways. As mentioned earlier, the *Fth1* heterozygous knockout mice model used here has a 2-fold reduction in systemic H-ferritin levels [293], and the *Fth1* in tumor cells is not otherwise modified. This study thus provides a unique opportunity to analyze the genetic modulation of systemic *Fth1* extrinsic to the tumor and its role in mice GBMs.

Our data suggest that there is a significant and sex-biased modulation of the tumor microenvironment associated with the decreased *Fth1*. Extracellular iron levels in the tumor microenvironment have previously been shown to impact anti-tumor immune responses in breast cancer cells [20]. This raises a possibility that extracellular FTH1, which is a significant iron delivery protein, might also impact the anti-tumor immune response. Indeed, that is what we observed in our unbiased topGO and GSEA pathway analyses. We observe that pathways related to the regulation of immune system processes and immune responses were greatly upregulated in the tumors of mice with the *Fth1*+/- background as compared to *Fth1* +/+ background. Moreover, these pathways were influenced by the sex of the animals with females having an activation of the immune related genes whereas males showing downregulation of these genes. To further analyze the relationship between the role of tumor extrinsic *Fth1* and the tumor microenvironment immune landscape we used the mMCP deconvolution algorithm to determine whether *Fth1* impacted infiltrating immune and stromal cell populations.

In our mMCP analysis, we identified 2 immune infiltrating cell populations, T and CD8+ T cells, that were significantly affected in the mice with *Fth1*+/- genetic background. We further observed that these effects were sexually biased where females with *Fth1*+/- had significantly reduced infiltration of T and

CD8+ T cells as compared to females with *Fth1*+/+. Our results support recent research on reduced T and CD8+ T cell infiltration associated with reduced survival in multiple different cancers, including GBM [10,36]. A question of the mechanism underlying our main finding of sex-biased survival is whether the effect is a direct effect of *Fth1* reduction on the tumor or an indirect effect of *Fth1* reduction influencing the immune system. In a study by L. Vanoaica *et al*., it was shown that conditional deletion of *Fth1* in mice T cells reduced the number of peripheral T cells in all lymphoid organs [309]. It was further demonstrated that reduced *Fth1* reduced T cell expansion by increasing labile iron pool and reactive oxygen species ultimately increasing the oxidative stress on the T cells [37]. This could mean that a similar mechanism is contributing to the overall reduction in T and CD8+ T cells, leading to the observed reduction in the infiltration of these cell types in the tumors, in this study. However, this is unlikely the major cause of the reduction in infiltration observed here because in the same model of conditional deletion of *Fth1*, increased proliferation of mouse T and B cell populations due to increased availability of labile iron pool was also seen. Increased proliferation of the cells counterbalanced the total reduction in the number of these cells making reduction of the cell population minimal. In our study, we observe upregulation of chemokine and cytokine production related genes in females with *Fth1*+/- knockdown as compared to controls further suggesting that a reduction in the T cells is an unlikely explanation in our findings. This suggests a possibility that the reduction In infiltration of T cells in *Fth1*+/- female GBM tissue is not a result of simple decrease in the T cell numbers. Additionally, our flow cytometry data establishing the baseline levels of circulatory T and CD8+ T cells, in the blood of these mice, further suggests that *Fth1* manipulation in these mice does not cause an inherent reduction in the number of these cells which could thereby reflect as low infiltration within the tumors.

The intratumoral cellular heterogeneity in GBMs also receives a significant contribution from stromal cells such as mast, endothelial, and fibroblast cells [38,39]. The specific role of mast cells (MCs) in tumorigenesis largely varies depending on the type of cancer. For example, MCs play a pro-tumorigenic role in thyroid [40] and prostate cancer [41] and their infiltration is associated with poor prognosis in these cancers [42,43]. Conversely, increased MC infiltration has been associated with a pronounced survival advantage in non-small-cell lung cancer [44]. In a previous study, MC infiltration was shown to contribute to glioma progression [42]. In our study, *Fth1*+/- females had a significantly higher infiltration of mast cells supporting the existing literature on pro-tumorigenic nature of MCs in gliomas. Increased MC along with reduced T and CD8+ T cells could be contributing to an aggressive phenotype in female *Fth1*+/- mice leading to overall poor survival outcomes. However, the exact molecular mechanisms of MC infiltration, its crosstalk with other immune components including T and CD8+ T cells, and its impact on tumor progression or overall survival are not clearly understood. One possibility could be the

promotion of tumor angiogenesis by MCs, which is well in line with the observed function of MCs in some other cancers such as squamous cell carcinoma [45]. MCs have been shown to secrete or activate angiogenic factors and ECM-degrading proteases such as matrix metalloprotease 9 (MMP-9) that could directly or indirectly degrade extracellular matrix (ECM) components thereby supporting vasculature growth [45]. Because of infiltration of MCs to the site of tumors is highly dependent on the tumor microenvironment and chemoattractants secreted from the tumors, we theorize that *Fth1* downregulation in female brains could be facilitating a tumor microenvironment for GBM growth, proliferation, and aggressiveness [46]. This might mean that *Fth1* is acting as a negative regulator of GBM tumors in females but has no such role in male tumors. Our observation of increased fibroblast cells in males with *Fth1*+/- but not females further highlight sex-specific intertumoral heterogeneity associated with *Fth1* expression levels. Fibroblast levels have been directly correlated with GBM epithelial-mesenchymal transition (EMT) [47], a regulatory mechanism implicated in the progression of GBMs; additionally, higher fibroblast levels were associated with worse prognosis [48]. In our study, males with *Fth1*+/- background had significantly higher levels of fibroblast infiltration while females with *Fth1*+/- (which also have poorer survival outcomes) did not. This shows that fibroblasts' association with poorer survival outcomes is specific to male GBMs but not females, further highlighting sex-specific differences in potential GBM progression mechanisms.

Lastly, it should be noted that the heterozygous *Fth1* knockout mice used in this study are healthy and do not present any apparent abnormalities but do have high levels of serum L-ferritin [22,49]. L-ferritin (FTL) is the L-chain polypeptide that combines with H-ferritin in a tissue-dependent manner to form the 24-polypeptide ferritin protein. Higher L-ferritin expression in tumor tissue, particularly in the infiltrating tumor-associated macrophage population, has been significantly correlated with high tumor grade and poorer GBM survival [50,51]. There was no significant increase in the number of infiltrating macrophages in the tumors that would have contributed to the poorer survival in the female *Fth1*+/- mice. Thus, it is unlikely that the elevated serum L-ferritin contributed to the differences observed in our study.

4.6 Conclusions

This study links the expression of extracellular FTH1, the immune system, and GBM survival and reveals that the relationship is sex biased. Sex-specific differences in iron metabolism, immune cell function and GBM survival are established. Importantly, this study uses a unique animal model to begin to identify the role of FTH1 as a specific and key component of that relationship indicating its importance, on a sex-

basis. When taken into consideration with our previous report that FTH1 binds to human brain tumors [19] and delivers iron to cancer cells in culture resulting in limiting their migration, the data herein are consistent with the loss of FTH1 in vivo promoting decreased survival. Moreover, this in vivo study further elucidates the role of FTH1 in tumor biology by revealing a sex effect and an effect on the tumor microenvironment.

Chapter 5 : Overarching Themes of the Role of FTH1 in GBMs

5.1. Summary of Main Findings of Dissertation

My thesis focuses on the role of ferritin in Glioblastoma (GBM) biology. The main findings from this body of work have revealed that H-ferritin plays a significant role in GBM tumors with an underlying premise of sexual bias in its role and effects.

In the first chapter, I have provided a comprehensive view of the role of ferritin in cancers. H-ferritin has been shown to impact angiogenesis, EMT, proliferation, therapeutic resistance, and many other hallmarks of cancer. In the same chapter, I also underscore multiple gaps in our understanding of the underlying mechanisms/biology of ferritin's role in multiple cancers including GBM. One such gap is in the understanding of H-ferritin's role in iron delivery to cancers. One of the roles of H-ferritin is to deliver iron to multiple cell types and organs. Considering cancer cells are iron-addicted, and ferritin carries significantly more amount of iron than Transferrin (a canonical iron acquisition protein), suggests a possibility of potential exploitation of this protein by iron-hungry cancer cells to acquire surplus iron.

With the above knowledge in mind, we hypothesized that GBM cancer stem cells might uptake H-ferritin protein for their iron needs. To test this hypothesis, I studied the binding and uptake of H-ferritin protein in human tumor membranes, and GBM cancer stem cells (GBM CSCs), in my second chapter. I showed that GBM male human tumors bind to H-ferritin significantly more than female tumors. I further showed that GBM CSCs uptake H-ferritin potentially via the TfR receptor. More interestingly, I found that the uptake of H-ferritin leads to diminished invasion capacity of the GBM CSCs. With this chapter, I demonstrated that GBM tumors and cells take up H-ferritin protein and that H-ferritin can deliver the iron payload it is carrying to the GBM cells. This ability of H-ferritin in delivering its payload to GBM cells has ramifications beyond just the biology of GBM tumors and is described in the coming sections.

In the next chapter, I investigated if known modulators of iron acquisition, HFE, and sex impacted the uptake of H-ferritin and TF proteins. Although my reports on HFE's role in mice survival were consistent with the existing literature, I showed that HFE did not significantly impact the uptake of the H-ferritin and Transferrin proteins in GBMs. I also showed although the binding of H-ferritin and Transferrin on human tissues is impacted by sex its uptake in mice models is not. The most important takeaway from this chapter is that the significant role of HFE in survival is driven by mechanisms other than just iron uptake by H-ferritin and Transferrin protein.

Lastly, my fourth chapter extends the H-ferritin research beyond the context of tumors i.e., it investigates whether tumor extrinsic H-ferritin levels impact GBM outcomes. In this chapter, I show that tumor extrinsic downregulation of *Fth1* in mice impacts survival in female mice but not male mice. Upon further investigation, I identified significantly reduced tumor infiltration of CD8+ T and T cell immune populations along with an increased mast cell infiltration in the female tumors with extrinsic *Fth1* downregulation as compared to female tumors with control *Fth1* levels.

I have distilled my thesis project into two broad themes and will explore them in this final chapter: (1) the relevance of ferritin in iron acquisition and its functional impact on cancers (2) H-ferritin and its role in tumor microenvironment modulation. Both these themes will be discussed with an underlying and parallel theme of sexual dimorphism observed in this thesis.

5.2 The relevance of ferritin in iron acquisition and its functional impact on cancers

To understand the relevance of H-ferritin uptake I would like to briefly go over the different modes of iron uptake by a cell. Iron is a critical nutrient required by the cells for their DNA repair and synthesis, mitochondrial functioning, and functioning of the various enzymes in the cells [235]. There are three modes of iron uptake by a cell: free iron uptake, iron uptake bound to transferrin protein, and iron uptake bound to ferritin protein [21]. These modes of iron uptake are activated in the cells depending on its type and context and can exist side-by-side in the cells. For example, free iron uptake is mainly seen in the

intestinal cell types, and in astrocytes and neurons during inflammation, transferrin bound iron uptake is seen in almost all cell types in the body, and ferritin uptake has been shown in multiple organs including brain[253,322]. Ferritin uptake has also been shown in some cancer cell lines such as K562[27,271]. Macrophages and hepatocytes on the other hand have been shown to acquire iron by all three mechanisms described above [235,253]. In terms of context dependence, iron requirements are higher during developmental stages and in cancer cells which have rapid turnover of nutrients [12]. Free iron uptake and iron uptake by the Tf/TfR axis has been studied widely in the literature but very little is known about ferritin mediated iron uptake. My thesis for the first time shows that H-ferritin can function as an iron delivery protein for Glioblastoma (GBM) stem cells. Glioblastoma stem cells are a small population of cells within the GBM tumors that play important roles in mediating cellular heterogeneity, disease recurrence, tumor growth, and response to therapeutics [90]. Many different cancers and cancer cell types have been known to be iron-addicted with higher needs of iron for their functioning. Uptake of H-ferritin which can carry significantly higher amounts of iron as compared to transferrin highlights the underlying mechanism deployed by cancer cells to acquire increasing iron amounts from the tumor microenvironment.

The mode of iron uptake, by a cell, also depends on the availability of the form of the iron in its microenvironment. This is highly important when studying glioblastoma because the GBM tumor microenvironment can be rich in extracellular H-ferritin. The source of ferritin in the GBM tumor microenvironment could be from the microglia, infiltrating macrophages, astrocytes, neurons, oligodendrocytes, and the extracellular ferritin pool from serum and cerebrospinal fluid[193,323]. Macrophages are a major source of secreted ferritin which can be detected in the serum and the cellular microenvironments. Hence, tumor associated macrophages (TAMs) which comprise around 30-40% of the GBM tumors could serve as a major source of ferritin in the tumor microenvironment. Additionally, the ferritin secreted by the macrophages is known to be iron rich, like the intracellular form of the ferritin, and has a higher H:L ratio. Moreover, tumor cells have shown increased proliferation in presence of ferritin from macrophages[109,235,324].

In my study, I show a reduction in the invasion capacity of the GBM stem cells and observe no significant change in the proliferation capacity of the cells. Although, it is not clear at this point of time whether these effects are strictly due to increase in labile iron pool of the cells or are due to non-iron dependent mechanisms of H-ferritin. However, the reduction in invasion capacity can be explained by more than one theory: (1) the ‘go or grow’ hypothesis; this hypothesis proposes two alternative fates for cancer cells within a tumor: invasive migration or cell proliferation. It suggests that cancer cells must make a critical

decision between two distinct phenotypic states: they can either adopt a highly proliferative state to promote tumor growth or switch to a migratory state to facilitate invasion and metastasis. According to this hypothesis, when resources such as nutrients and oxygen are limited within the tumor microenvironment, cancer cells face a trade-off between proliferating and invading. In favorable conditions with sufficient resources, cancer cells predominantly undergo cell division, leading to increased tumor growth. However, in conditions of limited resources or other unfavorable microenvironmental cues, cancer cells may switch to a migratory and invasive phenotype[325,326]. (2) Source of ferritin impacting the functional outcome; For example, ferritin secreted by cultured newborn mouse astrocytes did not stimulate apoptotic activity in GBM cells as opposed to the ferritin derived from the GBM cancer cells themselves[327]. Also, as I mentioned earlier, ferritin secreted by macrophages increased the proliferation of the cancer cells, but the ferritin utilized in this study did not. Moreover, most of the existing literature on the role of iron in cancer has been focused on understanding the proliferation capacity of the cells. Our study on GBM cancer stem cells studying invasion is one of the few studies that has investigated cell functions other than proliferation. In line with this another study from our lab has recently shown that GBM cells show reduction in invasion capacity upon increased iron uptake. This suggests a novel role of ferritin and iron in invasion capacity of the cells. All in all, the reasons for differences in the functional implications of ferritin uptake from different sources are not clear and neither is the clinical and pathophysiological significance at this point of time but do suggest a complex biology of GBM tumor cell iron acquisition and functional regulation via ferritin and iron.

Additional complexity in iron regulation and homeostasis in GBM is contributed by the sex of the patient. Due to their biological makeup women tend to lose iron stores through menstruation, pregnancy, and hormonal effects while men usually have higher iron stores than women [328]. A consequence of increased iron stores in men is high serum iron levels, mainly represented via high circulating ferritin levels, which have been associated with increased cancer risk [329]. Increased availability of circulating ferritin in men could suggest a possibility that tumors in males adapt iron acquisition mechanisms that help them tap into these easily available iron stores aka circulating ferritin. Moreover, pre-existing cellular iron status of K562 cells was shown to significantly affect the capacity of the cells to restore the equilibrium of their labile iron pool (LIP) post iron acquisition [139,330]. This suggests a possibility that pre-existing iron status in males and females' cells could further drive the differences in iron acquisition and homeostasis mechanisms in their cancer cells.

Overall, this theme establishes that cancer cells can uptake H-ferritin from the extracellular milieu and that there is a possible sex difference in its uptake. It highlights the dynamic nature of cancer cells and their ability to adapt to changing microenvironmental conditions. Targeting the signaling pathways involved in the decision-making process of cancer cells' ability to acquire iron could potentially lead to the development of novel therapeutic strategies aimed at inhibiting them.

5.3 H-ferritin and its role in tumor microenvironment modulation

My second and third chapter showed that extracellular H-ferritin can enter GBM cells, and that post entry has functional implications on the cells. This suggested that ferritin levels in the extracellular milieu of the GBM cells can modulate functional behavior of the cells. To understand if this was the case in vivo, I utilized a novel mice model, in my fourth chapter, which has a systemic H-ferritin heterozygous knockdown. With the aim to understand the role of tumor extrinsic H-ferritin in tumor development, I orthotopically injected these mice with tumor cells that had no modification in their H-ferritin levels. Survival studies with these GBM mice showed that reduction in systemic H-ferritin causes a significant decline in female mice's survival as compared to the control H-ferritin female mice. Whereas male mice do not have any effect on their survival. Further analyses of the tumors showed a significant reduction in T cells, CD8+ T cells, and a significant increase in mast cells in the GBM tumors of the female mice with H-ferritin knockdown as compared the female mice with control H-ferritin levels. Reduction in infiltration of CD8+ T cells and T cells in human GBMs studies have been shown to be significantly associated with poor survival status[275,308]. On the other hand, the association between increased mast cell infiltration in GBM and patient survival is still a subject of investigation, and the findings are not yet conclusive. For example, some studies have suggested that increased mast cell infiltration in GBM is associated with poorer prognosis and shorter overall survival. These studies have reported that higher mast cell density within the tumor microenvironment is correlated with more aggressive tumor behavior, increased angiogenesis, and worse clinical outcomes [314,331]. Whereas some others have not found a significant association between mast cell infiltration and survival in GBM patients[332]. It is important to keep in mind that the studies examining mast cell infiltration in GBM, and survival outcomes have been relatively small and have used different methodologies, making it challenging to draw definitive conclusions. Additionally, GBM is a highly heterogeneous disease, and the role of mast cells may vary between individual patients. In our study we show that increased mast cell infiltration in the female GBMs is associated with poor survival in context of H-ferritin downregulation. Overall, our study suggested that tumor extrinsic levels of H-ferritin were modulating the infiltration of the T cells, CD8+ T

cells, and mast cells in the GBM tissues of females but not males. This is a highly novel finding in understanding GBM biology beyond just the tumor and its composition. This is also an interesting finding because females generally exhibit more robust immune responses compared to males, potentially impacting GBM progression. For example, females tend to have higher levels of certain immune cells, such as natural killer cells and dendritic cells, which play a role in tumor surveillance and elimination[333,334].

The differences in survival and immune cell infiltration between male and female mice, upon H-ferritin knockdown, could be explained by two inter-related theories: (1) Downregulation of H-ferritin impacts the proper functioning of the immune system in the females but not males suggesting a sex-biased role of H-ferritin in immune function, (2) H-ferritin has a protective function in the female mice brain which is abrogated upon its knockdown creating a neuroimmune microenvironment that facilitates aggressive growth and progression of GBM. H-ferritin's role in immune modulation has been studied previously. Its levels in macrophages and dendritic cells influence their activation and function[335]. It regulates the maturation and antigen-presenting capacity of dendritic cells, which are crucial for initiating immune responses[102336]. H ferritin has also been shown to inhibit the production of pro-inflammatory cytokines and promote an anti-inflammatory environment[337]. Furthermore, studies have demonstrated a connection between H ferritin and various immune-related disorders and diseases such as rheumatoid arthritis, and systemic lupus erythematosus[338]. It is important to note that the role of H ferritin in the immune system is still an area of active research, and further studies are needed to fully elucidate its mechanisms and functions. However, the available evidence suggests that H ferritin not only participates in iron homeostasis but also exerts immunomodulatory effects, highlighting its significance in immune responses and potential implications for immune-related disorders. In our study, H-ferritin downregulation affecting survival in females but not males not only highlight the sex-specific immunomodulatory effects of H-ferritin it also suggests female sex specific protective role of H-ferritin in the neuroimmune system between males and females. Neuroimmune sex differences refer to the observed variations between males and females in the interactions between the nervous system and the immune system. These differences involve the complex interplay between immune cells, such as microglia and various components of the neural system. Multiple reports have shown that there are sex-specific variances in the immune responses within the central nervous system[339,340]. These include differences in the activation and function of immune cells, the release of cytokines, differences in number, morphology, and gene expression profiles of microglia, and the overall regulation of immune processes in the brain[339]. Neuroimmune sex differences could provide insights into the susceptibility, prevalence, and progression of GBM between

males and females. It is possible that H-ferritin downregulation critically alters the neuroimmune landscape in females creating a microenvironment that is susceptible for GBM growth and progression.

It is important to note here that survival in GBMs is an outcome of complex inter-relationships between multiple factors involving heterogeneity, activation/deactivation of crucial pathways, immune system effects, overall baseline health of the patient, etc. However, identifying the pathways or mechanisms that have the highest contribution to impacting overall survival and therapeutically targeting them, thereby increasing the survival period of the patients, is the current goal of all the research carried out in this field. Our research is one step in this direction. Studying the protective mechanisms that ferritin might have in female brain and understanding the sex-specific role of H-ferritin in immune modulation can provide directions into regulation of iron/ferritin levels in the male system. Mirroring certain protective/beneficial survival mechanisms of females in males could be one therapeutic approach in increasing the survival and treatment outcomes of male GBM patients.

5.4 Conclusions

In summary, my thesis research has significantly contributed to our understanding of extracellular H-ferritin and its implications in Glioblastoma (GBM). The findings presented in this dissertation introduce H-ferritin, as an iron delivery protein capable of transporting iron to GBM stem cells. Moreover, my research has elucidated the systemic role of H-ferritin in regulating the tumor microenvironment, thereby emphasizing its significance in GBM biology. These studies have laid the groundwork for establishing H-ferritin as a key member of the iron delivery protein family specifically within Glioblastoma tumors. Moving forward, the next crucial step will involve exploring the therapeutic potential of this molecule and the potential to therapeutically target the pathways it modulates. Additionally, the uptake of H-ferritin in GBM stem cells, via TfR, opens doors to its application in targeted drug delivery, as discussed in detail in my first chapter. Further investigation into this area holds promise for developing innovative treatment strategies.

Overall, my thesis research has provided valuable insights into the role of extracellular H-ferritin in GBM, paving the way for future studies and potential therapeutic applications.

Supplementary to Chapter 2

Materials

Catalog numbers of the materials used in the research are as follows: Neurobasal™ medium without phenol red (Gibco, Cat # 12348017), 2% B27 without vitamin A (Gibco, Cat # 12587010), sodium pyruvate (Gibco, Cat # 11360070), GlutaMax™ (Gibco, Cat # 35050079), Isopropyl-β-D-thio-galactoside (IPTG, Sigma, Cat # I6758), Atto 647N NHS ester dye (Sigma-Aldrich, Cat # 765082), Human Tf conjugated with Alexa 488 (ThermoFisher Scientific Cat # T13342), Geltrex™ (ThermoFisher Scientific, Cat # A1413201), mountant containing DAPI (ThermoFisher Scientific, Cat # P36966), FerroFarRed ™ (Sigma-Aldrich, Cat # SCT037), StemPro™ Accutase™ Cell Dissociation Reagent (ThermoFisher Scientific, Cat # A1110501), eBioscience™ Flow Cytometry Staining Buffer (ThermoFisher Scientific, Cat # 00-4222-26), Chlorpromazine (CPZ) (Sigma, Cat # C8138), anti-TfR antibody (R&D Systems, Cat # AF2474, 25µg/ml receptor blocking), anti-Tim-1 antibody (R&D Systems Cat # MAB1750, 25µg/ml receptor blocking), IgG antibody (R&D Systems, Cat # AB-108-C, 25µg/ml receptor blocking). alamarBlue™ cell viability reagent (Thermo Fisher, Cat # DAL1100), Nunc™ 96-well, U-bottom plates (ThermoFisher Scientific, Cat # 168136), TGX gradient SDS gel (BioRad, Cat # 5671093), Rap1A antibody (Cell Signaling # 2399S, 1:1000) and β-actin (Sigma-Aldrich, Cat # A5441, 1:5000).

Methods

Recombinant H-ferritin preparation

BL21 *E.coli* was transformed with pET30a (+) vector containing human Hft gene and a 6X poly-His tag. Positive selection was performed in the presence of kanamycin antibiotic. Positive clones were induced to express Hft by Isopropyl-β-D-thio-galactoside (Sigma) induction. Bacteria were then lysed, and protein was purified via nickel columns (GE Healthcare). Total protein was quantified using bicinchoninic acid assay (BCA, Pierce). Hft was conjugated with Atto 647N NHS ester dye (Sigma) following manufacturer's protocol.

Radiolabeling FTH1 protein

^{125}I labeling of proteins was carried out as previously described[341]. Briefly, 1mci of ^{125}I (Sigma-Aldrich) was added to Iodogen tubes (ThermoFisher Scientific, Cat # 28601) containing 1X PBS to obtain an aqueous ^{125}I. Iodogen tubes contain oxidants [1,3,4,6-tetrachloro-3α,6α-diphenyl glycoluril, Iodogen,

which is known to reduce oxidative damage to the proteins during the radiolabeling process. The aqueous ^{125}I solution was incubated at room temperature for 5 minutes with occasional shaking. Next, 100µg of protein, H-ferritin was added to the tube and incubated at room temperature for 5 minutes with occasional mixing. The radiolabeling reaction was terminated with the help of a scavenger buffer, a saturating solution of Tyrosine, containing 10 mg/ml Tyrosine in Tris Iodination Buffer pH 7.5. Non-radiolabeled protein was removed by spinning the labeled mixture on a spin column (Roche, cat # 11274015001). Finally, the radiolabeled protein present in the flow through of the spin columns was collected and stored, in a lead box, at 4°C. Radioactivity of the radiolabeled protein was checked on Gamma 4000 Analyzer for a minute.

Supplementary Figure and Table Legends

Fig. S1 Uptake of Hft does not robustly impact proliferation To determine viability of the Hft treated GICs, (a) T387 and (b) T3691, alamarBlue™ cell viability reagent (Thermo Fisher) was used according to the manufacturer guidelines. Hft treatment, 0-300 µg/mL, was performed. at 24, 48, or 72 hours at 37°C. The fluorescence was measured at each time point i.e. 24h, 48h, and 72h, with excitation wavelength at 560 nm and emission wavelength at 590 nm on plate reader**.** No robust reduction was observed on cell proliferation assay. Results representative of at least n = 3 replicates. Two-way ANOVA (significance represented for 72 hours only) treatment: *: $p < 0.05$, **: $p < 0.01$, ***: $p < 0.001$, ****: $p < 0.0001$

Fig. S2 Rap1A expression is increased in GBM as compared to normal tissues and high Rap1A expression is significantly corelated with poorer survival Datasets were accessed using Gliovis (TCGA_GBM Agilent-4502 platform, http://gliovis.bioinfo.cnio.es) (accessed on 25 January 2023). (a) GBM tumors have high expression of Rap1A as compared to non-tumors (GBM n=489, non-tumors n=10). Student's two-tailed t-test: (ns) non-significant, *: $p < 0.05$, **: $p < 0.01$, ***: $p < 0.001$, ****: $p < 0.0001$. (b) High Rap1A level correlated with poor survival as compared to low Rap1A level. Rap1A Low: n = 245, events = 210, median = 14.5, Rap1A High: n= 243, events = 206, median = 14, HR = 0.96, (0.8 - 1.1). Kaplan–Meier survival curves were compared by log-rank test. Not significant (ns), * $p < 0.05$, *** $p < 0.001$, **** $p < 0.0001$.

Fig. S3 IRE sequence on 3'UTR of Rap1B mRNA Searching for Iron Responsive Elements

(SIREs) was used to identify potential iron-responsive element sequence on the 3' UTR of Rap1B mRNA transcripts. A characteristic hairpin loop and a stem structure of IRE, motif 16, sequence was identified. A C8 bulge typical of canonical IRE sequence can also be seen in the stem of the stem-loop structure.

Table S1 Demographic Information of the GBM patient cohort Patient information on median age, sex, whether received chemotherapy, genetic information, and location of the tumor in the brain. Genetic information includes: Isocitrate Dehydrogenase-1 (IDH1) wildtype status (patients negative for IDH1 R132H were considered IDH wildtype), % positive for Glial Fibrillary Acidic Protein (GFAP) staining, % positive for Oligodendrocyte Transcription Factor 2 (OLIG2) staining, % of p53 and % of Ki67 staining, and % positive for Grade IV classification of the tumors. The location of the tumor is according to the brain region in which the tumor was present at diagnoses.

Figures

Fig. S1

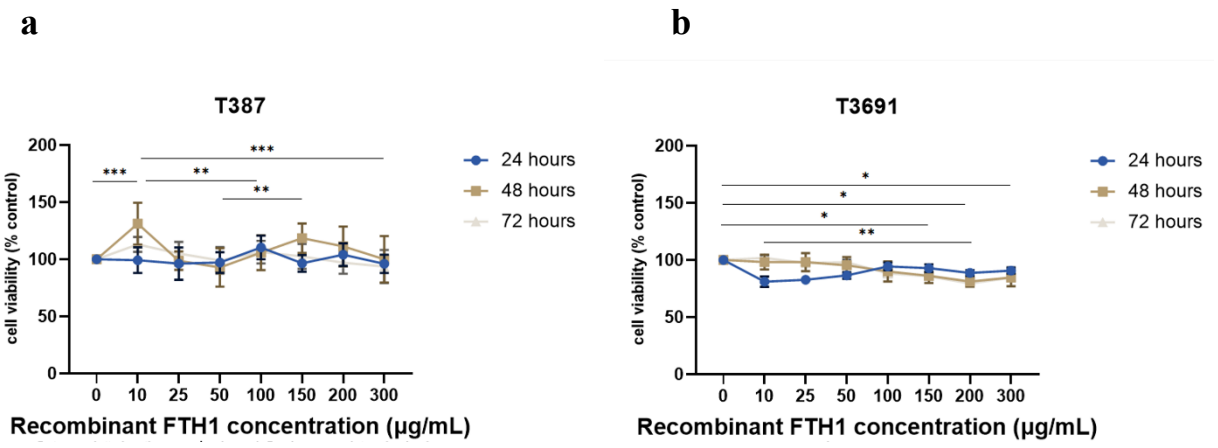

Fig. S2

a

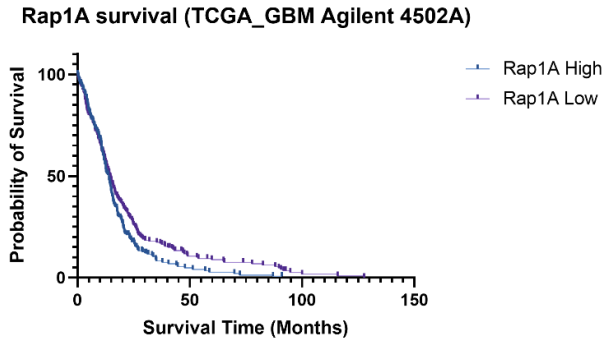

Rap1A Low: n = 245, events = 210, median = 14.5
Rap1A High: n= 243, events = 206, median = 14
HR = 0.96, (0.8 - 1.1),

b

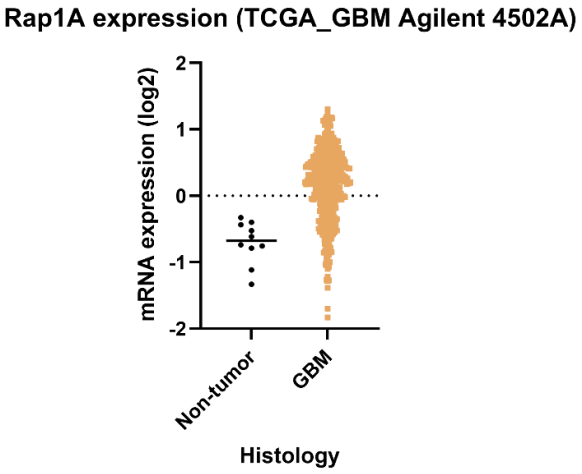

Fig. S3

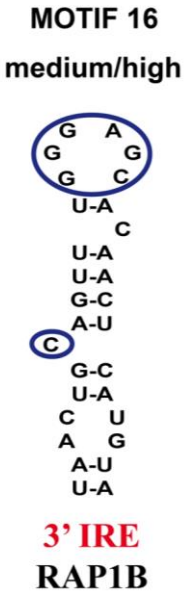

Table S1

	Male	Female
Number of Patients, n (% overall)	6 (50)	6 (50)
Continuous Variables		
Median age at Diagnosis	65.5	62
Treatment Status		
Received Chemotherapy, n (%)	2 (33.33)	0 (0)
Received Radiation, n (%)	2 (33.33)	0 (0)
Genetic		
IDH1 Wildtye, n (%)	6 (100)	3 (50)
Grade IV, n (%)	6 (100)	6 (100)
OLIG 2 +, n (%)	4 (66.67)	1 (16.6)
Average p53 nuclear labeling index	8%	12%
Average Ki67 nuclear labeling index	26%	28%
GFAP +, n (%)	6 (100)	3 (50)
Location		
Frontal lobe, n (%)	1 (16.67)	1 (16.67)
Parietal lobe, n (%)	1 (16.67)	0
Occipital lobe, n (%)	0	3 (50)
Left Temporal lobe, n (%)	2 (33.33)	1 (16.67)
Right Temporal lobe, n (%)	1 (16.67)	1 (16.67)

Supplementary to Chapter 4

Figures and Figure Legends

Fig. S1 Survival differences between male and female heterozygous *Fth1* knockout and control mice Survival outcomes in the mice GBM model, (a) there was no survival difference between the male and female mice with *Fth1*+/+ genetic backgrounds, (b) similarly, there was no survival difference between male and female mice with heterozygous *Fth1* genetic background. Kaplan–Meier survival curves were compared by log-rank test. Not significant (ns), * $p < 0.05$, *** $p < 0.001$, **** $p < 0.0001$.

Fig. S2 Circulating blood levels of T and Cd8+ T cells Circulating immune cells from male and female *Fth1*+/+ and *Fth1*+/- (n=3 animals in each group) groups were analyzed using flow cytometer (BD FACS Symphony). The gating for each individual replicate of the animal is represented (a) male *Fth1*+/+, (b) male *Fth1*+/-, (c) female *Fth1*+/+, (d) female *Fth1*+/-. The overall summary of the relative levels of T cell and CD8+ T cell in blood is represented in (e). We did not observe significant differences between the four groups. The groups were compared using one-way ANOVA. Markers used in the study are as follows:

Target	Fluor	Clone	BD catalogue #
CD45	APC	30-F11	559864
CD3	PE	145-2C11	553063
CD4	FITC	RM4-5	553046
CD8	BV421	53-6.7	563898
Viability stain	FVS780		565388

Figures

Fig. S1

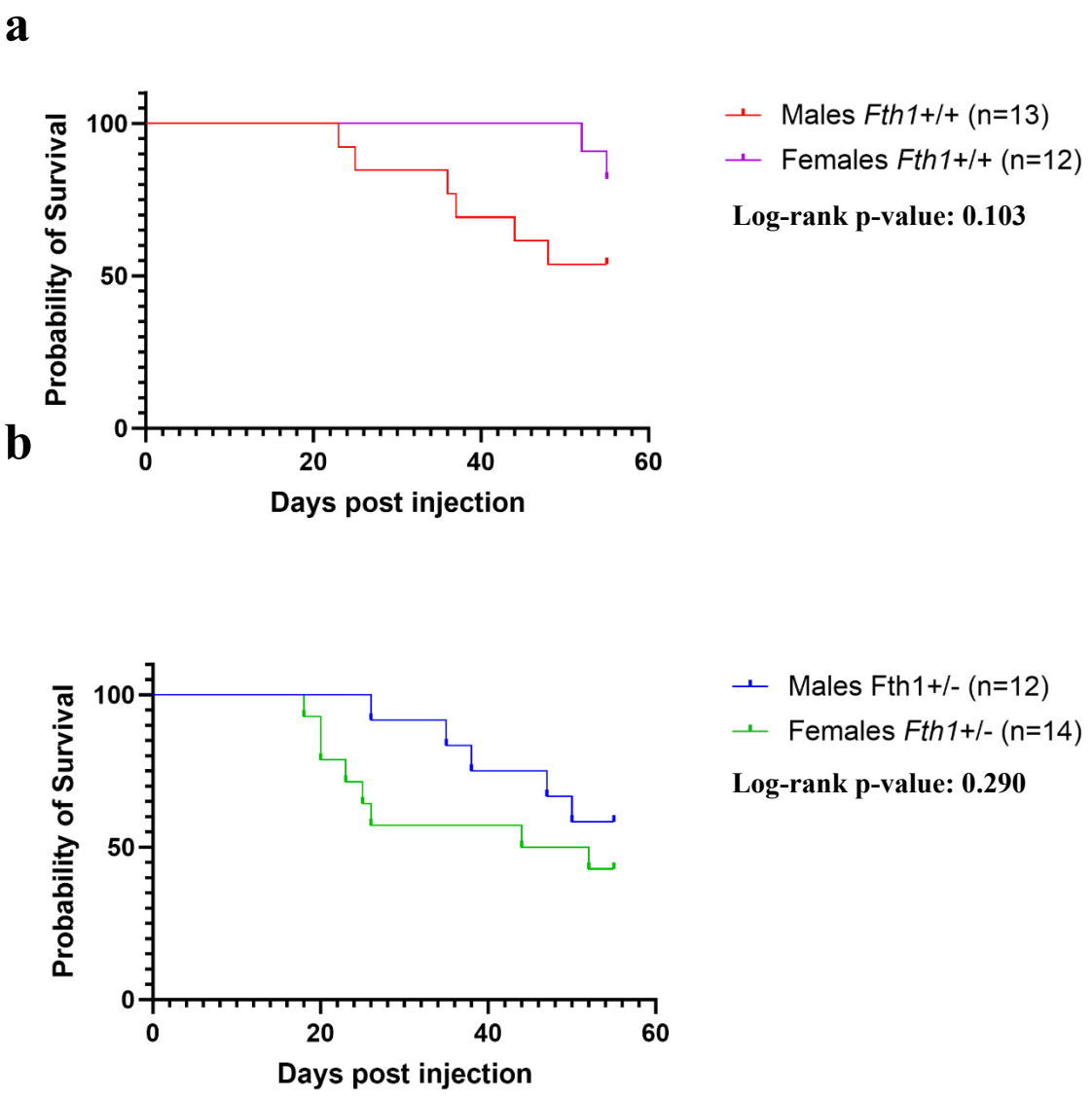

Fig. S2

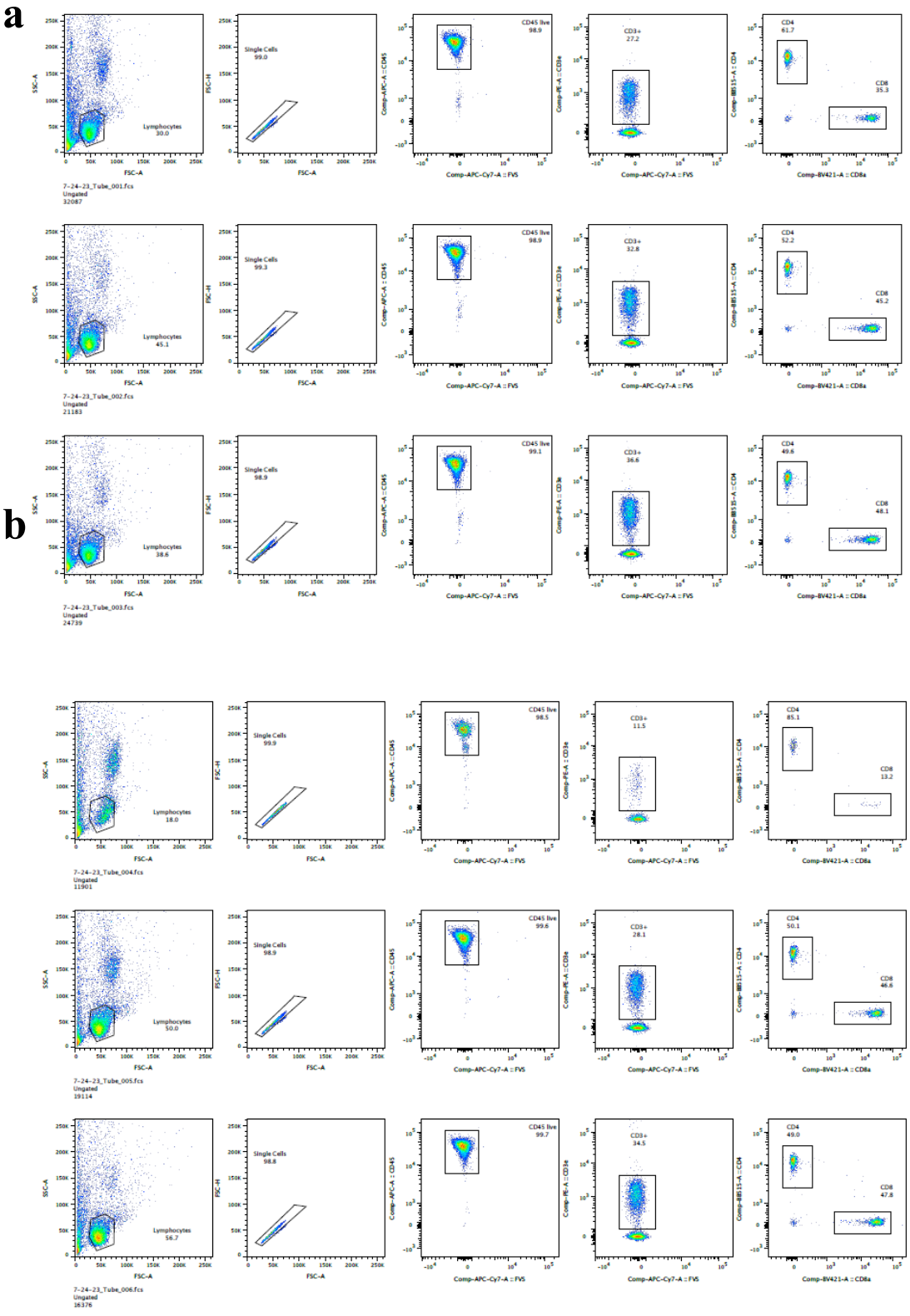
a
b
Lymphocytes
Single Cells
CD45 live
CD3+
CD4
CD8
FSC-A
SSC-A
FSC-H
Comp-APC-Cy7-A :: FVS
Comp-BV421-A :: CD8a
7-24-23_Tube_001.fcs
Ungated
32087
7-24-23_Tube_002.fcs
Ungated
21183
7-24-23_Tube_003.fcs
Ungated
24739
7-24-23_Tube_004.fcs
Ungated
11901
7-24-23_Tube_005.fcs
Ungated
19114
7-24-23_Tube_006.fcs
Ungated
16376

c

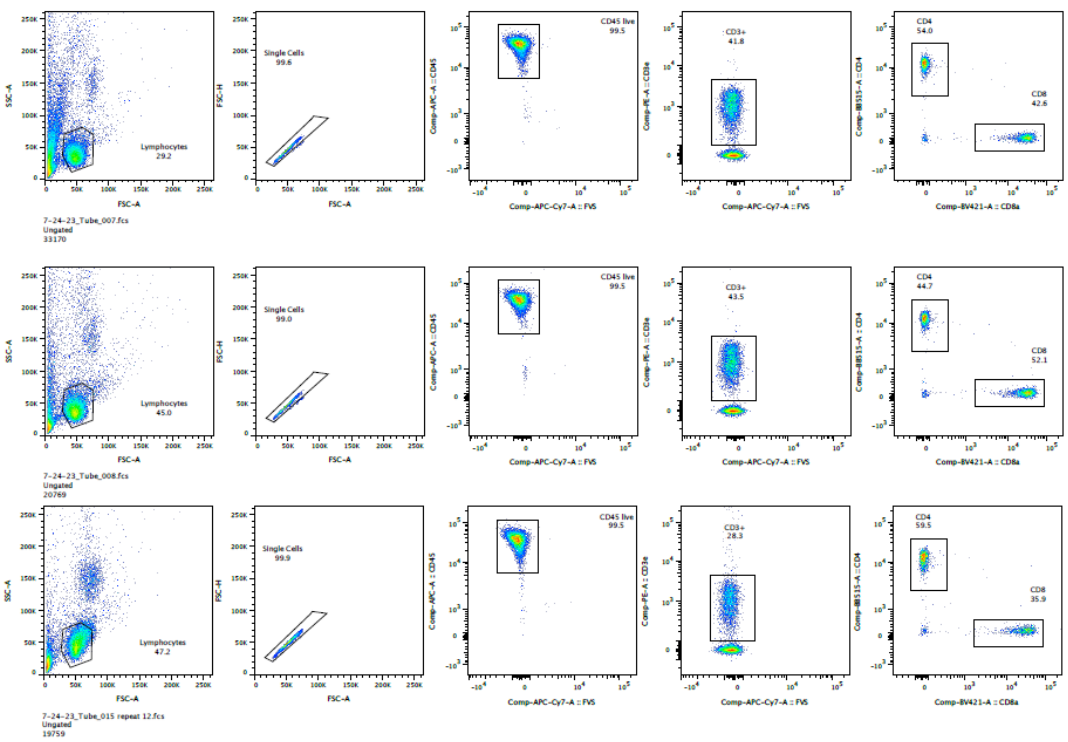
Lymphocytes 29.2
Single Cells 99.6
CD45 live 99.5
CD3+ 41.8
CD4 54.0
CD8 42.6
7-24-23_Tube_007.fcs
Ungated
33170
Lymphocytes 45.0
Single Cells 99.0
CD45 live 99.5
CD3+ 43.5
CD4 44.7
CD8 52.1
7-24-23_Tube_008.fcs
Ungated
20769
Lymphocytes 47.2
Single Cells 99.9
CD45 live 99.5
CD3+ 28.3
CD4 59.5
CD8 35.9
7-24-23_Tube_015 repeat 12.fcs
Ungated
19759

d

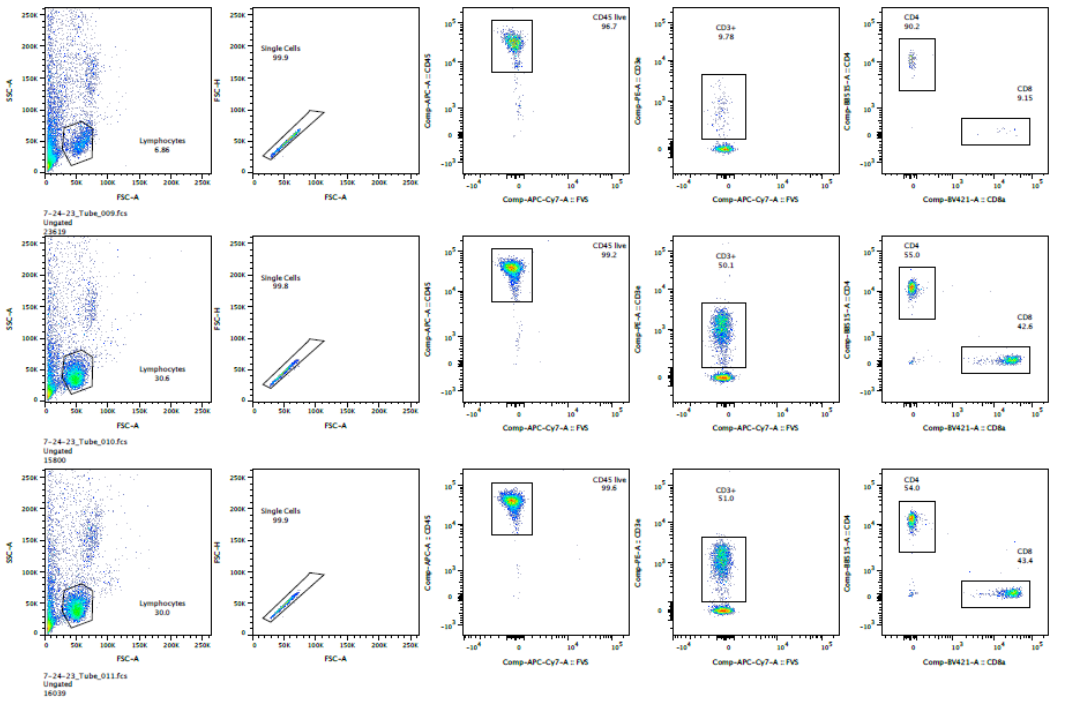
Lymphocytes 6.86
Single Cells 99.9
CD45 live 96.7
CD3+ 9.78
CD4 90.2
CD8 9.15
7-24-23_Tube_009.fcs
Ungated
23619
Lymphocytes 30.6
Single Cells 99.8
CD45 live 99.2
CD3+ 50.1
CD4 55.0
CD8 42.6
7-24-23_Tube_010.fcs
Ungated
15800
Lymphocytes 30.0
Single Cells 99.9
CD45 live 99.6
CD3+ 51.0
CD4 54.0
CD8 43.4
7-24-23_Tube_011.fcs
Ungated
16039

e

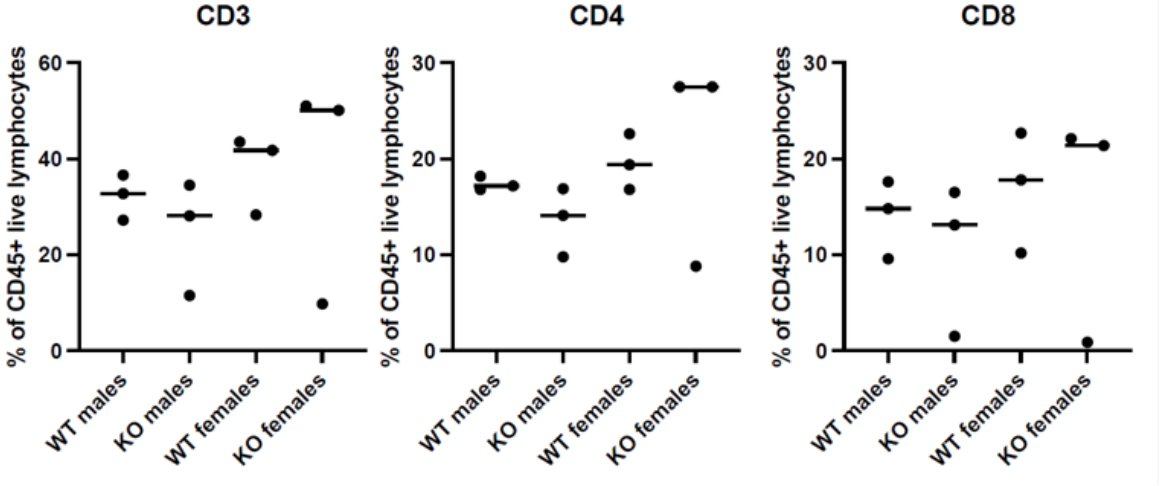
CD3
CD4
CD8
% of CD45+ live lymphocytes
60
40
20
0
30
20
10
0
WT males
KO males
WT females
KO females

References

1. Kim, M. *et al.* PH-dependent structures of ferritin and apoferritin in solution: Disassembly and reassembly. *Biomacromolecules* **12**, 1629–1640 (2011).
2. Lawson, D. M. *et al.* Solving the structure of human H ferritin by genetically engineering intermolecular crystal contacts. *Nat. 1991 3496309* **349**, 541–544 (1991).
3. Cairo, G., Rappocciolo, E., Tacchini, L. & Schiaffonati, L. Expression of the genes for the ferritin H and L subunits in rat liver and heart. Evidence for tissue-specific regulations at pre- and post-translational levels. *Biochem. J.* **275**, 813 (1991).
4. Pino, J. M. V. *et al.* Iron-restricted diet affects brain ferritin levels, dopamine metabolism and cellular prion protein in a region-specific manner. *Front. Mol. Neurosci.* **10**, 145 (2017).
5. Koorts, A. M. & Viljoen, M. Ferritin and ferritin isoforms I: Structure-function relationships, synthesis, degradation and secretion. *Arch. Physiol. Biochem.* **113**, 30–54 (2007).
6. Bradley, J. M., Moore, G. R. & Le Brun, N. E. Mechanisms of iron mineralization in ferritins: one size does not fit all. *J. Biol. Inorg. Chem.* **19**, 775–785 (2014).
7. Everett, J. *et al.* Iron stored in ferritin is chemically reduced in the presence of aggregating Aβ(1-42). *Sci. Rep.* **10**, (2020).
8. Hjelmeland, A. B. *et al.* Acidic stress promotes a glioma stem cell phenotype. *Cell Death Differ.* **18**, 829–840 (2011).
9. Torti, S. V. *et al.* The molecular cloning and characterization of murine ferritin heavy chain, a tumor necrosis factor-inducible gene. *J. Biol. Chem.* **263**, 12638–12644 (1988).
10. Knovich, M. A., Storey, J. A., Coffman, L. G., Torti, S. V. & Torti, F. M. Ferritin for the clinician. *Blood Rev.* **23**, 95–104 (2009).
11. Fisher, J. *et al.* Ferritin: A novel mechanism for delivery of iron to the brain and other organs. *Am. J. Physiol. - Cell Physiol.* **293**, 641–649 (2007).
12. Alkhateeb, A. A. & Connor, J. R. The significance of ferritin in cancer: Anti-oxidation, inflammation and tumorigenesis. *Biochim. Biophys. Acta - Rev. Cancer* **1836**, 245–254 (2013).
13. Zhang, C., Zhang, X. & Zhao, G. Ferritin Nanocage: A Versatile Nanocarrier Utilized in the Field of Food, Nutrition, and Medicine. *Nanomaterials* **10**, 1–25 (2020).
14. Honarmand Ebrahimi, K., Hagedoorn, P. L. & Hagen, W. R. Unity in the biochemistry of the iron-storage proteins ferritin and bacterioferritin. *Chem. Rev.* **115**, 295–326 (2015).
15. Gorobets, O., Gorobets, S. & Koralewski, M. Physiological origin of biogenic magnetic nanoparticles in health and disease: From bacteria to humans. *Int. J. Nanomedicine* **12**, 4371–4395 (2017).
16. Levisq, S. *et al.* Mechanism of Ferritin Iron Uptake: Activity of the H-chain and Deletion Mapping of the Ferro-oxidase Site. *J. Biol. Chem.* **263**, 180–18092 (1988).
17. Tosha, T. *et al.* Ferritin protein nanocage ion channels: Gating by N-terminal extensions. *J. Biol. Chem.* **287**, 13016–13025 (2012).
18. Aisen, P., Enns, C. & Wessling-Resnick, M. Chemistry and biology of eukaryotic iron metabolism. *Int. J. Biochem. Cell Biol.* **33**, 940–959 (2001).
19. Theil, E. C. Ferritin protein nanocages use ion channels, catalytic sites, and nucleation

channels to manage iron/oxygen chemistry. *Curr. Opin. Chem. Biol.* **15**, 304–311 (2011).
20. Chiou, B. *et al.* Endothelial cells are critical regulators of iron transport in a model of the human blood–brain barrier. *J. Cereb. Blood Flow Metab.* **39**, 2117 (2019).
21. Chiou, B. *et al.* Pharmaceutical iron formulations do not cross a model of the human blood-brain barrier. *PLoS One* **13**, (2018).
22. Simpson, I. A. *et al.* A novel model for brain iron uptake: introducing the concept of regulation. *J. Cereb. Blood Flow Metab.* **35**, 48 (2015).
23. Duck, K. A. & Connor, J. R. Iron uptake and transport across physiological barriers. *Biometals* **29**, 573 (2016).
24. Todorich, B., Zhang, X. & Connor, J. R. H-ferritin is the major source of iron for oligodendrocytes. *Glia* **59**, 927–935 (2011).
25. Sakamoto, S. *et al.* H-Ferritin Is Preferentially Incorporated by Human Erythroid Cells through Transferrin Receptor 1 in a Threshold-Dependent Manner. *PLoS One* **10**, e0139915 (2015).
26. Chiou, B. & Connor, J. R. Emerging and Dynamic Biomedical Uses of Ferritin. *Pharmaceuticals* **11**, (2018).
27. Kalgaonkar, S. & Lönnerdal, B. Receptor-mediated uptake of ferritin-bound iron by human intestinal Caco-2 cells. *J. Nutr. Biochem.* **20**, 304 (2009).
28. Li, L. *et al.* Binding and uptake of H-ferritin are mediated by human transferrin receptor-1. *Proc. Natl. Acad. Sci. U. S. A.* **107**, 3505–3510 (2010).
29. Chiou, B., Lucassen, E., Sather, M., Kallianpur, A. & Connor, J. Semaphorin4A and H-ferritin utilize Tim-1 on human oligodendrocytes: A novel neuro-immune axis. *Glia* **66**, 1317–1330 (2018).
30. Han, J. *et al.* Iron Uptake Mediated by Binding of H-Ferritin to the TIM-2 Receptor in Mouse Cells. *PLoS One* **6**, e23800 (2011).
31. Todorich, B., Zhang, X., Slagle-Webb, B., Seaman, W. E. & Connor, J. R. Tim-2 is the receptor for H-ferritin on oligodendrocytes. *J. Neurochem.* **107**, 1495–1505 (2008).
32. Li, R., Luo, C., Mines, M., Zhang, J. & Fan, G. H. Chemokine CXCL12 induces binding of ferritin heavy chain to the chemokine receptor CXCR4, alters CXCR4 signaling, and induces phosphorylation and nuclear translocation of ferritin heavy chain. *J. Biol. Chem.* **281**, 37616–37627 (2006).
33. Yu, B. *et al.* Interactions of ferritin with scavenger receptor class A members. *J. Biol. Chem.* **295**, 15727–15741 (2020).
34. Mendes-Jorge, L. *et al.* L-Ferritin Binding to Scara5: A New Iron Traffic Pathway Potentially Implicated in Retinopathy. *PLoS One* **9**, e106974 (2014).
35. Li, J. Y. *et al.* Scara5 Is a Ferritin Receptor Mediating Non-Transferrin Iron Delivery. *Dev. Cell* **16**, 35–46 (2009).
36. Akinc, A. & Battaglia, G. Exploiting Endocytosis for Nanomedicines. *Cold Spring Harb. Perspect. Biol.* **5**, (2013).
37. Zahringer, J., Baliga, B. S. & Munro, H. N. Novel mechanism for translational control in regulation of ferritin synthesis by iron. *Proc. Natl. Acad. Sci. U. S. A.* **73**, 857 (1976).
38. Torti, F. M. & Torti, S. V. Regulation of ferritin genes and protein. *Blood* **99**, 3505–3516 (2002).
39. Sammarco, M. C., Ditch, S., Banerjee, A. & Grabczyk, E. Ferritin L and H Subunits Are Differentially Regulated on a Post-transcriptional Level. *J. Biol. Chem.* **283**, 4578–4587

(2008).
40. Wang, W. *et al.* IRP2 regulates breast tumor growth. *Cancer Res.* **74**, 497–507 (2014).
41. Deng, Z., Manz, D. H., Torti, S. V. & Torti, F. M. Iron-responsive element-binding protein 2 plays an essential role in regulating prostate cancer cell growth. *Oncotarget* **8**, 82231–82243 (2017).
42. Li, X. *et al.* miR-335 promotes ferroptosis by targeting ferritin heavy chain 1 in in vivo and in vitro models of Parkinson's disease. *Int. J. Mol. Med.* **47**, 1–12 (2021).
43. Tsuji, Y. JunD activates transcription of the human ferritin H gene through an antioxidant response element during oxidative stress. *Oncogene* **24**, 7567 (2005).
44. Ringoldj, G. M., Myamboll, K. B., Young11, A. P. & Torti, F. M. The Molecular Cloning and Characterization of Murine Ferritin Heavy Chain, a Tumor Necrosis Factor-inducible Gene. *J. Biol. Chem.* **263**, 12638–12614 (1988).
45. Wei, Y., Miller, S. C., Tsuji, Y., Torti, S. V. & Torti, F. M. Interleukin 1 induces ferritin heavy chain in human muscle cells. *Biochem. Biophys. Res. Commun.* **169**, 289–296 (1990).
46. MacKenzie, E. L. & Tsuji, Y. Elevated Intracellular Calcium Increases Ferritin H Expression Through an NFAT-Independent Posttranscriptional Mechanism Involving mRNA Stabilization. *Biochem. J.* **411**, 107 (2008).
47. Pietsch, E. C., Chan, J. Y., Torti, F. M. & Torti, S. V. Nrf2 mediates the induction of ferritin H in response to xenobiotics and cancer chemopreventive dithiolethiones. *J. Biol. Chem.* **278**, 2361–2369 (2003).
48. Huang, B. W., Ray, P. D., Iwasaki, K. & Tsuji, Y. Transcriptional regulation of the human ferritin gene by coordinated regulation of Nrf2 and protein arginine methyltransferases PRMT1 and PRMT4. *FASEB J.* **27**, 3763 (2013).
49. Iwasaki, K., Hailemariam, K. & Tsuji, Y. PIAS3 interacts with ATF1 and regulates the human ferritin H gene through an antioxidant-responsive element. *J. Biol. Chem.* **282**, 22335–22343 (2007).
50. Liu, J. *et al.* Hypoxia induced ferritin light chain (FTL) promoted epithelia mesenchymal transition and chemoresistance of glioma. *J. Exp. Clin. Cancer Res.* **39**, 1–17 (2020).
51. Talks, K. L. *et al.* The Expression and Distribution of the Hypoxia-Inducible Factors HIF-1α and HIF-2α in Normal Human Tissues, Cancers, and Tumor-Associated Macrophages. *Am. J. Pathol.* **157**, 411 (2000).
52. Fuhrmann, D. C., Mondorf, A., Beifuß, J., Jung, M. & Brüne, B. Hypoxia inhibits ferritinophagy, increases mitochondrial ferritin, and protects from ferroptosis. *Redox Biol.* **36**, (2020).
53. Huang, B. W., Miyazawa, M. & Tsuji, Y. Distinct Regulatory Mechanisms of the Human Ferritin Gene by Hypoxia andHypoxia Mimetic Cobalt Chloride at the Transcriptional and Post-transcriptionalLevels. *Cell. Signal.* **26**, 2702 (2014).
54. Tsuji, Y., Kwak, E., Saika, T., Torti, S. V & Torti$, F. M. Preferential repression of the H subunit of ferritin by adenovirus E1A in NIH-3T3 mouse fibroblasts. *J. Biol. Chem.* **268**, 7270–7275 (1993).
55. Wu, K. J., Polack, A. & Dalla-Favera, R. Coordinated regulation of iron-controlling genes, H-ferritin and IRP2, by c-MYC. *Science (80-.).* **283**, 676–679 (1999).
56. Lv, H. & Shang, P. The significance, trafficking and determination of labile iron in cytosol, mitochondria and lysosomes. *Metallomics* **10**, 899–916 (2018).

57. Brown, R. A. M. *et al.* Altered Iron Metabolism and Impact in Cancer Biology, Metastasis, and Immunology. *Front. Oncol.* **10**, 476 (2020).
58. O'Donnell, K. A. *et al.* Activation of Transferrin Receptor 1 by c-Myc Enhances Cellular Proliferation and Tumorigenesis. *Mol. Cell. Biol.* **26**, 2373 (2006).
59. Zhang, F., Wang, W., Tsuji, Y., Torti, S. V. & Torti, F. M. Post-transcriptional Modulation of Iron Homeostasis during p53-dependent Growth Arrest. *J. Biol. Chem.* **283**, 33911 (2008).
60. Polyak, K., Xia, Y., Zweier, J. L., Kinzler, K. W. & Vogelstein, B. A model for p53-induced apoptosis. *Nature* **389**, 300–305 (1997).
61. Faniello, M. C. *et al.* p53-mediated downregulation of H ferritin promoter transcriptional efficiency via NF-Y. *Int. J. Biochem. Cell Biol.* **40**, 2110–2119 (2008).
62. Lee, J. H., Jang, H., Cho, E. J. & Youn, H. D. Ferritin binds and activates p53 under oxidative stress. *Biochem. Biophys. Res. Commun.* **389**, 399–404 (2009).
63. Biamonte, F. *et al.* Ferritin heavy subunit enhances apoptosis of non-small cell lung cancer cells through modulation of miR-125b/p53 axis. *Cell Death Dis. 2018 912* **9**, 1–10 (2018).
64. Pontrelli, P., Accetturo, M. & Gesualdo, L. miRNome analysis using real-time PCR. *Methods Mol. Biol.* **1186**, 201–232 (2014).
65. Biamonte, F. *et al.* H-Ferritin-Regulated MicroRNAs Modulate Gene Expression in K562 Cells. *PLoS One* **10**, (2015).
66. Shpyleva, S. I. *et al.* Role of ferritin alterations in human breast cancer cells. *Breast Cancer Res. Treat.* **126**, 63–71 (2011).
67. Chan, J. J. *et al.* A FTH1 gene:pseudogene:microRNA network regulates tumorigenesis in prostate cancer. *Nucleic Acids Res.* **46**, 1998 (2018).
68. Alkhateeb, A. A. & Connor, J. R. Nuclear ferritin: A new role for ferritin in cell biology. *Biochim. Biophys. Acta* **1800**, 793–797 (2010).
69. Surguladze, N., Patton, S., Cozzi, A., Fried, M. G. & Connor, J. R. Characterization of nuclear ferritin and mechanism of translocation. *Biochem. J.* **388**, 731–740 (2005).
70. Surguladze, N., Thompson, K. M., Beard, J. L., Connor, J. R. & Fried, M. G. Interactions and Reactions of Ferritin with DNA. *J. Biol. Chem.* **279**, 14694–14702 (2004).
71. Corsi, B. *et al.* Human mitochondrial ferritin expressed in HeLa cells incorporates iron and affects cellular iron metabolism. *J. Biol. Chem.* **277**, 22430–22437 (2002).
72. Bahr, T. M. *et al.* Ferritin in serum and urine: A pilot study. *Blood Cells. Mol. Dis.* **76**, 59–62 (2019).
73. Petzold, A. *et al.* Cerebrospinal fluid ferritin level, a sensitive diagnostic test in late-presenting subarachnoid hemorrhage. *J. Stroke Cerebrovasc. Dis.* **20**, 489–493 (2011).
74. Drysdale, J. *et al.* Mitochondrial ferritin: A new player in iron metabolism. *Blood Cells. Mol. Dis.* **29**, 376–383 (2002).
75. Shi, Z. H. *et al.* Mitochondrial ferritin, a new target for inhibiting neuronal tumor cell proliferation. *Cell. Mol. Life Sci.* **72**, 983–997 (2015).
76. Levi, S. *et al.* A human mitochondrial ferritin encoded by an intronless gene. *J. Biol. Chem.* **276**, 24437–24440 (2001).
77. Guaraldo, M. *et al.* Characterization of human mitochondrial ferritin promoter: identification of transcription factors and evidences of epigenetic control. *Sci. Reports 2016 61* **6**, 1–11 (2016).

78. Santambrogio, P. *et al.* Mitochondrial Ferritin Expression in Adult Mouse Tissues. *J. Histochem. Cytochem.* **55**, 1129 (2007).
79. Santambrogio, P. *et al.* Over-expression of mitochondrial ferritin affects the JAK2/STAT5 pathway in K562 cells and causes mitochondrial iron accumulation. *Haematologica* **96**, 1424–1432 (2011).
80. Wang, Y. Q. *et al.* The Protective Role of Mitochondrial Ferritin on Erastin-Induced Ferroptosis. *Front. Aging Neurosci.* **8**, (2016).
81. Nie, G., Sheftel, A. D., Kim, S. F. & Ponka, P. Overexpression of mitochondrial ferritin causes cytosolic iron depletion and changes cellular iron homeostasis. *Blood* **105**, 2161–2167 (2005).
82. Nie, G., Chen, G., Sheftel, A. D., Pantopoulos, K. & Ponka, P. In vivo tumor growth is inhibited by cytosolic iron deprivation caused by the expression of mitochondrial ferritin. *Blood* **108**, 2428–2434 (2006).
83. Gong, S. *et al.* Roflumilast restores cAMP/PKA/CREB signaling axis for FtMt-mediated tumor inhibition of ovarian cancer. *Oncotarget* **8**, 112341 (2017).
84. Gong, S. *et al.* Roflumilast enhances cisplatin-sensitivity and reverses cisplatin-resistance of ovarian cancer cells via cAMP/PKA/CREB-FtMt signalling axis. *Cell Prolif.* **51**, (2018).
85. Cai, C., Ching, A., Lagace, C. & Linsenmayer, T. Nuclear ferritin-mediated protection of corneal epithelial cells from oxidative damage to DNA. *Dev. Dyn.* **237**, 2676–2683 (2008).
86. Cai, C. X., Birk, D. E. & Linsenmayer, T. F. Nuclear ferritin protects DNA from UV damage in corneal epithelial cells. *Mol. Biol. Cell* **9**, 1037–1051 (1998).
87. Thompson, K. J., Fried, M. G., Ye, Z., Boyer, P. & Connor, J. R. Regulation, mechanisms and proposed function of ferritin translocation to cell nuclei. *J. Cell Sci.* **115**, 2165–2177 (2002).
88. Linsenmayer, T. F. *et al.* Corneal Epithelial Nuclear Ferritin and Its Transporter Ferritoid Afford Unique Protection to DNA from UV Light and Reactive Oxygen Species. *Oxidative Stress Appl. Basic Res. Clin. Pract.* 39–66 (2015) doi:10.1007/978-1-4939-1935-2_3.
89. Liu, X. *et al.* Heavy chain ferritin siRNA delivered by cationic liposomes increases sensitivity of cancer cells to chemotherapeutic agents. *Cancer Res.* **71**, 2240–2249 (2011).
90. Ravi, V., Madhankumar, A. B., Abraham, T., Slagle-Webb, B. & Connor, J. R. Liposomal delivery of ferritin heavy chain 1 (FTH1) siRNA in patient xenograft derived glioblastoma initiating cells suggests different sensitivities to radiation and distinct survival mechanisms. *PLoS One* **14**, e0221952 (2019).
91. Wang, W., Knovich, M. A., Coffman, L. G., Torti, F. M. & Torti, S. V. Serum Ferritin: Past, Present and Future. *Biochim. Biophys. Acta* **1800**, 760 (2010).
92. Daru, J. *et al.* Serum ferritin as an indicator of iron status: what do we need to know? *Am. J. Clin. Nutr.* **106**, 1634S (2017).
93. Shalitin, S. *et al.* Serum ferritin level as a predictor of impaired growth and puberty in thalassemia major patients. *Eur. J. Haematol.* **74**, 93–100 (2005).
94. Harrison-Findik, D. D. Gender-related variations in iron metabolism and liver diseases. *World J. Hepatol.* **2**, 302–310 (2010).
95. Kappert, K., Jahić, A. & Tauber, R. Assessment of serum ferritin as a biomarker in

COVID-19: bystander or participant? Insights by comparison with other infectious and non-infectious diseases. *https://doi.org/10.1080/1354750X.2020.1797880* **25**, 616–625 (2020).
96. Rosário, C., Zandman-Goddard, G., Meyron-Holtz, E. G., D'Cruz, D. P. & Shoenfeld, Y. The Hyperferritinemic Syndrome: Macrophage activation syndrome, Still's disease, septic shock and catastrophic antiphospholipid syndrome. *BMC Med.* **11**, 1–11 (2013).
97. Ramírez-Carmona, W. *et al.* Are Serum Ferritin Levels a Reliable Cancer Biomarker? A Systematic Review and Meta-Analysis. *https://doi.org/10.1080/01635581.2021.1982996* **74**, 1917–1926 (2021).
98. Arosio, P., Yokota, M. & Drysdale, J. W. Characterization of serum ferritin in iron overload: possible identity to natural apoferritin. *Br. J. Haematol.* **36**, 199–207 (1977).
99. Kate, J. Ten, Wolthuis, A., Westerhuis, B. & van Deursen, C. The iron content of serum ferritin: physiological importance and diagnostic value. *Eur. J. Clin. Chem. Clin. Biochem.* **35**, 53–56 (1997).
100. Anderson, E. R. & Shah, Y. M. Iron homeostasis in the liver. *Compr. Physiol.* **3**, 315 (2013).
101. Meyron-Holtz, E. G., Moshe-Belizowski, S. & Cohen, L. A. A possible role for secreted ferritin in tissue iron distribution. *J. Neural Transm.* **118**, 337–347 (2011).
102. Gray, C. P., Franco, A. V., Arosio, P. & Hersey, P. Immunosuppressive effects of melanoma-derived heavy-chain ferritin are dependent on stimulation of IL-10 production. *Int. J. cancer* **92**, 843–850 (2001).
103. Alkhateeb, A. A., Han, B. & Connor, J. R. Ferritin stimulates breast cancer cells through an iron-independent mechanism and is localized within tumor-associated macrophages. *Breast Cancer Res. Treat.* **137**, 733–744 (2013).
104. Gray CP, Arosio P, H. P. Association of Increased Levels of Heavy-Chain Ferritin with Increased CD4+ CD25+ Regulatory T-Cell Levels in Patients with Melanoma1 | Citedby Results | Clinical Cancer Research | American Association for Cancer Research. *Clinical Cancer Research* 9(7):2551-9 https://aacrjournals.org/clincancerres/crossref-citedby/203600 (2003).
105. De Almeida, S. M., Da Cunha, D. S., Yamada, E., Doi, E. M. & Ono, M. Quantification of cerebrospinal fluid ferritin as a biomarker for CNS malignant infiltration. *Arq. Neuropsiquiatr.* **66**, 720–724 (2008).
106. Koskiniemi, M. Malignancy markers in the cerebrospinal fluid. *Eur. J. Pediatr.* **148**, 3–8 (1988).
107. Sato, Y. *et al.* Cerebrospinal fluid ferritin in glioblastoma: Evidence for tumor synthesis. *J. Neurooncol.* **40**, 47–50 (1998).
108. Ghosh, S., Hevi, S. & Chuck, S. L. Regulated secretion of glycosylated human ferritin from hepatocytes. *Blood* **103**, 2369–2376 (2004).
109. Truman-Rosentsvit, M. *et al.* Ferritin is secreted via 2 distinct nonclassical vesicular pathways. *Blood* **131**, 342–352 (2018).
110. Cohen, L. A. *et al.* Serum ferritin is derived primarily from macrophages through a nonclassical secretory pathway. *Blood* **116**, 1574–1584 (2010).
111. Brown, C. W. *et al.* Prominin2 Drives Ferroptosis Resistance by Stimulating Multivesicular Body/Exosome-Mediated Iron Export. *Dev. Cell* **51**, 575 (2019).
112. Mrowczynski, O. D. *et al.* HFE genotype affects exosome phenotype in cancer. *Biochim.*

Biophys. acta. Gen. Subj. **1861**, 1921–1928 (2017).
113. Mrowczynski, O. D., Zacharia, B. E. & Connor, J. R. Exosomes and their implications in central nervous system tumor biology. *Prog. Neurobiol.* **172**, 71–83 (2019).
114. Palsa, K., Baringer, S. L., Shenoy, G., Simpson, I. A. & Connor, J. R. Exosomes are involved in iron transport from human blood-brain barrier endothelial cells and are modified by endothelial cell iron status. *J. Biol. Chem.* **299**, 102868 (2023).
115. Basuli, D. *et al.* Iron addiction: a novel therapeutic target in ovarian cancer. *Oncogene 2017 3629* **36**, 4089–4099 (2017).
116. Schonberg, D. L. *et al.* Preferential Iron Trafficking Characterizes Glioblastoma Stem-like Cells. *Cancer Cell* **28**, 441–455 (2015).
117. Lu, C., Zhao, H., Luo, C., Lei, T. & Zhang, M. Knockdown of ferritin heavy chain (FTH) inhibits the migration of prostate cancer through reducing S100A4, S100A2, and S100P expression. *Transl. Cancer Res.* **9**, 5418–5429 (2020).
118. Hu, W. *et al.* FTH promotes the proliferation and renders the HCC cells specifically resist to ferroptosis by maintaining iron homeostasis. *Cancer Cell Int.* **21**, 1–18 (2021).
119. Wu, T. *et al.* Expression of Ferritin Light Chain (FTL) Is Elevated in Glioblastoma, and FTL Silencing Inhibits Glioblastoma Cell Proliferation via the GADD45/JNK Pathway. *PLoS One* **11**, e0149361 (2016).
120. Cozzi, A. *et al.* Analysis of the biologic functions of H- and L-ferritins in HeLa cells by transfection with siRNAs and cDNAs: evidence for a proliferative role of L-ferritin. *Blood* **103**, 2377–2383 (2004).
121. Yu, G. H., Fu, L., Chen, J., Wei, F. & Shi, W. X. Decreased expression of ferritin light chain in osteosarcoma and its correlation with epithelial-mesenchymal transition. *Eur. Rev. Med. Pharmacol. Sci.* **22**, 2580–2587 (2018).
122. Zhang, J. & Chen, X. p53 Tumor Suppressor and Iron Homeostasis. *FEBS J.* **286**, 620 (2019).
123. Yang DC, Jiang X, Elliott RL, H. J. Antisense ferritin oligonucleotides inhibit growth and induce apoptosis in human breast carcinoma cells - PubMed. *Anticancer Res.* 22(3):1513-24 (2002).
124. Cozzi, A. *et al.* Role of iron and ferritin in TNFα-induced apoptosis in HeLa cells. *FEBS Lett.* **537**, 187–192 (2003).
125. Chang, C. M., Fitch, M. E., Yuan, M., Parslow, T. G. & Shu, H. G. Bax can associate with ferritin heavy chain (FHC) resulting in inhibition of bax-mediated apoptosis. *Int. J. Radiat. Oncol.* **51**, 189 (2001).
126. Baldi, A. *et al.* Ferritin Contributes to Melanoma Progression by Modulating Cell Growth and Sensitivity to Oxidative Stress. *Clin. Cancer Res.* **11**, 3175–3183 (2005).
127. Ribatti, D., Tamma, R. & Annese, T. Epithelial-Mesenchymal Transition in Cancer: A Historical Overview. *Transl. Oncol.* **13**, 100773 (2020).
128. Sioutas, A. *et al.* Oxidant-induced autophagy and ferritin degradation contribute to epithelial–mesenchymal transition through lysosomal iron. *J. Inflamm. Res.* **10**, 29 (2017).
129. Zhang, K. H. *et al.* Ferritin heavy chain-mediated iron homeostasis and subsequent increased reactive oxygen species production are essential for epithelial-mesenchymal transition. *Cancer Res.* **69**, 5340–5348 (2009).
130. Liu, J. *et al.* Hypoxia induced ferritin light chain (FTL) promoted epithelia mesenchymal transition and chemoresistance of glioma. *J. Exp. Clin. Cancer Res.* **39**, 1–17 (2020).

131. Son, H. & Moon, A. Epithelial-mesenchymal Transition and Cell Invasion. *Toxicol. Res.* **26**, 245 (2010).
132. Coffman, L. G., Parsonage, D., D'Agostino, R., Torti, F. M. & Torti, S. V. Regulatory effects of ferritin on angiogenesis. *Proc. Natl. Acad. Sci. U. S. A.* **106**, 570–575 (2009).
133. Tesfay, L., Huhn, A. J., Hatcher, H., Torti, F. M. & Torti, S. V. Ferritin Blocks Inhibitory Effects of Two-Chain High Molecular Weight Kininogen (HKa) on Adhesion and Survival Signaling in Endothelial Cells. *PLoS One* **7**, e40030 (2012).
134. Jin, P., Kang, J., Lee, M. K. & Park, J. W. Ferritin heavy chain controls the HIF-driven hypoxic response by activating the asparaginyl hydroxylase FIH. *Biochem. Biophys. Res. Commun.* **499**, 475–481 (2018).
135. Zimna, A. & Kurpisz, M. Hypoxia-Inducible Factor-1 in Physiological and Pathophysiological Angiogenesis: Applications and Therapies. *Biomed Res. Int.* **2015**, (2015).
136. Labrie, M., Brugge, J. S., Mills, G. B. & Zervantonakis, I. K. Therapy resistance: opportunities created by adaptive responses to targeted therapies in cancer. *Nat. Rev. Cancer 2022 226* **22**, 323–339 (2022).
137. Nie, Z. *et al.* Ferroptosis and Tumor Drug Resistance: Current Status and Major Challenges. *Front. Pharmacol.* **13**, 1647 (2022).
138. Lin, F. & Girotti, A. W. Elevated ferritin production, iron containment, and oxidant resistance in hemin-treated leukemia cells. *Arch. Biochem. Biophys.* **346**, 131–141 (1997).
139. S Epsztejn, H Glickstein, V Picard, I N Slotki, W Breuer, C Beaumont, Z. I. C. H-ferritin subunit overexpression in erythroid cells reduces the oxidative stress response and induces multidrug resistance properties - PubMed. *Blood* 15;94(10):3593-603 https://pubmed.ncbi.nlm.nih.gov/10552971/.
140. Chekhun, V. F. *et al.* Iron metabolism disturbances in the MCF-7 human breast cancer cells with acquired resistance to doxorubicin and cisplatin. *Int. J. Oncol.* **43**, 1481–1486 (2013).
141. Wu, J. *et al.* Antileukemia Effect of Ciclopirox Olamine Is Mediated by Downregulation of Intracellular Ferritin and Inhibition β-Catenin-c-Myc Signaling Pathway in Glucocorticoid Resistant T-ALL Cell Lines. *PLoS One* **11**, (2016).
142. R. Connor, J. Role of H-Ferritin in Radiosensitivity of Human Glioma Cells. *Cancer Biol. Treat.* **3**, 1–10 (2016).
143. Tirinato, L. *et al.* Lipid droplets and ferritin heavy chain: A devilish liaison in human cancer cell radioresistance. *Elife* **10**, (2021).
144. Aversa, I. *et al.* Chemoresistance in H-Ferritin Silenced Cells: The Role of NF-κB. *Int. J. Mol. Sci.* **19**, (2018).
145. Rychtarcikova, Z. *et al.* Tumor-initiating cells of breast and prostate origin show alterations in the expression of genes related to iron metabolism. *Oncotarget* **8**, 6376 (2017).
146. Raggi, C. *et al.* Dysregulation of Iron Metabolism in Cholangiocarcinoma Stem-like Cells. *Sci. Reports 2017 71* **7**, 1–12 (2017).
147. Cozzi, A. *et al.* Analysis of the biologic functions of H- and L-ferritins in HeLa cells by transfection with siRNAs and cDNAs: evidence for a proliferative role of L-ferritin. *Blood* **103**, 2377–2383 (2004).
148. Mancias, J. D., Wang, X., Gygi, S. P., Harper, J. W. & Kimmelman, A. C. Quantitative

proteomics identifies NCOA4 as the cargo receptor mediating ferritinophagy. *Nat. 2014 5097498* **509**, 105–109 (2014).
149. Mancias, J. D. & Kimmelman, A. C. Mechanisms of Selective Autophagy in Normal Physiology and Cancer. *J. Mol. Biol.* **428**, 1659–1680 (2016).
150. Rockfield, S., Flores, I. & Nanjundan, M. Expression and function of nuclear receptor coactivator 4 isoforms in transformed endometriotic and malignant ovarian cells. *Oncotarget* **9**, 5344 (2018).
151. Santana-Codina, N. *et al.* NCOA4-mediated ferritinophagy is a pancreatic cancer dependency via maintenance of iron bioavailability for iron-sulfur cluster proteins. *Cancer Discov.* **12**, 2180 (2022).
152. Mou, Y. *et al.* Low expression of ferritinophagy-related NCOA4 gene in relation to unfavorable outcome and defective immune cells infiltration in clear cell renal carcinoma. *BMC Cancer* **21**, 1–12 (2021).
153. Dixon, S. J. & Stockwell, B. R. The Hallmarks of Ferroptosis. *https://doi.org/10.1146/annurev-cancerbio-030518-055844* **3**, 35–54 (2019).
154. Lu, B. *et al.* The Role of Ferroptosis in Cancer Development and Treatment Response. *Front. Pharmacol.* **8**, (2017).
155. Yang, W. S. & Stockwell, B. R. Synthetic lethal screening identifies compounds activating iron-dependent, nonapoptotic cell death in oncogenic-RAS-harboring cancer cells. *Chem. Biol.* **15**, 234–245 (2008).
156. Dixon, S. J. *et al.* Ferroptosis: An iron-dependent form of nonapoptotic cell death. *Cell* (2012) doi:10.1016/j.cell.2012.03.042.
157. Mou, Y. *et al.* Ferroptosis, a new form of cell death: Opportunities and challenges in cancer. *J. Hematol. Oncol.* **12**, (2019).
158. Lang, X. *et al.* Radiotherapy and Immunotherapy Promote Tumoral Lipid Oxidation and Ferroptosis via Synergistic Repression of SLC7A11. *Cancer Discov.* **9**, 1673–1685 (2019).
159. Wang, W. *et al.* CD8+ T cells regulate tumor ferroptosis during cancer immunotherapy. *Nature* **569**, 270 (2019).
160. Zhang, C., Liu, X., Jin, S., Chen, Y. & Guo, R. Ferroptosis in cancer therapy: a novel approach to reversing drug resistance. *Mol. Cancer* **21**, 1–12 (2022).
161. Du, J. *et al.* DHA exhibits synergistic therapeutic efficacy with cisplatin to induce ferroptosis in pancreatic ductal adenocarcinoma via modulation of iron metabolism. *Cell Death Dis.* **12**, (2021).
162. Turcu, A. L. *et al.* DMT1 Inhibitors Kill Cancer Stem Cells by Blocking Lysosomal Iron Translocation. *Chem. – A Eur. J.* **26**, 7369–7373 (2020).
163. Xie, Y. *et al.* Ferroptosis: Process and function. *Cell Death and Differentiation* (2016) doi:10.1038/cdd.2015.158.
164. Yang, N. Di *et al.* Artesunate induces cell death in human cancer cells via enhancing lysosomal function and lysosomal degradation of ferritin. *J. Biol. Chem.* **289**, 33425–33441 (2014).
165. Eling, N., Reuter, L., Hazin, J., Hamacher-Brady, A. & Brady, N. R. Identification of artesunate as a specific activator of ferroptosis in pancreatic cancer cells. *Oncoscience* **2**, 517–532 (2015).
166. Chen, X., Yu, C., Kang, R. & Tang, D. Iron Metabolism in Ferroptosis. *Front. Cell Dev.*

Biol. **8**, 1089 (2020).
167. Hou, W. *et al.* Autophagy promotes ferroptosis by degradation of ferritin. *Autophagy* **12**, 1425–1428 (2016).
168. Zhang, Y. *et al.* Loss of COPZ1 induces NCOA4 mediated autophagy and ferroptosis in glioblastoma cell lines. *Oncogene* **40**, 1425 (2021).
169. Fan, K. *et al.* Ferritin Nanocarrier Traverses the Blood Brain Barrier and Kills Glioma. *ACS Nano* **12**, 4105–4115 (2018).
170. Palombarini, F., Fabio, E. Di, Boffi, A., Macone, A. & Bonamore, A. Ferritin Nanocages for Protein Delivery to Tumor Cells. *Molecules* **25**, (2020).
171. Reutovich, A. A., Srivastava, A. K., Arosio, P. & Bou-Abdallah, F. Ferritin nanocages as efficient nanocarriers and promising platforms for COVID-19 and other vaccines development. *Biochim. Biophys. acta. Gen. Subj.* **1867**, (2023).
172. Palombarini, F. *et al.* Self-assembling ferritin-dendrimer nanoparticles for targeted delivery of nucleic acids to myeloid leukemia cells. *J. Nanobiotechnology* **19**, (2021).
173. Theil, E. C. Ferritin protein nanocages—the story. *Nanotechnol. perceptions* **8**, 7 (2012).
174. Jiang, B. *et al.* Ferritin nanocages for early theranostics of tumors via inflammation-enhanced active targeting. *Sci. China Life Sci.* **65**, 328–340 (2022).
175. Harrison, P. M. & Arosio, P. The ferritins: molecular properties, iron storage function and cellular regulation. *Biochim. Biophys. Acta* **1275**, 161–203 (1996).
176. Santambrogios, P. *et al.* Evidence that a salt bridge in the light chain contributes to the physical stability difference between heavy and light human ferritins. **287**, 14077–14083 (1992).
177. Bellini, M. *et al.* Protein nanocages for self-triggered nuclear delivery of DNA-targeted chemotherapeutics in Cancer Cells. *J. Control. Release* **196**, 184–196 (2014).
178. Kang, S. *et al.* Controlled assembly of bifunctional chimeric protein cages and composition analysis using noncovalent mass spectrometry. *J. Am. Chem. Soc.* **130**, 16527–16529 (2008).
179. Belletti, D. *et al.* Protein cage nanostructure as drug delivery system: magnifying glass on apoferritin. *http://dx.doi.org/10.1080/17425247.2017.1243528* **14**, 825–840 (2016).
180. Sun, X., Hong, Y., Gong, Y., Zheng, S. & Xie, D. Bioengineered Ferritin Nanocarriers for Cancer Therapy. *Int. J. Mol. Sci.* **22**, (2021).
181. Khoshnejad, M., Parhiz, H., Shuvaev, V. V., Dmochowski, I. J. & Muzykantov, V. R. Ferritin-based drug delivery systems: Hybrid nanocarriers for vascular immunotargeting. *J. Control. Release* **282**, 13–24 (2018).
182. Bellini, M. *et al.* Engineered Ferritin Nanoparticles for the Bioluminescence Tracking of Nanodrug Delivery in Cancer. *Small* **16**, 2001450 (2020).
183. Zhang, B., Tang, G., He, J., Yan, X. & Fan, K. Ferritin nanocage: A promising and designable multi-module platform for constructing dynamic nanoassembly-based drug nanocarrier. *Adv. Drug Deliv. Rev.* **176**, (2021).
184. Mohanty, A., Parida, A., Raut, R. K. & Behera, R. K. Ferritin: A Promising Nanoreactor and Nanocarrier for Bionanotechnology. *ACS Bio Med Chem Au* **2**, 258–281 (2022).
185. Yin, S., Davey, K., Dai, S., Liu, Y. & Bi, J. A critical review of ferritin as a drug nanocarrier: Structure, properties, comparative advantages and challenges. *Particuology* **64**, 65–84 (2022).
186. Truffi, M. *et al.* Ferritin nanocages: A biological platform for drug delivery, imaging and

theranostics in cancer. *Pharmacol. Res.* **107**, 57–65 (2016).
187. Zhen, Z. *et al.* RGD Modified Apoferritin Nanoparticles for Efficient Drug Delivery to Tumors. *ACS Nano* **7**, 4830 (2013).
188. Kuruppu, A. I. *et al.* An Apoferritin-based Drug Delivery System for the Tyrosine Kinase Inhibitor Gefitinib. *Adv. Healthc. Mater.* **4**, 2816–2821 (2015).
189. Luo, Y., Wang, X., Du, D. & Lin, Y. Hyaluronic acid-conjugated apoferritin nanocages for lung cancer targeted drug delivery. *Biomater. Sci.* **3**, 1386–1394 (2015).
190. Huang, C. W. *et al.* Integrin α2β1-targeting ferritin nanocarrier traverses the blood–brain barrier for effective glioma chemotherapy. *J. Nanobiotechnology* **19**, 1–17 (2021).
191. Chen, Z. *et al.* Apoferritin Nanocage for Brain Targeted Doxorubicin Delivery. *Mol. Pharm.* **14**, 3087–3097 (2017).
192. Bhavyata (Pandya) Shesh. Iron profiling in GBMs. (Penn State University, 2023).
193. Chiou, B., Neely, E. B., Mcdevitt, D. S., Simpson, I. A. & Connor, J. R. Transferrin and H-ferritin involvement in brain iron acquisition during postnatal development: impact of sex and genotype. *J. Neurochem.* **152**, 381 (2020).
194. Li, L. *et al.* Ferritin-mediated siRNA delivery and gene silencing in human tumor and primary cells. *Biomaterials* **98**, 143–151 (2016).
195. Yuan, Z. *et al.* Rational design of engineered H-ferritin nanoparticles with improved siRNA delivery efficacy across an in vitro model of the mouse BBB. *Nanoscale* **14**, 6449–6464 (2022).
196. Pediconi, N. *et al.* Design and Synthesis of Piperazine-Based Compounds Conjugated to Humanized Ferritin as Delivery System of siRNA in Cancer Cells. *Bioconjug. Chem.* **32**, 1105–1116 (2021).
197. Zhao, Y. *et al.* Bioengineered Magnetoferritin Nanoprobes for Single-Dose Nuclear-Magnetic Resonance Tumor Imaging. *ACS Nano* **10**, 4184–4191 (2016).
198. Crich, S. G. *et al.* Magnetic resonance visualization of tumor angiogenesis by targeting neural cell adhesion molecules with the highly sensitive gadolinium-loaded apoferritin probe. *Cancer Res.* **66**, 9196–9201 (2006).
199. Sitia, L. *et al.* Development of Tumor-Targeted Indocyanine Green-Loaded Ferritin Nanoparticles for Intraoperative Detection of Cancers. *ACS Omega* **5**, 12035–12045 (2020).
200. Lin, X. *et al.* Hybrid Ferritin Nanoparticles as Activatable Probes for Tumor Imaging. *Angew. Chem. Int. Ed. Engl.* **50**, 1569 (2011).
201. The unique physiology of solid tumors: opportunities (and problems) for cancer therapy - PubMed. https://pubmed.ncbi.nlm.nih.gov/9537241/.
202. Huang, P. *et al.* Dye Loaded Ferritin Nanocages for Multimodal Imaging and Photothermal Therapy. *Adv. Mater.* **26**, 6401 (2014).
203. Lin, C. Y. & Shieh, M. J. Near-Infrared Fluorescent Dye-Decorated Nanocages to Form Grenade-like Nanoparticles with Dual Control Release for Photothermal Theranostics and Chemotherapy. *Bioconjug. Chem.* **29**, 1384–1398 (2018).
204. Lakkaraju, A. & Rodriguez-Boulan, E. Itinerant exosomes: emerging roles in cell and tissue polarity. *Trends in Cell Biology* (2008) doi:10.1016/j.tcb.2008.03.002.
205. Joyce, M. G. *et al.* A SARS-CoV-2 ferritin nanoparticle vaccine elicits protective immune responses in nonhuman primates. *Sci. Transl. Med.* **14**, 5735 (2022).
206. Carmen, J. M. *et al.* SARS-CoV-2 ferritin nanoparticle vaccine induces robust innate

immune activity driving polyfunctional spike-specific T cell responses. *npj Vaccines 2021 61* **6**, 1–18 (2021).
207. Powell, A. E. *et al.* A Single Immunization with Spike-Functionalized Ferritin Vaccines Elicits Neutralizing Antibody Responses against SARS-CoV-2 in Mice. *ACS Cent. Sci.* **7**, 183–199 (2021).
208. Masoomi Nomandan, S. Z., Azimzadeh Irani, M. & Hosseini, S. M. In silico design of refined ferritin-SARS-CoV-2 glyco-RBD nanoparticle vaccine. *Front. Mol. Biosci.* **9**, 972 (2022).
209. Johnston, S. C. *et al.* A SARS-CoV-2 Spike Ferritin Nanoparticle Vaccine Is Protective and Promotes a Strong Immunological Response in the Cynomolgus Macaque Coronavirus Disease 2019 (COVID-19) Model. *Vaccines* **10**, 717 (2022).
210. Yang, R. *et al.* Doxorubicin loaded ferritin nanoparticles for ferroptosis enhanced targeted killing of cancer cells. *RSC Adv.* **9**, 28548–28553 (2019).
211. Grochans, S. *et al.* Epidemiology of Glioblastoma Multiforme–Literature Review. *Cancers (Basel).* **14**, (2022).
212. Hatoum, A., Mohammed, R. & Zakieh, O. The unique invasiveness of glioblastoma and possible drug targets on extracellular matrix. *Cancer Manag. Res.* **11**, 1843 (2019).
213. Friedmann-Morvinski, D. Glioblastoma heterogeneity and cancer cell plasticity. *Crit. Rev. Oncog.* **19**, 327–336 (2014).
214. Rivera, M., Sukhdeo, K. & Yu, J. Ionizing radiation in glioblastoma initiating cells. *Front. Oncol.* **3 APR**, 74 (2013).
215. Goffart, N., Kroonen, J. & Rogister, B. Glioblastoma-Initiating Cells: Relationship with Neural Stem Cells and the Micro-Environment. *Cancers (Basel).* **5**, 1049 (2013).
216. Lathia, J. D., Mack, S. C., Mulkearns-Hubert, E. E., Valentim, C. L. L. & Rich, J. N. Cancer stem cells in glioblastoma. *Genes Dev.* **29**, 1203 (2015).
217. Eyler, C. E. & Rich, J. N. Survival of the Fittest: Cancer Stem Cells in Therapeutic Resistance and Angiogenesis. *J. Clin. Oncol.* **26**, 2839 (2008).
218. Treps, L., Perret, R., Edmond, S., Ricard, D. & Gavard, J. Glioblastoma stem-like cells secrete the pro-angiogenic VEGF-A factor in extracellular vesicles. *J. Extracell. Vesicles* **6**, (2017).
219. Cheng, L. *et al.* Elevated Invasive Potential of Glioblastoma Stem Cells. *Biochem. Biophys. Res. Commun.* **406**, 643 (2011).
220. Inoue, A. *et al.* Cancer stem-like cells of glioblastoma characteristically express MMP-13 and display highly invasive activity. *Int. J. Oncol.* **37**, 1121–1131 (2010).
221. Pearson, J. R. D. *et al.* Immune Escape in Glioblastoma Multiforme and the Adaptation of Immunotherapies for Treatment. *Front. Immunol.* **11**, 1 (2020).
222. Sesé, B. *et al.* Glioblastoma Embryonic-like Stem Cells Exhibit Immune-Evasive Phenotype. *Cancers (Basel).* **14**, 2070 (2022).
223. Jiang, H. *et al.* Ferrous iron–activatable drug conjugate achieves potent MAPK blockade in KRAS-driven tumors. *J. Exp. Med.* **219**, (2022).
224. Chen, Y., Fan, Z., Yang, Y. & Gu, C. Iron metabolism and its contribution to cancer (Review). *Int. J. Oncol.* **54**, 1143–1154 (2019).
225. Hu, W. *et al.* FTH promotes the proliferation and renders the HCC cells specifically resist to ferroptosis by maintaining iron homeostasis. *Cancer Cell Int.* **21**, 1–18 (2021).
226. Volovetz, J. *et al.* Identifying conserved molecular targets required for cell migration of

glioblastoma cancer stem cells. *Cell Death Dis.* **11**, (2020).
227. Prionisti, I., Bühler, L. H., Walker, P. R. & Jolivet, R. B. Harnessing Microglia and Macrophages for the Treatment of Glioblastoma. *Front. Pharmacol.* **10**, (2019).
228. Fisher, J. *et al.* Ferritin: a novel mechanism for delivery of iron to the brain and other organs. *Am. J. Physiol. Cell Physiol.* **293**, (2007).
229. Glick, R. P., Gettleman, R., Patel, K., Lakshman, R. & Tsibris, J. C. M. Insulin and insulin-like growth factor I in brain tumors: binding and in vitro effects. *Neurosurgery* **24**, 791–797 (1989).
230. Chang, C. C., Wu, M. & Yuan, F. Role of specific endocytic pathways in electrotransfection of cells. *Mol. Ther. - Methods Clin. Dev.* **1**, 14058 (2014).
231. Lamb, R. *et al.* Antibiotics that target mitochondria effectively eradicate cancer stem cells, across multiple tumor types: Treating cancer like an infectious disease. *Oncotarget* **6**, 4569 (2015).
232. Konijn, A. M. *et al.* The Cellular Labile Iron Pool and Intracellular Ferritin in K562 Cells. *Blood* **94**, 2128–2134 (1999).
233. Koneru, T. *et al.* Transferrin: Biology and Use in Receptor-Targeted Nanotherapy of Gliomas. *ACS Omega* **6**, 8727–8733 (2021).
234. Sun, T. *et al.* Targeting transferrin receptor delivery of temozolomide for a potential glioma stem cell-mediated therapy. *Oncotarget* **8**, 74451 (2017).
235. Brown, R. A. M. *et al.* Altered Iron Metabolism and Impact in Cancer Biology, Metastasis, and Immunology. *Front. Oncol.* **10**, 476 (2020).
236. Prager, B. C., Xie, Q., Bao, S. & Rich, J. N. Cancer Stem Cells: The Architects of the Tumor Ecosystem. *Cell Stem Cell* **24**, 41 (2019).
237. Lobello, N. *et al.* Ferritin heavy chain is a negative regulator of ovarian cancer stem cell expansion and epithelial to mesenchymal transition. *Oncotarget* **7**, 62019 (2016).
238. Di Sanzo, M. *et al.* Ferritin Heavy Chain Binds Peroxiredoxin 6 and Inhibits Cell Proliferation and Migration. *Int. J. Mol. Sci.* **23**, 12987 (2022).
239. Sodek, K. L., Ringuette, M. J. & Brown, T. J. Compact spheroid formation by ovarian cancer cells is associated with contractile behavior and an invasive phenotype. *Int. J. Cancer* **124**, 2060–2070 (2009).
240. Boylan, K. L. M., Manion, R. D., Shah, H., Skubitz, K. M. & Skubitz, A. P. N. Inhibition of Ovarian Cancer Cell Spheroid Formation by Synthetic Peptides Derived from Nectin-4. *Int. J. Mol. Sci.* **21**, 1–16 (2020).
241. Beunk, L. *et al.* Actomyosin contractility requirements and reciprocal cell–tissue mechanics for cancer cell invasion through collagen-based channels. *Eur. Phys. J. E. Soft Matter* **45**, 48 (2022).
242. Zhang, Y. L., Wang, R. C., Cheng, K., Ring, B. Z. & Su, L. Roles of Rap1 signaling in tumor cell migration and invasion. *Cancer Biol. Med.* **14**, 90 (2017).
243. Looi, C. K., Hii, L. W., Ngai, S. C., Leong, C. O. & Mai, C. W. The Role of Ras-Associated Protein 1 (Rap1) in Cancer: Bad Actor or Good Player? *Biomed. 2020, Vol. 8, Page 334* **8**, 334 (2020).
244. Bailey, C. L., Kelly, P. & Casey, P. J. Activation of Rap1 promotes prostate cancer metastasis. *Cancer Res.* **69**, 4962–4968 (2009).
245. You, G. R. *et al.* Molecular Interplays Between Cell Invasion and Radioresistance That Lead to Poor Prognosis in Head-Neck Cancer. *Front. Oncol.* **11**, 2724 (2021).

246. Wilkinson, N. & Pantopoulos, K. The IRP/IRE system in vivo: insights from mouse models. *Front. Pharmacol.* **5**, (2014).
247. Sanchez, M. *et al.* Iron regulation and the cell cycle: Identification of an iron-responsive element in the 3′-untranslated region of human cell division cycle 14A mRNA by a refined microarray-based screening strategy. *J. Biol. Chem.* **281**, 22865–22874 (2006).
248. Fukuyama, T. *et al.* Involvement of the c-Src-Crk-C3G-Rap1 signaling in the nectin-induced activation of Cdc42 and formation of adherens junctions. *J. Biol. Chem.* **280**, 815–825 (2005).
249. Lattmann, E., Deng, T. & Hajnal, A. To Divide or Invade: A Look Behind the Scenes of the Proliferation-Invasion Interplay in the Caenorhabditis elegans Anchor Cell. *Front. Cell Dev. Biol.* **8**, 1727 (2021).
250. Gerlee, P. & Nelander, S. The Impact of Phenotypic Switching on Glioblastoma Growth and Invasion. *PLoS Comput. Biol.* **8**, 1002556 (2012).
251. Hatzikirou, H., Basanta, D., Simon, M., Schaller, K. & Deutsch, A. 'Go or Grow': the key to the emergence of invasion in tumour progression? *Math. Med. Biol. A J. IMA* **29**, 49–65 (2012).
252. Landry, A. P., Balas, M., Alli, S., Spears, J. & Zador, Z. Distinct regional ontogeny and activation of tumor associated macrophages in human glioblastoma. *Sci. Reports 2020 101* **10**, 1–13 (2020).
253. Duck, K. A. & Connor, J. R. Iron uptake and transport across physiological barriers. *Biometals* **29**, 573 (2016).
254. Lopes-Ramos, C. M., Quackenbush, J. & DeMeo, D. L. Genome-Wide Sex and Gender Differences in Cancer. *Front. Oncol.* **10**, 2486 (2020).
255. Zhu, Y., Shao, X., Wang, X., Liu, L. & Liang, H. Sex disparities in cancer. *Cancer Lett.* **466**, 35–38 (2019).
256. Carrano, A., Juarez, J. J., Incontri, D., Ibarra, A. & Cazares, H. G. Sex-Specific Differences in Glioblastoma. *Cells* **10**, (2021).
257. Franceschi, E. *et al.* The Prognostic Roles of Gender and O6-Methylguanine-DNA Methyltransferase Methylation Status in Glioblastoma Patients: The Female Power. *World Neurosurg.* **112**, e342–e347 (2018).
258. Whitmire, P. *et al.* Sex-specific impact of patterns of imageable tumor growth on survival of primary glioblastoma patients. *bioRxiv* 325464 (2018) doi:10.1101/325464.
259. Yang, W. *et al. Sex differences in GBM revealed by analysis of patient imaging, transcriptome, and survival data*. *Sci. Transl. Med* vol. 11 http://stm.sciencemag.org/ (2019).
260. Nesterova, D. S. *et al.* Sexually dimorphic impact of the iron-regulating gene, HFE, on survival in glioblastoma. *Neuro-Oncology Adv.* **2**, (2020).
261. Zhang, A. S., Davies, P. S., Carlson, H. L. & Enns, C. A. Mechanisms of HFE-induced regulation of iron homeostasis: Insights from the W81A HFE mutation. *Proc. Natl. Acad. Sci. U. S. A.* **100**, 9500 (2003).
262. Fleming, R. E. Iron Sensing as a Partnership: HFE and Transferrin Receptor 2. *Cell Metab.* **9**, 211–212 (2009).
263. Schmidt, P. J., Toran, P. T., Giannetti, A. M., Bjorkman, P. J. & Andrews, N. C. Transferrin receptor modulates Hfe-dependent regulation of hepcidin expression. *Cell Metab.* **7**, 205 (2008).

264. Vujić, M. Molecular basis of HFE-hemochromatosis. *Front. Pharmacol.* **5 MAR**, 42 (2014).
265. Alexander, J. & Kowdley, K. V. HFE-associated hereditary hemochromatosis. *Genet. Med.* **11**, 307–313 (2009).
266. Montosi, G. *et al.* Wild-type HFE protein normalizes transferrin iron accumulation in macrophages from subjects with hereditary hemochromatosis. *Blood* **96**, 1125–1129 (2000).
267. Drakesmith, H. *et al.* The hemochromatosis protein HFE inhibits iron export from macrophages. *Proc. Natl. Acad. Sci. U. S. A.* **99**, 15602 (2002).
268. Nesterova, D. S. *et al.* Sexually dimorphic impact of the iron-regulating gene, HFE, on survival in glioblastoma. *Neuro-oncology Adv.* **2**, (2020).
269. Troike, K. M. *et al.* Tumor cell-intrinsic HFE drives glioblastoma growth. doi:10.1101/2022.04.13.487917.
270. Baringer, S. L., Neely, E. B., Palsa, K., Simpson, I. A. & Connor, J. R. Regulation of brain iron uptake by apo- and holo-transferrin is dependent on sex and delivery protein. *Fluids Barriers CNS* **19**, (2022).
271. Li, L. *et al.* Binding and uptake of H-ferritin are mediated by human transferrin receptor-1. *Proc. Natl. Acad. Sci. U. S. A.* **107**, 3505–3510 (2010).
272. Kawabata, H. Transferrin and transferrin receptors update. *Free Radic. Biol. Med.* **133**, 46–54 (2019).
273. Todorich, B., Zhang, X., Slagle-Webb, B., Seaman, W. E. & Connor, J. R. Tim-2 is the receptor for H-ferritin on oligodendrocytes. *J. Neurochem.* **107**, 1495–1505 (2008).
274. Haddad, A. F. *et al.* Mouse models of glioblastoma for the evaluation of novel therapeutic strategies. *Neuro-oncology Adv.* **3**, 1–16 (2021).
275. Genoud, V. *et al.* Responsiveness to anti-PD-1 and anti-CTLA-4 immune checkpoint blockade in SB28 and GL261 mouse glioma models. *Oncoimmunology* **7**, (2018).
276. Khan, F. *et al.* Macrophages and microglia in glioblastoma: heterogeneity, plasticity, and therapy. *J. Clin. Invest.* **133**, (2023).
277. Wang, G. *et al.* Tumor-associated microglia and macrophages in glioblastoma: From basic insights to therapeutic opportunities. *Front. Immunol.* **13**, (2022).
278. DeRosa, A. & Leftin, A. The Iron Curtain: Macrophages at the Interface of Systemic and Microenvironmental Iron Metabolism and Immune Response in Cancer. *Front. Immunol.* **12**, (2021).
279. Gürsel, D. B. *et al.* Control of proliferation in astrocytoma cells by the receptor tyrosine kinase/PI3K/AKT signaling axis and the use of PI-103 and TCN as potential anti-astrocytoma therapies. *Neuro. Oncol.* **13**, 610 (2011).
280. Shenoy, G. *et al.* TAMI-42. THE ROLE OF HFE AND IRON IN CELL ADHESION AND MIGRATION IN GLIOBLASTOMA. *Neuro. Oncol.* **23**, vi207–vi207 (2021).
281. Ouzounova, M. *et al.* Monocytic and granulocytic myeloid derived suppressor cells differentially regulate spatiotemporal tumour plasticity during metastatic cascade. *Nat. Commun. 2017 81* **8**, 1–13 (2017).
282. (Pandya) Shesh, B. *et al.* Uptake of H-ferritin by Glioblastoma stem cells and its impact on their invasion capacity. *J. Cancer Res. Clin. Oncol.* (2023) doi:10.1007/S00432-023-04864-2.
283. Shenoy, G. *et al.* Iron Inhibits Glioblastoma Cell Migration and Polarization. *bioRxiv*

2022.10.13.512175 (2022) doi:10.1101/2022.10.13.512175.
284. Tamimi, A. F. & Juweid, M. Epidemiology and Outcome of Glioblastoma. *Glioblastoma* 143–153 (2017) doi:10.15586/CODON.GLIOBLASTOMA.2017.CH8.
285. McLendon, R. E. & Halperin, E. C. Is the long-term survival of patients with intracranial glioblastoma multiforme overstated? *Cancer* **98**, 1745–1748 (2003).
286. Khan, M. T. *et al.* Identification of Gender-Specific Molecular Differences in Glioblastoma (GBM) and Low-Grade Glioma (LGG) by the Analysis of Large Transcriptomic and Epigenomic Datasets. *Front. Oncol.* **11**, 3634 (2021).
287. Ma, J., Yao, Y., Tian, Y., Chen, K. & Liu, B. Advances in sex disparities for cancer immunotherapy: unveiling the dilemma of Yin and Yang. *Biol. Sex Differ. 2022 131* **13**, 1–12 (2022).
288. Irelli, A., Sirufo, M. M., D'Ugo, C., Ginaldi, L. & De Martinis, M. Sex and Gender Influences on Cancer Immunotherapy Response. *Biomedicines* **8**, (2020).
289. Han, J. *et al.* Pan-cancer analysis reveals sex-specific signatures in the tumor microenvironment. *Mol. Oncol.* **16**, 2153–2173 (2022).
290. Mackenzie, E. L., Iwasaki, K. & Tsuji, Y. Intracellular Iron Transport and Storage: From Molecular Mechanisms to Health Implications. *Antioxid. Redox Signal.* **10**, 997 (2008).
291. Blight, G. D. & Morgan, E. H. Ferritin and iron uptake by reticulocytes. *Br. J. Haematol.* **55**, 59–71 (1983).
292. Sacco, A. *et al.* Iron Metabolism in the Tumor Microenvironment—Implications for Anti-Cancer Immune Response. *Cells* **10**, 1–17 (2021).
293. Ferreira, C. *et al.* H ferritin knockout mice: a model of hyperferritinemia in the absence of iron overload. *Blood* **98**, 525–532 (2001).
294. Thompson, K. *et al.* Mouse brains deficient in H-ferritin have normal iron concentration but a protein profile of iron deficiency and increased evidence of oxidative stress. *J. Neurosci. Res.* **71**, 46–63 (2003).
295. Troike, K. M. *et al.* Tumor cell-intrinsic HFE drives glioblastoma growth. *bioRxiv* 2022.04.13.487917 (2022) doi:10.1101/2022.04.13.487917.
296. Biskup, E., Schejbel, L., de Oliveira, D. N. P. & Høgdall, E. Test of the FlashFREEZE unit in tissue samples freezing for biobanking purposes. *Cell Tissue Bank.* 1–13 (2022) doi:10.1007/S10561-022-10045-1/FIGURES/6.
297. Becht, E. *et al.* Estimating the population abundance of tissue-infiltrating immune and stromal cell populations using gene expression. *Genome Biol.* **17**, 1–20 (2016).
298. Petitprez, F. *et al.* The murine Microenvironment Cell Population counter method to estimate abundance of tissue-infiltrating immune and stromal cell populations in murine samples using gene expression. *Genome Med.* **12**, 1–15 (2020).
299. Risso, D., Ngai, J., Speed, T. P. & Dudoit, S. Normalization of RNA-seq data using factor analysis of control genes or samples. *Nat. Biotechnol. 2014 329* **32**, 896–902 (2014).
300. Ho, K. H. & Patrizi, A. Assessment of common housekeeping genes as reference for gene expression studies using RT-qPCR in mouse choroid plexus. *Sci. Rep.* **11**, 3278 (2021).
301. Robinson, M. D., McCarthy, D. J. & Smyth, G. K. edgeR: a Bioconductor package for differential expression analysis of digital gene expression data. *Bioinformatics* **26**, 139 (2010).
302. Mootha, V. K. *et al.* PGC-1α-responsive genes involved in oxidative phosphorylation are coordinately downregulated in human diabetes. *Nat. Genet. 2003 343* **34**, 267–273 (2003).

303. Rahnenfuhrer AA. Bioconductor - topGO. *Bioconductor* 1 https://bioconductor.org/packages/release/bioc/html/topGO.html (2022).
304. Marisetty, A. *et al.* MiR-181 Family Modulates Osteopontin in Glioblastoma Multiforme. *Cancers 2020, Vol. 12, Page 3813* **12**, 3813 (2020).
305. Wen, X. *et al.* miR-181a-5p inhibits the proliferation and invasion of drug-resistant glioblastoma cells by targeting F-box protein 11 expression. *Oncol. Lett.* **20**, (2020).
306. Lv, Z. & Yang, L. MiR-124 inhibits the growth of glioblastoma through the downregulation of SOS1. *Mol. Med. Rep.* **8**, 345–349 (2013).
307. Silber, J. *et al.* miR-124 and miR-137 inhibit proliferation of glioblastoma multiforme cells and induce differentiation of brain tumor stem cells. *BMC Med.* **6**, 1–17 (2008).
308. Mauldin, I. S. *et al.* Proliferating CD8+ T cell infiltrates are associated with improved survival in glioblastoma. *Cells* **10**, 3378 (2021).
309. Vanoaica, L. *et al.* Conditional Deletion of Ferritin H in Mice Reduces B and T Lymphocyte Populations. *PLoS One* **9**, e89270 (2014).
310. Vickman, R. E. *et al.* Deconstructing tumor heterogeneity: the stromal perspective. *Oncotarget* **11**, 3621 (2020).
311. Khalafallah, A. M. *et al.* 'zooming in' on Glioblastoma: Understanding Tumor Heterogeneity and its Clinical Implications in the Era of Single-Cell Ribonucleic Acid Sequencing. *Neurosurgery* **88**, 477–486 (2021).
312. Melillo, R. M. *et al.* Mast cells have a protumorigenic role in human thyroid cancer. *Oncogene* **29**, 6203–6215 (2010).
313. Johansson, A. *et al.* Mast cells are novel independent prognostic markers in prostate cancer and represent a target for therapy. *Am. J. Pathol.* **177**, 1031–1041 (2010).
314. Põlajeva, J. *et al.* Mast Cell Accumulation in Glioblastoma with a Potential Role for Stem Cell Factor and Chemokine CXCL12. *PLoS One* **6**, (2011).
315. Welsh, T. J. *et al.* Macrophage and mast-cell invasion of tumor cell islets confers a marked survival advantage in non-small-cell lung cancer. *J. Clin. Oncol.* **23**, 8959–8967 (2005).
316. Ribatti, D. & Crivellato, E. The controversial role of mast cells in tumor growth. *Int. Rev. Cell Mol. Biol.* **275**, 89–131 (2009).
317. Seidel, H. *et al.* Effects of Primary Mast Cell Disease on Hemostasis and Erythropoiesis. *Int. J. Mol. Sci.* **22**, (2021).
318. Asif, P. J., Longobardi, C., Hahne, M. & Medema, J. P. The Role of Cancer-Associated Fibroblasts in Cancer Invasion and Metastasis. *Cancers (Basel).* **13**, (2021).
319. Song, H., Fu, X., Wu, C. & Li, S. Aging-related tumor associated fibroblasts changes could worsen the prognosis of GBM patients. *Cancer Cell Int.* **20**, (2020).
320. Ferreira, C. *et al.* H ferritin knockout mice: A model of hyperferritinemia in the absence of iron overload. *Blood* **98**, 525–532 (2001).
321. Ann Mari Rosager, Mia D. Sørensen, Rikke H. Dahlrot, Steinbjørn Hansen, David L. Schonberg, Jeremy N. Rich, Justin D. Lathia, B. W. K. Transferrin receptor-1 and ferritin heavy and light chains in astrocytic brain tumors: Expression and prognostic value. *PLoS One* **12(8)**, e0182954. (2017).
322. Todorich, B., Zhang, X. & Connor, J. R. H-ferritin is the major source of iron for oligodendrocytes. *Glia* **59**, 927–935 (2011).
323. Cheli, V. T. *et al.* H-ferritin expression in astrocytes is necessary for proper

oligodendrocyte development and myelination. *Glia* **69**, 2981–2998 (2021).
324. Leimberg, J. M., Konijn, A. M. & Fibach, E. Macrophages promote development of human erythroid precursors in transferrin-free culture medium. *Hematology* **10**, 73–76 (2005).
325. Garay, T. *et al.* Cell migration or cytokinesis and proliferation?--revisiting the 'go or grow' hypothesis in cancer cells in vitro. *Exp. Cell Res.* **319**, 3094–3103 (2013).
326. Corcoran, A., Del Maestro, R. F., Berger, M. S., Canoll, P. D. & Bruce, J. N. Testing the 'Go or Grow' hypothesis in human medulloblastoma cell lines in two and three dimensions. *Neurosurgery* **53**, 174–185 (2003).
327. Jaksch-Bogensperger, H. *et al.* Ferritin in glioblastoma. *Br. J. Cancer 2020 12210* **122**, 1441–1444 (2020).
328. Coad, J. & Conlon, C. Iron deficiency in women: assessment, causes and consequences. *Curr. Opin. Clin. Nutr. Metab. Care* **14**, 625–634 (2011).
329. Wen, C. P. *et al.* High serum iron is associated with increased cancer risk. *Cancer Res.* **74**, 6589–6597 (2014).
330. Condeles, A. L. & Toledo Junior, J. C. The labile iron pool reacts rapidly and catalytically with peroxynitrite. *Biomolecules* **11**, (2021).
331. Komi, D. E. A. & Redegeld, F. A. Role of Mast Cells in Shaping the Tumor Microenvironment. *Clin. Rev. Allergy Immunol.* **58**, 313 (2020).
332. Maciel, T. T., Moura, I. C. & Hermine, O. The role of mast cells in cancers. *F1000Prime Rep.* **7**, (2015).
333. Shireman, J. M., Ammanuel, S., Eickhoff, J. C. & Dey, M. Sexual dimorphism of the immune system predicts clinical outcomes in glioblastoma immunotherapy: A systematic review and meta-analysis. *Neuro-oncology Adv.* **4**, 1–14 (2022).
334. Gal-Oz, S. T. *et al.* ImmGen report: sexual dimorphism in the immune system transcriptome. *Nat. Commun.* **10**, (2019).
335. Gray, C. P., Arosio, P. & Mersey, P. Heavy chain ferritin activates regulatory T cells by induction of changes in dendritic cells. *Blood* **99**, 3326–3334 (2002).
336. Liang, W. & Ferrara, N. Iron Metabolism in the Tumor Microenvironment: Contributions of Innate Immune Cells. *Front. Immunol.* **11**, (2020).
337. Sciacqua, A. *et al.* Ferritin modifies the relationship between inflammation and arterial stiffness in hypertensive patients with different glucose tolerance. *Cardiovasc. Diabetol.* **19**, 1–10 (2020).
338. Seyhan, S., Pamuk, Ö. N., Pamuk, G. E. & Çakır, N. The correlation between ferritin level and acute phase parameters in rheumatoid arthritis and systemic lupus erythematosus. *Eur. J. Rheumatol.* **1**, 92 (2014).
339. Osborne, B. F., Turano, A. & Schwarz, J. M. Sex differences in the neuroimmune system. *Curr. Opin. Behav. Sci.* **23**, 118–123 (2018).
340. McCarthy, M. M., Herold, K. & Stockman, S. L. Fast, Furious and Enduring: Sensitive versus Critical Periods in Sexual Differentiation of the Brain. *Physiol. Behav.* **187**, 13 (2018).
341. Bailey, G. S. The Iodogen Method for Radiolabeling Protein. *Protein Protoc. Handb.* 673–674 (1996) doi:10.1007/978-1-60327-259-9_115.

VITA

Bhavyata Shesh

Education

2020- Present	Penn State Harrisburg, MBA, General Management
2018- Present	Penn State Hershey College of Medicine, PhD, Biomedical Sciences
2011	Sardar Patel University, India, M.S. Medical Biotechnology

Internships

2022	Global Business Development and Strategy Intern, Viatris, NY
2021	Business Development and Strategy Intern, Rallybio, CT

Research

2016-2018	Research Technologist II, Penn State Cancer Institute, PA
2011-2015	Research Associate and Junior Research Fellow, India

Selected Publications

Bhavyata (Pandya) Shesh, James R. Connor, A novel view of ferritin in cancer, Biochimica et Biophysica Acta (BBA) - Reviews on Cancer, 2023

Bhavyata (Pandya) Shesh, Becky Slagle-Webb, Ganesh Shenoy, Vladimir Khristov, Brad E. Zacharia, James R. Connor, Uptake of H-ferritin by Glioblastoma stem cells and its impact on their invasion capacity, Journal of Cancer Research and Clinical Oncology, 2023

Bhavyata (Pandya) Shesh, Vonn Walter, Becky Slagle-Webb, Elizabeth Neely, James R. Connor, Sexually dimorphic effect of H-ferritin genetic manipulation on survival and tumor microenvironment in a mouse model of Glioblastoma, Journal of Neuro - Oncology, 2023 (submitted)

Vladimir Khristov, Darya Nesterova, Mara Trifoi, Taylor Clegg, Annika Daya, Thomas Barrett, Emily Tufano, Ganesh Shenoy, **Bhavyata Pandya**, Gela Beselia, Nataliya Smith, Oliver Mrowczynski, Brad Zacharia, Kristin Waite, Justin Lathia, Jill Barnholtz-Sloan, James Connor, Plasma IL13Rα2 as a novel liquid biopsy biomarker for glioblastoma, Journal of Neuro - Oncology, 2022

Ganesh Shenoy, Becky Slagle-Webb, Chachrit Khunsriraksakul, **Bhavyata Pandya**, Jingqin Luo, Vladimir, Khristov, Nataliya Smith, Alireza Mansouri, Brad E. Zacharia, Sheldon Holder, Justin D. Lathia, Jill S. Barnholtz-Sloan, James R. Connor, Association of Anemia, and Iron Supplementation with Sex-Specific Survival in Glioblastoma Patients, (Preprint)

Alicia C. McDonald, Jay D. Raman, Jing Shen, Jason Liao, **Bhavyata Pandya**, Manish A. Vira, Circulating microRNAs in plasma before and after radical prostatectomy, Urologic Oncology, 2019

Vaibhav Bhatt, **Bhavyata Pandya**, Chaitanya Joshi, Anju Nagee, Curcuma longa: an alternative to antibiotics to combat mastitis in cattle, WJAS, 2013